

**MOLECULAR CLONING, EXPRESSION AND  
CHARACTERIZATION OF MU-OPIOID RECEPTORS WITH  
SPECIAL REFERENCE TO ITS INTERACTION WITH BOVINE  
BETA-CASOMORPHINS**



**THESIS SUBMITTED TO THE  
ICAR-NATIONAL DAIRY RESEARCH INSTITUTE, KARNAL  
(DEEMED UNIVERSITY)  
IN PARTIAL FULFILLMENT OF THE REQUIREMENTS  
FOR THE AWARD OF THE DEGREE OF**

**MASTER OF TECHNOLOGY  
IN  
ANIMAL BIOTECHNOLOGY  
BY**

**AMARJEET  
B.TECH (BIOTECHNOLOGY)**

**ANIMAL BIOTECHNOLOGY CENTRE (ABTC)  
ICAR-NATIONAL DAIRY RESEARCH INSTITUTE  
(DEEMED UNIVERSITY)  
KARNAL-132001 (HARYANA), INDIA**

**2019**

**Regn. No. 16-M-BT-13**

*Dedicated  
To My  
Father  
Late Ramdeen  
&  
My Parents*



# Molecular Cloning, Expression and Characterization of Mu- opioid Receptors with special reference to its Interaction with Bovine Beta-casomorphins

BY

AMARJEET


THESIS SUBMITTED TO THE  
NATIONAL DAIRY RESEARCH INSTITUTE, KARNAL  
(DEEMED UNIVERSITY)  
IN PARTIAL FULFILMENT OF THE REQUIREMENTS  
FOR THE AWARD OF THE DEGREE OF

MASTER OF TECHNOLOGY

IN

ANIMAL BIOTECHNOLOGY

Approved by:


  
(EXTERNAL EXAMINER)

  
Dr. (Mrs.) Monika Sodhi  
(MAJOR ADVISOR & CHAIRPERSON)

## Members of Advisory Committee

**Dr. RS Kataria**

Principal Scientist, AB Division, NBAGR

  
\_\_\_\_\_


**Dr. Manishi Mukesh**

Principal Scientist, AB Division, NBAGR

  
\_\_\_\_\_

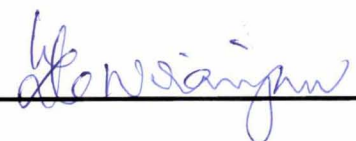
**Dr. Sudarshan Kumar**

Scientist, Animal Biotech Centre, NDRI

  
\_\_\_\_\_


**Dr. SK Niranjana**

Principal Scientist, AGB Division, NBAGR

  
\_\_\_\_\_

**Dr. Suneel Kumar Onteru**

Principal Scientist, ABC Division, NDRI  
(Joint Director's Nominee)

  
\_\_\_\_\_



राष्ट्रीय पशु आनुवंशिक संसाधन ब्यूरो  
**NATIONAL BUREAU OF ANIMAL GENETIC RESOURCES**  
(I.C.A.R.)



Makrapur Campus, G.T. Road Bye Pass, Near Basant Vihar,  
P.O. Box. No. 129, KARNAL - 132 001 (Haryana)

**Dr. Monika Sodhi**

Principal Scientist

(Animal Biotechnology Division)

ICAR-NBAGR, Karnal-132001, Haryana, India

**Certificate**

This is to certify that the thesis entitled “**Molecular Cloning, Expression and Characterization of Mu-opioid Receptors with special reference to its Interaction with Bovine Beta-casomorphins**” submitted by **MR. AMARJEET** in partial fulfilment of the requirement for the award of the degree of **MASTER OF TECHNOLOGY** in **ANIMAL BIOTECHNOLOGY** of the **ICAR-NATIONAL DAIRY RESEARCH INSTITUTE (DEEMED UNIVERSITY)-KARNAL-132001 (HARYANA) INDIA**, is a bonafide research work carried out by him under my supervision and guidance, and no part of the thesis has been submitted for any other degree or diploma.

Dated: 31-05-2019

**Dr. Monika Sodhi**

Major Advisor & chairperson (Guide)

## *Acknowledgements.....*

*With all the experiences of joys and sorrows God has always been kind to me and helped me in every step of my life to make me understand the value of life.*

*Words in my lexicon fail to express my profound sense of veneration and indebtedness to my mentor **Dr. Monika Sodhi**, Principal Scientist, Animal Biotechnology Division, NBAGR, Karnal, for his inspiring guidance, outstanding cooperation and constant encouragement during the entire course of study. His constant support, critical appreciation and parental concern gave a glitter of confidence to my work. His intense hard work and countless efforts to provide every possible facility in the lab made this strenuous task achievable.*

*I am extremely indebted to all the members of my advisory committee Dr. R.S. Kataria, Principal Scientist, Animal Biotechnology Division, Dr. Manishi Mukesh, Principal Scientist, Animal Biotechnology Division, Dr. Sudarshan Kumar, Scientist, Animal Biotechnology Division, Dr. S.K. Niranjan, Principal Scientist, Animal Genetics and Breeding Division, Dr. Suneel Kumar Onteru, Principal Scientist, Animal Biochemistry Division, for their valuable suggestion and encouragement throughout the research.*

*I am deeply gratified to Director, NDRI Karnal. Dr. R. R. B. Singh and Director, NBAGR, KARNAL, Dr. R.K. Viji for providing me all the necessary facilities and financial support in the form of institutional fellowship during the entire period of my studies.*

*Thanks to **Dr. P. Palta**, Head, all faculty members and staff of Animal Biotechnology Division for their co-operation and support.*

*I consider myself greatly privileged and fortunate to have worked under the supervision and guidance of Dr. Saravanan Matheshwaran, Assistant Professor, IIT Kanpur for helping me in cloning and expression of mu receptor genes. I feel grateful to him for his kind affection, inspiring words, invaluable guidance, whole-hearted encouragement and critical appreciation and for all the trust he showed for me. I am also thankful to all the help from lab and division members of DNA repair and Antimicrobial Resistance (AMR) lab, Department of Biological Sciences and Bioengineering without which it was not possible to complete my studies.*

*I express a sincere thanks to my friends – Dr. Manoj Kumar Singh, Dr. Ankita Sharma, Dr. Prince Vivek, Pervash Kumari, Dr. Preeti Verma, Dr. Amandeep kaur, Dr. Aashaq Hussain Dar, Preeti Swami, Vipul Chudhari, Amandeep Just, Dr. Gourav, Manish Tiwari, Nephher, Aekagra Singh, Chitral Chatterjee, Umang Gupta, Hariharan V. C., Prem Anand, Priyanka Amule, Shreya Ghosh, Deepanjan Mishra, Mr. Devender Kumar, Mr. Balwan Singh for providing a very supportive environment in lab. I would like to thank my friends for making my stay at campus so memorable.*

*I would like to acknowledge all my teachers for making my fundamentals and concepts sound enough that eventually helped me to appreciate what I do. I am grateful to all my family members including my Mother, Brothers and cousins for all care and attention. I feel incapable of finding words to thank my parents for all the efforts and sacrifices made by them. I devote heartiest gratitude to my Mother. She has been my inspiration to improve as a person. I dedicate all my achievements to these people.*

*Finally, I would like take this opportunity to thank everybody who was important to the successful realization of this thesis, as well as expressing my apology if I failed to mention anyone personally in this acknowledgement.*

Dated: 31-05-2019

  
(Amarjeet)

## CONTENTS

Chapter No.	Title	Page No.
<b>1.0</b>	<b>INTRODUCTION</b>	<b>1-3</b>
<b>2.0</b>	<b>REVIEW OF LITERATURE</b>	<b>4-20</b>
2.1	Contribution of milk	4
2.1.1	Beta casein and bioactive peptides	5
2.1.2	Bioactive peptides from different types of milk	6
2.1.3	Regulatory mechanism of milk derived peptides	8
2.2	Pharmacologically defined $\mu$ -receptor subtypes	10
2.3	Molecular mechanism of opioid receptor dependent signaling and behavior	11
2.3.1	Molecular mechanisms of opioid tolerance	11
2.3.2	Opioid receptors and arrestin recruitment	12
2.4.	Epigenetic effect of casein derived opioid peptide	13
2.5	Structure and function of MOR agonist	15
2.6	Molecular docking	15
2.6.1	MORs binding and interaction study	17
2.7	Expression of a Membrane-inserted OPRM in bacterial system ( <i>E.coli</i> )	18
2.7.1	Isolation of OPRM	19
<b>3.0</b>	<b>MATERIALS AND METHODS</b>	<b>21-36</b>
3.1	To characterize mu opioid receptor (MOR) and its spliced variants in brain and gut tissues of mice	21
3.1.1.	Chemicals, Enzymes, Solutions, Buffers and Equipment's	21
3.1.2	RNA isolation from brain and gut	21
3.1.3	cDNA Synthesis	23
3.1.4	PCR amplification of MOR	24
3.1.5	Gel extraction purification	24
3.1.6	Sequencing of different transcript variants of MORs	25
3.2	To clone MOR in Pichia / Bacterial expression system for their over expression and purification	26
3.2.1	Vector System	27
3.2.2	Restriction digestion of vector and PCR product	28
3.2.3	Ligation of digested PCR product of MOR with the digested cloning/expression cloning vector pET28a (+)	28
3.2.4	Transformation	28

	3.2.5	Expression of recombinant MOR	29
	3.2.6	Detergent screening and purification	30
	3.2.7	Isolation of recombinant MOR	31
	3.2.8	Ammonium sulphate precipitation of MOR Protein	31
	3.2.9	SDS-PAGE analysis	32
	3.3	To undertake interaction studies of MOR with BCM7/9 by <i>in silico</i> approach	34
	3.3.1	Mice $\mu$ -opioid receptor gene	34
	3.3.2	Homology modelling of receptor and ligands	34
	3.3.3	Active Site Analysis and Residues Recognition	35
	3.3.4	3D model validation	35
	3.3.5	<i>In Silico</i> Protein-Protein Interaction Study	35
<b>4.0</b>	<b>RESULT AND DISCUSSION</b>		<b>37-81</b>
	4.1	To characterize mu opioid receptor (MOR) and its splice variants in brain and gut tissues of mice	37
	4.1.1	Sampling details, RNA isolation and cDNA synthesis	37
	4.1.2	PCR amplification of $\mu$ opioid receptor (MOR)	38
	4.1.3	Identification and retrieval of $\mu$ -opioid receptor gene	39
	4.1.4	Domain structure of MOR-1 gene	41
	4.1.5	Splicing and generation of different variants	44
	4.1.6	Sequence homology of OPRM-1 across and within species	49
	4.1.7	Phylogenetic analysis	50
	4.1.8	physicochemical properties and the abundance of amino acids in MORs transcript variants protein	55
	<b>4.2</b>	To clone MOR in Bacterial expression system for their over expression and purification	56
	4.2.1	Molecular cloning	56
	4.2.2	Transformation of <i>Escherichia coli</i> (DH5 $\alpha$ ) with pET28a (+) containing insert	57
	4.2.3	Analysis of pET28a (+) containing insert by restriction enzyme	58
	4.2.4	Expression of mice MOR in E.coli	58
	4.2.5	MOR-1M Solubilisation and purification	59
	4.2.6	Confirmation for the binding properties of purified receptor protein	61

	4.3	To undertake interaction studies of MOR with BCM7/9 by Insilco approach	62
	4.3.1	Homology modelling of the 3D Structure of 7TM mu-opioid receptor protein	63
	4.3.2	Active site analysis and residues recognition	64
	4.3.3	3D modelling of beta-casomorphins	66
	4.3.4	Secondary structure prediction and 3D Structure validation	68
	4.3.5	Molecular docking and receptor protein interaction study	73
	4.3.6	Hydrophobic interactions and functional activity	77
	4.3.7	MOR-BCMs complex energy minimization	79
<b>5.0</b>	<b>SUMMARY AND CONCLUSIONS</b>		<b>85-87</b>
<b>BIBLIOGRAPHY</b>			<b>i-xv</b>
<b>APPENDIX I</b>			<b>Xvi</b>

## **LIST OF TABLES**

<b>Table No.</b>	<b>Title</b>	<b>Page No.</b>
2.1	Comparison of nutritional value of mother milk and cow milk	5
2.2	Bioactive peptides of bovine milk	6
2.3	Pharmacologically defined $\mu$ -receptor subtypes	10
3.1	Composition of master mix1 for cDNA synthesis	23
3.2	Composition of reagents for preparation of Mix1I for cDNA synthesis	24
3.3	Primer details of mu-opioid receptor (MOR)	24
3.4	Bacterial strains used for cloning, expression and propagation	28
3.5	Ammonium sulphate precipitaion of MOR protein	32
3.6	Composition of SDS-PAGE running buffer and protein loading dye	33
3.7	Composition of resolving and stacking gel	33
3.8	Protein staining and de-staining solutions (1L)	34
4.1	Purity and quantity of RNA from brain and gut tissue of mice	38
4.2	Characteristics of mice mu opioid receptor (MOR) transcript variants	40
4.3	Structural domain groups of mice mu opioid receptor transcripts	42
4.4	Characterixation and localization of OPRM-1 transcript variants/isoforms	43
4.5	MOR transcript variants and its canonical sequence position for alternate spicing	45
4.6	Estimates of evolutionary divergence between amino acid sequences of different MOR receptors	52
4.7	Physiochemical properties of $\mu$ -opioid receptor transcript variants.	53
4.7	Quality estimation scores of the predicted 3D structures by I-TASSER.	62
4.8	Enzym'e Commission (EC) and number of active site of MORs	63
4.9	Gene ontology term of MOR	64

4.10	Predicted ligand binding sites in the <i>MOR</i> using the homologue model generated by I-TASSER.	66
4.11	Calculated alpha helix, extended strand, beta turn and random coil for the secondary structures predicted for $\mu$ -opioid receptor isoforms by SOPMA	67
4.12	PROSA Z-score for homology model structure	68
4.13	Ramachandran plot analysis of molecular docking results of $\mu$ -opioid receptor	70
4.14	Patch Dock and Fire Dock results for each MORs energy for the solution in kcal/mol.	73
4.15	Energy minimization of complex (MORs-BCMs)	80

## **LIST OF FIGURES**

<b>Figure No.</b>	<b>Title</b>	<b>Page No.</b>
2.1	Percentage contribution of milk by different livestock species	5
2.2	Structural components of BCM-7 as an opioid peptide	7
2.3	Different variants of beta casein gene	7
2.4	Enzymatic digestion of A1 and A2 variants of bovine beta-casein.	8
2.5	The fate of milk consumed for beta-casomorphine-7 formation and effects exerted by beta-casomorphine-7 on various organs.	9
2.6	Molecular mechanism of opioid receptor dependent signaling	11
2.7	The effects bBCM7, hBCM-7 and morphine vary greatly in DNA methylation	14
2.8	Crystal structure of bioactive peptide. [A] Bovine rhodopsin (PDB ID: 1u19), [B] $\beta$ 2-adrenergic receptor	15
2.9	Molecular structure of morphine (agonist)	16
2.10	Schematics of $\mu$ -opioid receptor interaction	18
3.1	Vector Map pET28a (+) expression system	27
3.2	Orientation of MOR gene cloned in pET28a (+) expression vector	29
4.1	Representative gel picture of isolated RNA from brain and gut tissue	37
4.2	Amplified products of ACTB on 2% agarose gel indicating quality of cDNA prepared from Brain and Gut derived RNA samples	38
4.3	Amplified MOR transcript variants on 2 % Agarose gel,	39
4.4	Interaction near the NPxxY motif.	46-47
4.5	G-protein couple receptor (GPCRs) DRY motif.	47
4.6	Splice variants of OPRM-1 gene generated from splicing at different exons	48
4.7	Alignment of OPRM-1 gene transcripts based on aminoacid sequences.	51-53
4.8	Amino acid based phylogenetic analysis of OPRM-1 transcript variants	54

4.9	Electrophoresis of amplified MOR transcript variants MOR-1M (1.1 kb 1.5 % Agarose gel	56
4.10	Preparation of Vector pET28a (+) and MOR insert after digestion with EcoR I and Xho I restriction enzyme.	57
4.11	pET 28 (a+)-MOR-1M recombinant Lb plate	57
4.12	Electrophoresis of cloned plasmid on 1.5 % Agarose gel	58
4.13	Electrophoresis of cloned plasmid after double digestin on 1.5% agarose gel for release of insert	58
4.14	SDS-PAGE analysis for expression of MOR protein from E.coli strain C41 (DE3).	59
4.15	Chromatogram representation of purified MOR-1 protein through Hi-Trap Ni-NTA column from <i>E. coli</i> C41 (DE3)	60
4.16	SDS-PAGE analysis for purified MOR protein from E.coli strain C41 (DE3).	61
4.17	SDS-PAGE analysis for MOR protein precipitation from E.coli strain C41 (DE3).	61
4.18	Chromatogram representation of purified MOR-1 protein through Hi-Trap Heparin column from <i>E. coli</i> C41 (DE3)	62
4.19	SDS-PAGE analysis of post dialysis MOR protein purification from E.coli strain C41 (DE3).	62
4.20	Homology Model of MOR gene. [A] Mice mMOR, [B] Human hOPRM-1: Helix is represented by blue coils, $\beta$ -sheet as red and H-bond as blue line	67
4.21	3D Modelled structure of $\beta$ -casomorphine ligands	68
4.22	Secondary structure of MOR protein	71
4.23	Ramachandran plot of mu opioid receptor by PROCHECK server	72
4.24	Residue interaction energy profile for the MOR drawn with PROSA	73
4.22	Molecular Docking of MOR with BCMs:	74
4.26	Representation of H-bonding between MOR and BCM7/9.	76
4.27	Molecular docking and binding pocking site of $\mu$ -opioid receptor	77
4.28	Ligand binding pocket with polar interactions	78
4.29	The homology model where the ligand forming hydrogen bonds and hydrophobic interaction.	79

4.30	PDBsum's ligplot results for $\mu$ -OR-BCM7/9	81-82
4.31	Mice and Human MOR Comparative energy analysis of BCMs complex	83-84

## LIST OF ABBREVIATIONS

---

ACTB	-	Beta actin
Bp	-	Base pair
BCM-7	-	Beta- casomorphine 7
BCM-9	-	Beta- casomorphine 9
CaCl <sub>2</sub>	-	Calcium chloride
CTD	-	C-terminal domain
cDNA	-	Complementary deoxyribonucleic acid
DNA	-	Deoxy Ribonucleic Acid
dNTP	-	Deoxyribonucleotide tri phosphate
EDTA	-	Ethylene Diamine Trichloro Acetic Acid
GAPDH	-	Glyceraldehyde 3-phosphate dehydrogenase
GPCRs	-	G-protein couple receptor
IPTG	-	Isopropyl $\beta$ -D-1-thiogalactopyranoside
I-TASSER	-	Iterative Threading ASSEmbly Refinement
Kb	-	Kilo base
kDa	-	Kilo Dalton
LB	-	Luria Bertani
MgCl <sub>2</sub>	-	Magnesium Chloride
mRNA	-	Messenger Ribonucleic acid
MCS	-	Multiple cloning site
MOR	-	Mu-opioid receptor
MW	-	Molecular Weight
NTD	-	N-terminal domain
NCBI	-	National Centre for Biotechnology Information
OD	-	Optical density
pET28a (+)	-	pET28a (+) expression vector
SDS	-	Sodium dodecyl sulphate
PAGE	-	Polyacrylamide gel electrophoresis
TAE	-	Tris acetate EDTA
TBE	-	Tris buffer saline
TEMED	-	Tetra methyl ethylene diamine

## **ABSTRACT**

The A1 and A2 variants of bovine  $\beta$ -casein differ at amino acid position 67 with histidine in A1 and proline in A2 milk. This polymorphism leads to key conformational changes in the secondary structure of expressed  $\beta$ -casein protein and gastrointestinal proteolytic digestion of A1  $\beta$ -casein (raw/processed milk) releases a 7 amino acid bioactive peptide 'opioid' called beta-casomorphins-7 (BCM-7) in small intestine, while proline in A2 milk at 67 position prevents the split at this particular site and generates nine amino acid peptide BCM-9. BCM-7 binds to the mu opioid receptors distributed in the gut and brain which may affect the brain regions integrated with dopaminergic and serotonergic system, interfere with these pathways and disturb cortical association or functional connections which may be implicated in different diseases associated with as a risk factor for type I diabetes mellitus coronary heart disease arteriosclerosis sudden infant death syndrome Schizophrenia and autism. The present study, was undertaken to ascertain the binding of BCM 7/9 with mu-opioid receptor. The mu receptors have different splice variants, hence attempt was made to amplify the cDNA from gut and brain tissue of mice. Six splice variants were identified and efforts were also made to clone and express the mu receptor MOR. Induced expression mu opioid receptor genes in pET28a (+) vector and E.coli C41 (DE3) host yielded purified protein in large quantities, which could be a good resource for future studies. Further, different databases and literature was searched to identify these variants. In total 31 splice variants were identified and characterized. As the crystal structure for mice mu receptors as well as ligands (BCM7/9) was unavailable in the PDB databank, the strategy of homology modelling was utilized to generate their 3D structure. For structure prediction, the sequences for major 12 mu receptor isoform were used, Three templates (4n6hA, 5zbh, 4dk1A), satisfying all the criterion for the stable structure were used for homology modelling using I-TASSER. The homology of these templates with mu receptors was 95-98% with percent identity and positivity score of >90 %. The generated model of mu receptor was visualized using Chimera and PyMOLE Server. Using RAMPAGE Server, 98 % residues of mu receptors were observed to be in the most favored regions indicating energetically and sterically stable conformations of residues. The structures for BCM7 and BCM9 ligands modelled by MODELLER serve, displayed DOPE score of 0.97 and 0.98, respectively indicating good quality of structure prediction. The PDB files of ligand and target receptor were uploaded to Patch Dock server for docking, using cluster RMSD at default value of 4Å°. Interacting amino acidic residues and prominent binding sites were predicted by PDBsum server and LIGPLOT server respectively. Docking of BCM7/9 with mu receptors indicated stable binding of BCM7 with mu receptors as compared to BCM9 in terms of interacting amino acids (TYR<sup>128</sup>, TRP<sup>318</sup>, ASN<sup>127</sup>, LYS<sup>233</sup>, GLU<sup>310</sup> LEU<sup>219</sup>), ligand and protein atoms involve in hydrogen bonding (BCM7 = LYS<sup>233</sup> (2.22 Å°), BCM9 = LYS<sup>233</sup> (3.09 Å°)), number of hydrophobic interacting amino acid residues (15 in case of BCM7 while 13 in BCM9). The comparative energy minimization of docked model for  $\mu$ -OR-BCM7 (-191105.7 KJ/mole) and for  $\mu$ -OR-BCM9 (-1898520 KJ/mole) using YASARA server also indicated greater binding affinity of BCM7 towards mu opioid receptor. This might explain the probable ill effects of BCM7 in comparison to BCM9.

## सार

ए<sub>1</sub> तथा ए<sub>2</sub> गौ जातीय बीटा केसिन के दो व्यापक प्रकार हैं जोकि एमिनोअम्ल की स्थिति/ अनुक्रम 67 पर आपस में भिन्न हैं। ए<sub>2</sub> प्रकार में एमिनोअम्ल प्रोलीन होता है जबकि ए<sub>1</sub> प्रकार में यह बदलकर हिस्टीडीन हो जाता है। यह बहुरूपता व्यक्त बीटा केसिन प्रोटीन की द्वितीय संरचना में महत्वपूर्ण रूप से परिवर्तन करता है और ए<sub>1</sub> बीटा केसिन युक्त दूध (कच्चा/ प्रसंकृत) का छोटी आंत में प्रोटीओलिटिक पाचन 7 एमिनो एसिड बायोएक्टिव पेप्टाइड ओपियोड उत्पन्न करता है जिसे बीटा कैसोमोर्फिन-7 (बीसीएम-7) कहा जाता है जबकि 67 स्थिति में ए<sub>2</sub> दूध में प्रोलाइन इस विशेष साइट पर विभाजन को रोकता है और नौ एमिनो एसिड पेप्टाइड बीसीएम-9 उत्पन्न करता है। बीसीएम-7 आंत और मस्तिष्क में वितरित म्यू-ओपीओड रिसेप्टर्स को बाइंड करता है और यह डोपामिनजिक और सेरोटोनिनजिक प्रणाली के साथ एकीकृत होकर मस्तिष्क क्षेत्रों को प्रभावित कर सकता है और विभिन्न प्रकार के रोगों जैसे कि टाइप-1 डायबिटीज मेलिटस, कोरोनरी हार्ट डिजीज, आर्टिरियोस्क्लेरोसिस, शिशु मृत्यु सिंड्रोम, स्किज़ोफ्रेनिया का कारक बन सकता है। वर्तमान अध्ययन म्यू ओपेटाइड रिसेप्टर व बी सी एम् 7/ बी सी एम् 9 के बंधन की तुलनात्मक स्थिरता पता लगाने के लिए किया गया। म्यू-रिसेप्टर्स में अलग अलग सपलाईस वेरिएंट होते हैं इसलिए चूहों की आंत और मस्तिष्क के उतकों से सीडीएनए का प्रवर्धन किया गया और 6 सपलाईस वेरिएंट का पता लगाया गया। म्यू रिसेप्टर वेरिएंट को क्लोन और व्यक्त करने के प्रयास भी किए गए। PET28a (+) वेक्टर और E.coli C41 (DE3) होस्ट में अभिव्यक्ति के उपरांत शुद्ध म्यू अपियोड रिसेप्टर प्रोटीन पर्याप्त मात्रा में प्राप्त हुई जो भविष्य के अध्ययन के लिए एक अच्छा संसाधन हो सकता है। इसके अतिरिक्त अन्य उपस्थित वेरिएंट का पता लगाने के लिए विभिन्न डेटाबेस व लिटरेचर को भी सर्च किया और कुल 31 वेरिएंट पाये गए, जिनका निरूपण किया गया।

चूहों के म्यू रिसेप्टर और लिगेंड (बीसीएम 7/9) इंटरैक्शन के अध्ययन के लिए अपेक्षित क्रिस्टल संरचना की पीडीबी डेटाबैंक में अनुपलब्धता के कारण, इनकी 3डी संरचना को प्राप्त करने के लिए होमोलोजी मॉडल का प्रयोग किया गया। संरचना के अनुमान के लिए प्रमुख 12 म्यू- रिसेप्टर आइसोफॉर्म के अनुक्रमों का उपयोग किया गया था, तीन टेम्प्लेट (4n6hA, 5zbh, 4dk1A) जिन्होंने स्थिर संरचना के लिए सभी कसौटियों को पूरा किया, का उपयोग होमोलॉग मॉडलिंग के लिए किया गया। म्यू-रिसेप्टर्स के साथ इन टेम्प्लेट्स की होमोलॉजी 95-98% पाई गई। प्रतिशत पहचान के संबंध में म्यू-रिसेप्टर्स के साथ चयनित टेम्प्लेटों की समरूपता 90% से ऊपर थी। म्यू-रिसेप्टर से उत्पन्न मॉडल को Chimera और PyMole सर्वर का उपयोग करके देखा गया। बीसीएम 7/9 के मॉडल को मोडेलर सर्वर में निर्मित संरचनाएं 0.97 और 0.98 के डीओपीई स्कोर को प्रदर्शित करती हैं, जोकि लीजेंड संरचना में होमोलॉजी मॉडल की गुणवत्ता का आकलन करने के लिए एक विश्वसनीय सांख्यिकीय क्षमता है। रामचंद्रन प्लॉट के वांछित क्षेत्र उर्जा और स्टेरिकल स्थिरता को दर्शाते हैं और 90% से अधिक अवशेषों वाले मॉडल को अच्छी गुणवत्ता वाले मॉडल माना जाता है। रामपेज सर्वर का उपयोग करते हुए, म्यू-रिसेप्टर्स के 98% अवशेषों को सबसे पसंदीदा क्षेत्रों में देखा गया। लीजेंड और रिसेप्टर्स कि PDB फाईल को patchDock सर्वर में RMSD कलस्टर का प्रयोग करते हुए अपलोड किया गया। डाकिंग नतीजों से हमें पता चला कि बीसीएम7 का म्यू-रिसेप्टर्स के साथ बंधन, बीसीएम-9 कि तुलना में अधिक स्थिर था और इसमें (TYR<sup>128</sup>, TRP<sup>318</sup>, ASN<sup>127</sup>, LYS<sup>233</sup>, GLU<sup>310</sup> LEU<sup>219</sup>) एमिनो एसिड शामिल थे। लीजेंड व म्यू-रिसेप्टर के दौरान बीसीएम-7 में 15 एमिनो अम्ल हाइड्रोफोबिक इंटरैक्शन में शामिल थे। जबकि बीसीएम-9 के बंधन में इनकी संख्या केवल 13 थी, जोकि बीसीएम-7 की अधिक स्थिरता को दर्शाती है। इस बंधन में उर्जा न्युनिकरण का YASARA सर्वर के प्रयोग द्वारा भी पता लगाया गया। जोकि बीसीएम-7 में -191105.7 KJ/mole और बीसीएम-9 में -1898520 KJ/mole थी। यह नतीजे प्रत्यक्ष रूप से बताते हैं कि बीसीएम-7 का म्यू-रिसेप्टर्स के साथ बंधन अधिक स्थिर है।

# **CHAPTER -1**

---

---

## **Introduction**

---

---

## INTRODUCTION

---

Cow milk is considered as the best replacement of mother milk as it contains not only proteins and carbohydrates but also has minerals and vitamins which are essential for growth. The protein content in milk is 3.5% composed mainly of caseins (80%) and whey protein (20%). There are 4 caseins in bovine milk including alpha S1 ( $\alpha$ -S1), alpha S2 ( $\alpha$ -S2), Beta ( $\beta$ -CN), and kappa ( $\kappa$ -CN) contributing 39–46% , 8–11%, 25–35%, and 8–15% of total caseins respectively. Another form is gamma-casein, which is actually a product of  $\beta$ -casein's degradation. Caseins are encoded by members of a multigene family. The genes encoding for all the four caseins are found on bovine chromosome 6. Among the caseins, with 35% contribution,  $\beta$  casein is the second most contributor after alpha S1 ( $\alpha$ -S1). The bovine  $\beta$ -CN gene has 12 different genetic variants (A1, A2, A3, B, C, D, E, F, H1, H2, I, G). The variants A1 and A2 are most studied. The SNP C to A; CCT (proline A2) to CAT (histidine, A1) at amino acid position 67 is responsible for this variation. These two variants have gained attention recently due to the association of these variants with human health (Elliot *et al.*, 1999; McLachlan, 2001).. There is a general belief that due to change from proline to histidine, the secondary structure of beta casein is changed and the bioactive peptides generated after digestion of A1/A2 milk are different. Gastrointestinal proteolytic digestion of A1 milk (histidine at position 67) releases a 7 amino acid bioactive peptide 'opioid' known as  $\beta$ -casomorphin7 (BCM-7), while digestion of A2 milk (proline at 67 position) releases nine amino acid peptide BCM-9 (Roginski 2003; Kostya *et al.*, 2004). The BCMs behave like opioids and may have ill effects on human health. The main diseases associated with consumption of A1 milk or precisely opioid BCM7 include type I diabetes mellitus, coronary heart disease arteriosclerosis, Schizophrenia, autism and sudden infant death syndrome (Elliot *et al.*, 1999; Thorsdottir *et al.*, 2000; McLachlan, 2001; Tailford *et al.*, 2003; Sun *et al.*, 2003 and Woodford, 2008). However, the association of A1milk/BCM7 is based only on the epidemiological evidences and experimental evidences to ascertain the association of A1milk or bioactive peptides with human health are scanty.

The hypothesis is that the bioactive peptides, BCM 7/9 can mimic the effects of opioids and demonstrate opioid and pharmacological activities. The opioid receptors are located in the nervous, endocrine, and immune systems as well as in the intestinal tract of the mammalian organism and can interact with their endogenous (BCM7) as well as with exogenous opioids (Teschmacher, 2003). BCMs are  $\mu$ -receptor agonists and can have functional significance (Trompette *et al.*, 2003). For the experimental evidences to establish effect of milk derived

bioactive peptides studies are being carried out using mice as model. However, to ascertain the effectiveness of these models it is essential to study the structure of opioid receptor and interaction with probable ligands (BCM7/9). Both BCM7 and BCM9 are exogenous opioid agonist and unlike “typical” opioid peptides (endogenous), the beta-casomorphins are “atypical” in the sense that N-terminal tetrapeptide of these “atypical” opioid peptides represents the minimum sequence required for full opioid activity (Brantl *et al.*, 1979). In the bovine BCM7, presence of tyrosine residue at the N terminal and a phenylalanine residue at the 3<sup>rd</sup> or 4<sup>th</sup> position forms the motif, enabling it to bind to the opioid receptor pharmacophoric residues. The proline present at the 2<sup>nd</sup> position is crucial for the formation of bioactive conformation of the peptide in order to bind to the receptors. The proline at 2<sup>nd</sup> position along with the pharmacophoric residues forms the “messenger sequence”. The remaining C terminal sequence forms the “address sequence”. It has been shown that ligand recognition requires pharmacophoric residues and aromatic ring (Filizola *et al.*, 2001). In human, opioid receptors belong to superfamily G-protein couple receptor (GPCR) which is the largest family of integral trans membrane proteins coded by the human genome (Rosenbaum *et al.*, 2009). GPCRs facilitate most of the cellular transduction pathways usually in response to hormones, neurotransmitters and environmental stimulants, and some bioactive peptides. All G-proteins (GPCR) are made of seven transmembrane (7TM) helical segment comprising of an extracellular N terminus (NH<sub>3</sub>), separated by alternating intracellular and extracellular loop regions, and an intracellular C terminus (COOH) (Rosenbaum *et al.*, 2009, Pierce *et al.*, 2002, Hanson *et al.*, 2009). Opioid receptors have structural organisation similar to receptors for epinephrine, dopamine, serotonin, and adenosine (Lagerstrom *et al.*, 2008). Among different opioid receptors, MORs are primary transmembrane receptor in the brain responsible for binding of endogenous opioid neuropeptides (endorphin) as well as exogenously administered opioid compounds (morphine) (Kieffer *et al.*, 2009, Moles *et al.*, 2004). Potent drugs such as morphine, heroin, fentanyl and methadone induce their pharmacological effects and activation of cellular pathways through this receptor (Contet *et al.*, 2004). These mu receptors hold special importance for human health aspects as many bioactive peptides generated from food act as ligands for these receptors and trigger the different cellular pathways. Recently it has been observed that biomolecules generated after digestion of bovine milk protein behave like opioid receptor ligands address opioidergic systems and in the neonates, (Janecka *et al.*, 2002). Bovine milk is an integral part of human diet and hence it is pertinent to look into the interaction of bioactive peptides generated from milk with mu opioid receptors and their probable effects on human health. For *in vitro*

studies, it is important to clone and express the mu opioid receptors, so that large quantities of proteins are available to study the interactions of receptors and milk derived bioactive peptides. However, due to the hydrophobic nature, low natural abundance and lower stability after extraction, the overexpression and purification of that protein is not very easy (Sarramegna *et al.*, 2003). The previous experiments have reported a very low expression of MORs in different expression system such as bacteria (Stanasila *et al.*, 1993, Weiss *et al.*, 2002), yeast (Andreet *et al.*, 2006, Grunewald S *et al.*, 2004, Sarramegna *et al.*, 2002), while higher expression was reported in eukaryotic host systems (Akeroun *et al.*, 2005, Hassaine *et al.*, 2006, Massotte *et al.*, 1993). In few studies, expression of human mu ( $\mu$ ), delta ( $\delta$ ) and kappa ( $\kappa$ ) opioid receptor has been reported in E.coli (Stanasila *et al.*, 1999). In the present study, efforts were made to clone and express the mu receptor in Pichia /Bacterial expression system to get the quantities of proteins sufficient for in vivo experimentation. Expression in E.coli is easier and quick as bacterial expression system are easy to scale up and escapes problems like posttranslational modifications and GPCR heterooligomerization with GPCRs of the host cells (Maggio *et al.*, 2005). However, most of the membrane protein are expressed either in inclusion bodies or in pellet form and also sometimes are toxic to the host organism leading to reduction in yields (Wagner *et al.*, 2007). Thus in the previous studies molecular cloning, expression and purification of mice MOR gene by heterologous expression in E.coli, was carried out with his-tag. That is generally considered as an efficient strategy for expression and purification in *E.coli*. In India 55% of cow milk production is contributed by exotic/crossbred cows (Livestock-animal-husbandry-statistics 2018) which are known to possess higher frequency of A1 allele of beta casein as compared to Indian native cattle breeds (Ikonen *et al.*, 1997; Kaminski *et al.*, 2006, 2006a; 2007; Olenski *et al.* 2010; Sodhi *et al.*, 2011, 2013; Mishra *et al.*, 2009.), it is need of the hour to understand the mechanism of binding of BCMs to MOR that the disease related pathways. However, till date not much information is available on the characterization of mu receptors of mice distributed across various cells and tissue types and their interaction with BCM7/9. Keeping in view the gaps of knowledge, the present study was proposed with following objectives.

- 1. To characterize mu opioid receptor (MOR) and its splice variants in brain and gut tissues of mice**
- 2. To clone MOR in Pichia / Bacterial expression system for their over expression and purification**
- 3. To undertake interaction studies of MOR with BCM7/9 by in silico approach.**

# **CHAPTER -2**

---

---

## **Review of Literature**

---

---

## REVIEW OF LITERATURE

---

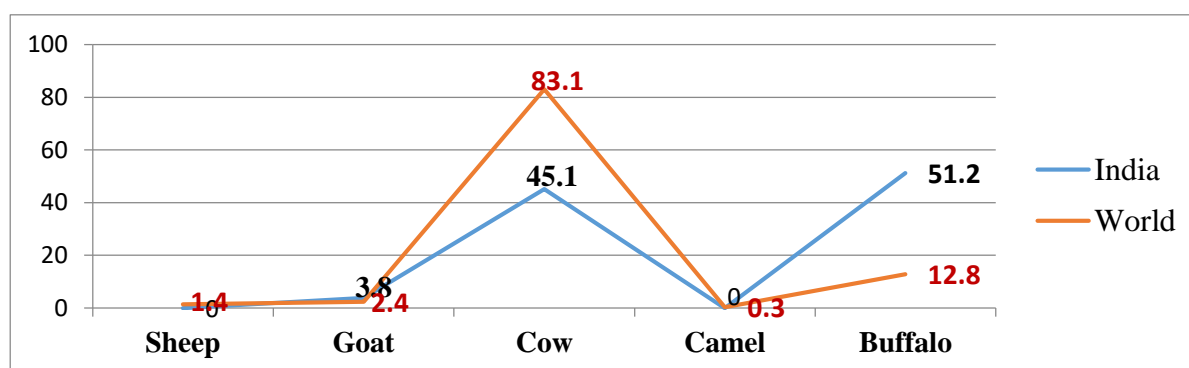
Milk is regarded as natural source of proteins, minerals and vitamins. Cow milk generally contains about 3.5 % proteins and more than 95% of these are constituted by caseins and whey proteins remaining 5% include peptones/low molecular weight peptides milk fat globule membrane proteins. Caseins, make up about 80% of the milk proteins and comprise of alpha S1 (39-46% of total caseins), alpha S2 (8-11%),  $\beta$  (25-35%), and kappa (8-15%) casein (Eigel *et al.*, 1984). Whey proteins (20%) contain two major proteins alpha lactalbumin and  $\beta$  lactoglobulin. (Marten *et al.* 1994). It is important to study single nucleotide polymorphism (SNP) located in the coding regions of genes as these variations lead to differences in quality or quantity of milk. Amongst the caseins, beta casein ( $\beta$ -casein) ranks second most abundant protein in bovine milk (40%).  $\beta$ -casein is a source of active peptides, mainly opioids (Bell *et al.* 2006; Givens *et al.* 2013; Nguyena *et al.* 2015).

### 2.1 Contribution of milk

It also contains immunoglobulins, hormones, growth factors, cytokines, nucleotides, peptides, polyamines, enzymes and other bioactive peptides. Milk and milk products are considered as functional foods, as these have a direct and significant effect on health (Marshall *et al.*, 2004). Milk and other dairy products have been recognized as important foods as early as 4000 BC as evidenced by stone drawings from the Sahara desert. It is one of the most important components of the human diet in the Western world in Asia. It is considered to be the only food that contains almost all substances known to be essential for human nutrition (Laakkonen and Pukkala *et al.*, 2008). Milk makes a significant contribution to meeting the body's needs for calcium, magnesium, selenium, the B-group vitamins (thiamin, riboflavin, niacin, vitamin B6, and folate), and provides vitamin A, vitamin C, magnesium, and zinc as well (Table 2.1) (Jelen *et al.*, 2005). Worldwide the major sources of milk are cow, buffalo, goat, sheep and camel. Across the globe, amongst different livestock species, cow milk contribution is 83.1% while in Indian it is 45.1% (Fig 2.1).

$\beta$ -casein is the second most prevalent protein in milk after  $\alpha$ -casein. The gene coding for  $\beta$ -casein (CSN2) is located on the 6th bovine chromosome among the cluster containing other casein genes *i.e.*  $\alpha$ -casein and  $\kappa$ -casein. The nutritive value of bovine caseins is not only determined by their amino acid content but also by bioactive peptides which are encrypted in an inactive form within the proteins and released during *in vivo* or *in vitro* digestion  $\beta$ -casein is the second most prevalent protein in milk after  $\alpha$ -casein. The gene coding for  $\beta$ -casein

(CSN2) is located on the 6th bovine chromosome among the cluster containing other casein genes *i.e.*  $\alpha$ -casein and  $\kappa$ -casein. The nutritive value of bovine caseins is not only determined by their amino acid content but also by bioactive peptides which are encrypted in an inactive form within the proteins and released during *in vivo* or *in vitro* digestion (Korhonen & Pihlanto, 2006; Park 2009). In the human, these bioactive peptides may act as hormone-like regulatory that may affect specific physiological functions (Kostyra et al. 2004; Silva and Malcata 2005). Bovine are a source of bioactive peptides that manifest antimicrobiological, antihypertensive, antithrombotic, immunomodulatory and mineral-binding activities (Clare and Swaisgood 2000; McLachlan, 200; Phelan et al. 2009).



Source: FAOSTAT, 2012

**Fig: 2.1** Percentage contribution of milk by different livestock species

**Table 2.1 Comparison of nutritional value of mother milk and cow milk**

Nutrients (per cup)	Mother's Milk	Cow's Milk
Calories	172	146
Protein (g)	2.5	7.9
Fat (g)	10.8	7.9
Saturated fat (g)	4.9	4.6
Monosaturated fat (g)	4.1	2.0
Polysaturated fat (g)	1.2	0.5
Carbohydrate (g)	17.0	11.0
Folate (mcg)	12	12
Vitamin C (mg)	12.3	0
Sodium (mg)	42	98
Iron (mg)	0.07	0.07
Calcium (mg)	79	276

### 2.1.1 Beta casein and bioactive peptides

Different bioactive peptides are produced after digestion of beta casein (Table 2.2) and amongst these; opioid  $\beta$ -casomorphin-7 generated from digestion of specific type of beta casein has been a focus of attention. The genetic variants in the beta casein are the reason behind generation of these diverse bioactive peptides.

**Table 2.2 Bioactive peptides of bovine milk**

Name	Sequence	Fragment	Bio-activity/Function
Beta-casomorphin 5	YPFPG	60-64	Opioid agonist
Beta-casomorphin 7	YPFPGPI	60-66	Opioidagonist, immunomodulatory, cytomodulatory, ACE inhibitory
Beta-casomorphin 9	YPFPGPIP	60-68	Opioid agonist
Beta-casomorphin 11	YPFPGPIPNSL	60-70	Opioid agonist
Immuno-peptide	PGPIP	63-68	Opioid agonist

### 2.1.2 Bioactive peptides from Different types of milk

A1/A2 type of milk differ in the type of beta casein and A1 and A2 variants of bovine  $\beta$ -casein differ at amino acid position 67 with histidine in A1 and proline in A2 milk. This polymorphism leads to key conformational changes in the secondary structure of expressed  $\beta$ -casein protein. Due to presence of histidine at amino acid 67 position, gastrointestinal proteolytic digestion (leucine aminopeptidase, elastase and carboxypeptidase Y) of A1  $\beta$ -casein (raw/processed milk) releases a 7 amino acid bioactive peptide ‘opioid’ called beta-casomorphin 7 (BCM-7) in small intestine, while proline in A2 milk at 67 position prevents the split at this particular site and generates nine amino acid peptide BCM-9 (Roginski *et al.*, 2003; Kostyra *et al.*, 2004). In hydrolyzed milk with A1 beta-casein variant, BCM-7 level is 4-fold higher than in A2 milk.

The word casomorphin suggest the opiate properties similar to morphine that includes affinity to opioid receptors, especially the MOP ( $\mu$ -opioid receptor peptide). The beta-casomorphine-7 has been identified as the “atypical” opioid peptide and exerts its influence on nervous, digestive, and immune functions via the MOR. In addition to BCM7/9, digestion of beta casein results in the release of other encrypted casomorphins along with other peptides including the non-opioid peptides (BCM5, BCM11, and Immuno-peptides). The BCM-9 is also an opioid agonist but with lesser affinity for  $\mu$  opioid receptor. The BCM-5, which is the more potent than BCM-7 and BCM-9, is primarily released from further proteolytic digestion of BCM-7 and BCM-9 by brush border peptidases.

Both in vitro and in vivo studies have suggested the absorption and transport of BCM-7 across epithelial barrier of small intestine. The opioid receptors (mu opioid receptors and delta opioid receptors) are widely distributed over the intestinal lining. Once the BCM-7 is formed in GI tract, it comes in contact with brush border of enterocytes. The brush border peptidase *i.e.* DPP IV (Dipeptidyl peptidase IV), is a cell-surface protease belonging to the

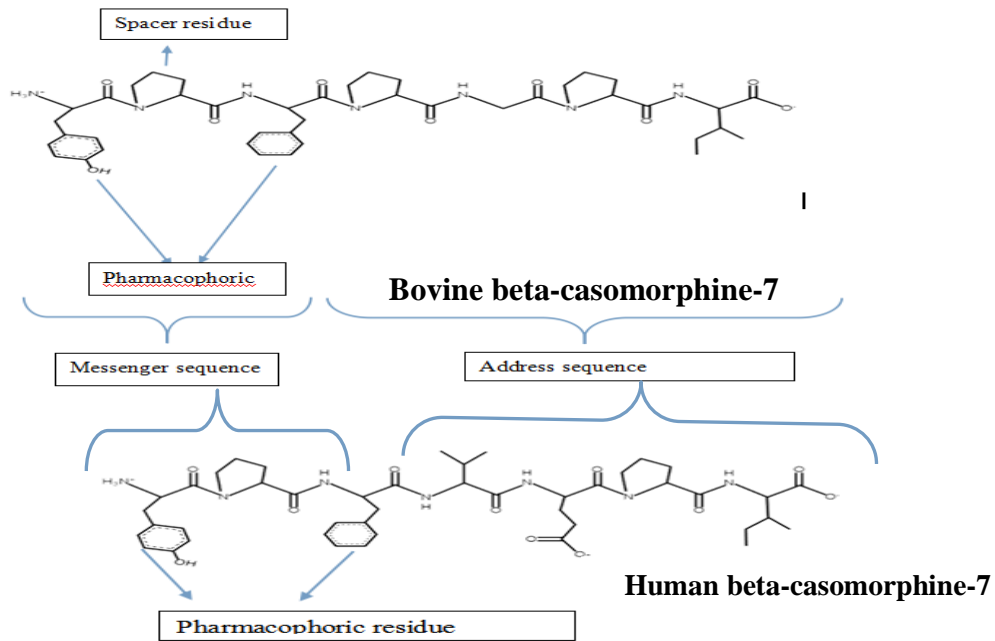


**Fig. 2.2** Structural components of BCM-7 as an opioid peptide

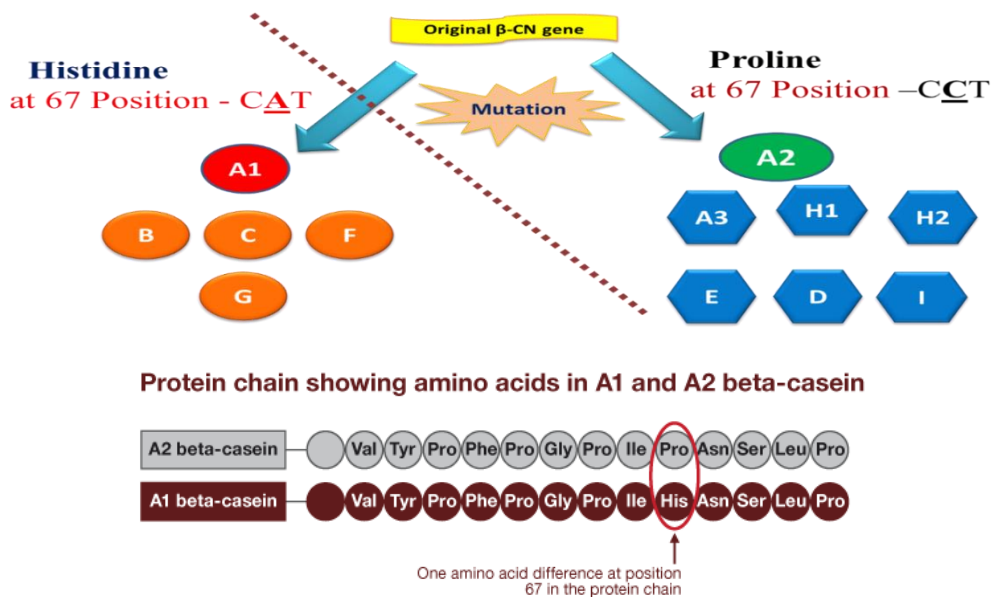


**Fig. 2.3** Different variants of beta casein gene

prolyloligopeptidase family which primarily metabolize BCM-7. Moreover, DPPIV is known to restrict activity of proinflammatory peptides. BCM7 is considered to modulate an immune response by affecting MOR and DPPIV genes expression. The weak activity of DPP IV in infants suggests the severity of symptoms arising from intact beta-casomorphine-7. In either cases *i.e* intact BCM-7 or hydrolysed to smaller peptides, they cross the epithelial barrier as evident from *in vivo* study on Caco-2 cell line. None of the *in vitro* studies have indicated the presence of BCM-7 in detectable amount in adult human's plasma; but has been detected in

infant plasma and urine. *In vivo* studies on newborn pups and calves have demonstrated immuno reactive beta-casomorphine to be transported across epithelial cell membrane. Hence, BCM-7 can pass through intestinal barrier in neonates as they have increased permeability for improved nutrient absorption. However intestinal permeability reduces as the age progresses. Also in adults with compromised digestive health or conditions such as celiac disease, stomach ulcers or autism have increased intestinal permeability which means that BCM-7 can enter the bloodstream more easily in adults as well. But in the case of BCM-9, there are no studies suggesting the trans-epithelial movement. The difficulty for beta-casomorphines to pass the epithelial membrane is may attributed to the high hydrophobicity value of the peptide.

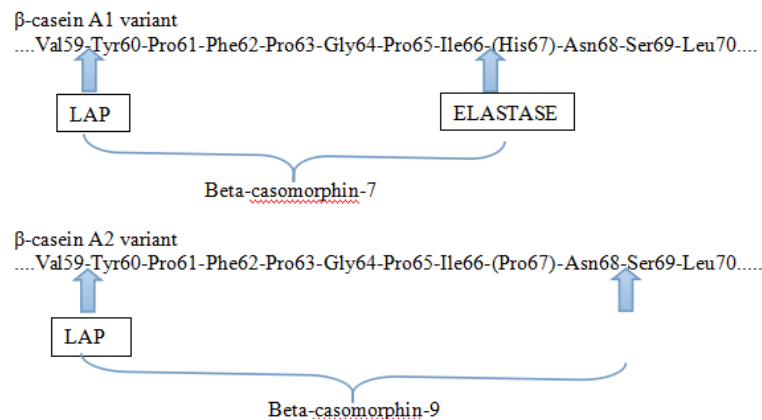


**Fig 2.4** Enzymatic digestion of A1 and A2 variants of bovine beta-casein.

### 2.1.3 Regulatory mechanism of milk derived peptides

Beta-casomorphines (beta-casomorphine-7, 9), are exogenous opioid agonist. Unlike a “typical” opioid peptide (endogenous), the beta-casomorphines are “atypical” in the sense that N-terminal tetrapeptide of most “atypical” opioid peptides represents the minimum sequence required for full opioid activity (Janecka *et al.*, 2004) . The beta-casomorphine-7 was identified as the “atypical” opioid peptide by (Brantl *et al.*, 1979). In the bovine beta-casomorphine-7 ,presence of tyrosine residue at the N terminal and a phenylalanine residue at the 3<sup>rd</sup> or 4<sup>th</sup> forms the motif enabling it’s binding to the opioid receptor, which are pharmacophoric residues. The proline present at the 2<sup>nd</sup> position is crucial for the formation of bioactive conformation of the peptide in order to bind receptor. The proline at 2<sup>nd</sup> position along with the pharmacophoric residues forms the “messenger sequence”. The remaining C terminal sequence forms the “address sequence” (Boutrou *et al.*, 2013), whereas in the case of human beta-casomorphine-7, only the 4<sup>th</sup> and 5<sup>th</sup> position is replaced by valine and glutamine instead of proline and glycine respectively. Since, there is no change in the messenger

sequence and pharmacophoric residues, the basic opioid activity and affinity for serotonin receptor remains the same as in the case of bovine casomorphine-7. The BCMs binds to opioid receptors with high affinity for  $\mu$  type opioid receptor (MOR). The MOP receptor have numerous effect on physiological processes upon activation by endogenous or exogenous opioid ligands .They have been identified on cell surfaces of various cells and tissue types in central nervous system, apart from that MOR have been characterized on cell surfaces of gastrointestinal tract , immune cells and pancreatic cells.. The receptor is a seven trans membrane spanning domain coupled to G inhibitory protein. After binding of exogenous ligand such as BCM-7, the  $G_{\beta\gamma}$  subunit dissociates from  $G_{\alpha}$  and various intracellular pathways are initiated (Fig.2.5).

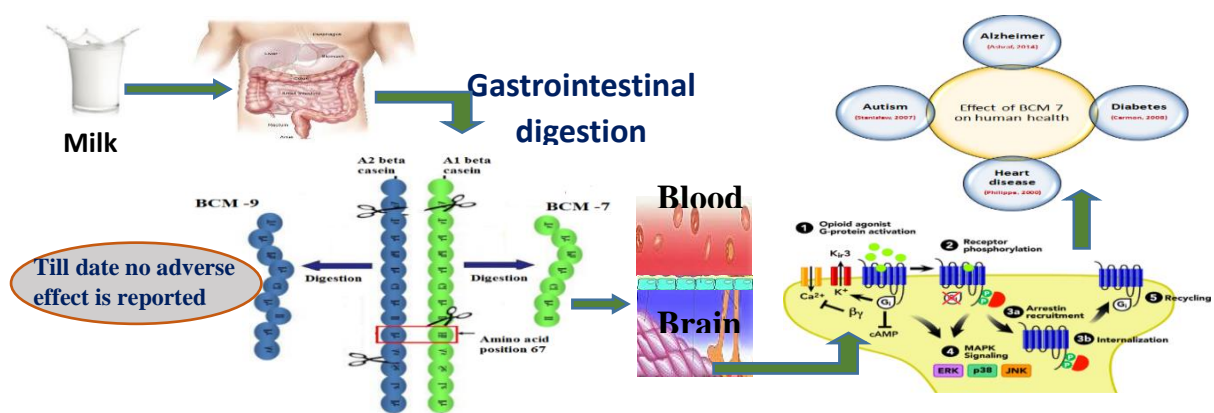


**Fig 2.5** The fate of milk consumed for beta-casomorphine-7 formation and effects exerted by beta-casomorphine-7 on various organs.

Another class of mechanism is by the virtue of non-opioid mediated effects of milk derived peptides. Among the  $\beta$ -casein derived peptides, beta-casomorphine-7 (YPFP GPI), beta-casokinin (YQQPVLGPVR), caseinophospopeptides (RELEELNVPGEIV ESLSSSEESITR and KNTMEHVSSSEESIISQETYKQEKMAINPSK) and immunopeptides (PGPIP and LLY) have immunomodulatory function. These peptides are reported to inhibit lymphocyte proliferation and inflammatory responses (Brantl *et al.*, 1979). Several studies have indicated the physiological effects of  $\beta$ -casomorphin immunoreactive material (BCMIR) in neonates (canines), but not in the adults (Janecka *et al.*, 2004, and Yamazaki *et al.*, 1993). This indicates the physiological significance of beta-casomorphines in early developmental stage of infants. In the either ways the beta-casomorphines and other bio-peptides from milk are able to elicit responses apart from the nutritional aspects. So, it is must to evaluate the effect of these peptides on different tissue types and metabolism. Another point need to clarify is, whether there are any combitorial effects of various beta-casomorphines and other immunopeptides derived from milk.

## 2.2 Pharmacologically defined $\mu$ -receptor subtypes

It was suggested that morphine like ligands bind with higher affinity to  $\mu$ 1 receptors (Ling GS *et al.*, 1985, Andoh T *et al.*, 2008). Proposed distribution, pharmacology and function of putative receptor subtypes of the MOP (mu-opioid receptor peptide), DOP (delta opioid receptor peptide), and KOP (kappa opioid receptor), receptors is given in (Table 2.3).

**Table 2.3 Pharmacologically defined  $\mu$ -receptor subtypes**

Pharmacological subtypes	Distribution	Possible discriminatory ligands	Other relevant ligands	Function/effect
$\mu$ 1	Brain, spinal cord, periphery	Naloxonazine (antagonist)	Morphine (agonist), TRIMU-5 (antagonist), $\beta$ -FNA (antagonist), Dihydromorphine (agonist), Naloxone (antagonist), Nalorphine (agonist) Codeine (agonist), Oxycodone ( $\downarrow$ agonist)	Analgesia
$\mu$ 2	Brain, spinal cord, periphery	TRIMU-5 (agonist), M6G (agonist)	Morphine ( $\downarrow$ agonist)*, naloxone ( $\downarrow$ antagonist)*, Dihydromorphine ( $\downarrow$ agonist)*, $\beta$ -FNA (antagonist), M6G (agonist), heroin (agonist),	Analgesia, GI transit, respiratory depression, itching
$\mu$ 3	Immune cells, amygdala, peripheral neural,	(opioid peptide insensitivity)	Morphine ( $\downarrow$ agonist)*, naloxone ( $\downarrow$ antagonist)*, dihydromorphine ( $\downarrow$ agonist)*, $\beta$ -FNA (antagonist),	Various including NO release
$\delta$ 1	Brain, periphery	DPDPE (agonist), BNTX (antagonist), DALCE (antagonist)	Enkephalin (agonist), deltorphin-D (agonist), naltrexone (antagonist)	Analgesia, cardioprotection
$\delta$ 2	Brain and spinal	Deltorphin-II (agonist), DSLET (agonist) 5-NTII (antagonist), Naltriben (antagonist)	Enkephalin (agonist), deltorphin-D (agonist), naltrexone (antagonist), deltorphin-II (agonist)	Analgesia, cardioprotection, thermoregulation
$\kappa$ 1a	Brain (nucleus accumbens, neocortex, cerebellum)	Dynorphin A (agonist), U50,488H (agonist)	nor-BNI (antagonist), U69,593 (agonist),	Analgesia, feeding
$\kappa$ 1b		Dynorphin B (agonist), $\alpha$ -neoendorphin (agonist)		
$\kappa$ 2a	Brain (hippocampus, thalamus, brainstem)		nor-BNI ( $\downarrow$ antagonist)*, bremazocine (agonist)	Analgesia, diuresis, neuroendocrine
$\kappa$ 2b		Leu-enkephalin (antagonist), oxycodone (agonist)		
$\kappa$ 3#	Brain	NalBzOH	Nalorphine (agonist), nor-BNI ( $\downarrow$ antagonist)*	Spinal analgesia, peripheral effects

**Abbreviations :** Opioid receptor: Mu( $\mu$ 1),delta ( $\delta$ 1), kappa( $\kappa$ 1a), mu-opioid receptor antagonist, L-tyrosyl-N-[(3-methylbutyl)amino]acetyl]-D-alaninamide (TRIMU-5), inhibitory effect ( $\downarrow$ agonist)\* and ( $\downarrow$  antagonist)\*, $\beta$ -FNA(beta-Funaltrexamine antagonist of mu-opioid receptor).

## 2.3 Molecular mechanism of opioid receptor dependent signaling and behavior

Opioid receptors are expressed in different regions of brain including medulla, locus coeruleus, and periaqueductal gray area. They are also expressed in limbic, midbrain, and cortical structures. The activation of opioid receptors at these locations directly inhibits neurons, which in turn inhibits spinal cord signal transmissions (McNicol *et al.*, 2003). All four opioid receptors (MOP, DOP, KOP and ORL-1) are seven-transmembrane spanning proteins that couple to inhibitory G proteins. After being activated by an agonist such as the endogenous opioid peptide endorphin, or exogenous agonists, such as betacasomorphins, morphine and fentanyl; the  $G\alpha$  and  $G\beta\gamma$  subunits dissociate (Fig 2.6) from one another and subsequently act on various intracellular pathways. (Childers *et al.*, 1979).

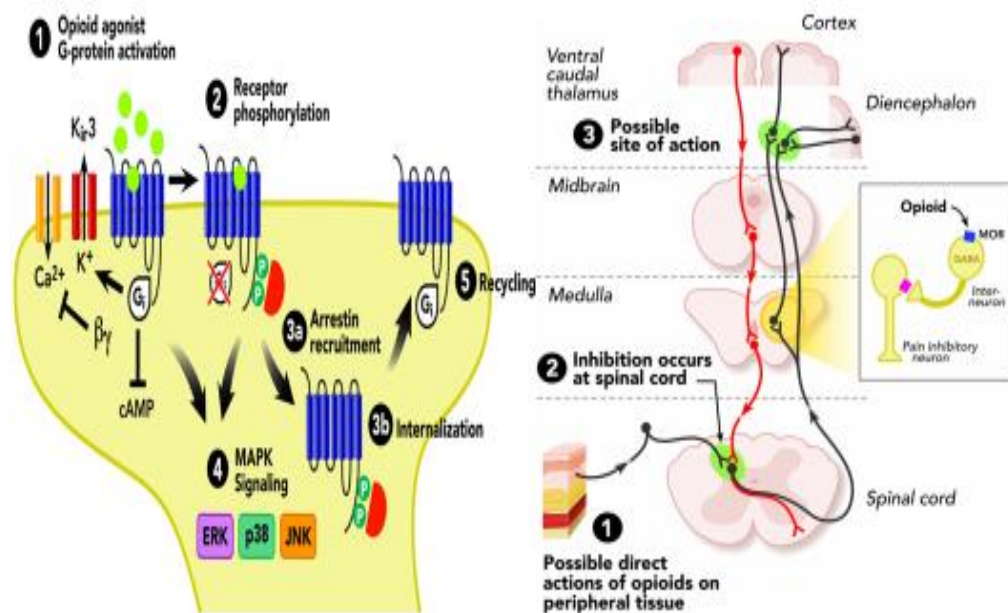


**Fig. 2.6** Molecular mechanism of opioid receptor dependent signaling

### 2.3.1 Molecular mechanisms of opioid tolerance

To date, the molecular and cellular mechanisms mediating the development of tolerance to morphine remain a matter of controversy. Traditionally, it was thought that the down regulation of opioid receptors after chronic agonist exposure induces tolerance, as reported in *in vitro* studies. (Dang *et al.*, 2012) However, recent *in vivo* studies show that down-regulation does not occur consistently with each and every agonist and may not completely explain tolerance. In light of these findings, it has been suggested that MOR proteins are in fact not down regulated but instead may be desensitized and uncoupled from downstream signalling pathways (Hasani *et al.*, 2011). It has been observed that after chronic morphine

exposure, levels of the second messenger cAMP are increased. However, this elevation in cAMP may not be attributable to opioid receptor uncoupling from inhibitory G proteins but instead could reflect cellular adaptive changes, including the up-regulation of adenylyl cyclase, protein kinase A, and cAMP response element-binding protein. (Hasani *et al.*, 2011) It is this ineffective regulation of cAMP by morphine that some believe induces tolerance. It has also been proposed that the regulation of opioid receptors by endocytosis reduces the development of tolerance and therefore serves a protective role. (Hasani *et al.*, 2011) After endocytosis, the cellular response is desensitized to the agonist, but the receptors can be recycled to the cell surface in an active state, resensitizing the receptor to the agonist. Morphine-activated opioid receptors signal for long periods of time, thereby enhancing the production of cAMP, which is thought to result in tolerance. *In vivo* studies have shown that facilitation of MOR endocytosis in response to morphine prevents the development of morphine tolerance. (Hasani *et al.*, 2011) In addition, it has been shown *in vivo* that the lack of arrestin 2 prevents the desensitization of MOR after chronic morphine treatment, and these mice also failed to develop ant nociceptive tolerance (Hasani *et al.*, 2011).

Present studies have identified how ligand-directed responses, more commonly known as biased agonism, are crucial in understanding the complexity of opioid-induced tolerance. The work of Bohn and colleagues showed how arrestin 1 and arrestin 2 differentially mediate the regulation of MOR. arrestins are required for internalization, but only arrestin 2 can rescue morphine-induced MOR internalization, whereas both arrestin 1 and arrestin 2 can rescue [d-Ala<sup>2</sup>, N-Me-Phe<sup>4</sup>, Gly-<sup>o</sup>15] enkephalin (DAMGO)-induced MOR internalization. These findings suggest that MOR regulation is dependent on the agonist and may be critical in understanding the mechanism involved in the development of tolerance.

### **2.3.2 Opioid receptors and arrestin recruitment**

Phosphorylation by GRK-2 or -3 of and opioid receptors leads to arrestin 2 or 3 recruitment. Arrestin molecules are key proteins that bind phosphorylated GPCRs to regulate their desensitization, sequestration, and sorting and ultimately assist in determining receptor fate. Opioid receptors are regulated by arrestin 2 and arrestin 3 binding (also called arrestin 1 and arrestin 2, respectively), and this interaction depends on the model system and agonist treatment procedure. Mice lacking arrestin 3 have been shown to have a reduced tolerance to opioids such as morphine, suggesting that MOR regulation requires arrestin (Walwyn *et al.*, 2010). With the use of surface plasmon resonance methods, glutathione s-transferase pull-down assays, and classic immune precipitation methods, the C-terminal tails of DOR, MOR,

KOR have been shown to be crucial for arrestin 2 or 3 binding. C-terminal carboxyl mutant opioid receptors have been studied widely, and these serine mutant receptors show decreased agonist-induced receptor internalization and arrestin recruitment. Dominant positive arrestins (such as Arrestin- 2-R169E or Arrestin-3-R170E) that bind the non-phosphorylated receptors can rescue internalization of serine mutated MOR/DOR/KOR, (Bruchas *et al.*, 2006) further implicating arrestin dependence in opioid-receptor trafficking.

#### **2.4 Epigenetic effect of casein derived opioid peptide**

Casein-free, gluten-free diets have been reported to mitigate some of the inflammatory gastrointestinal and behavioral traits associated with autism, but the mechanism for this palliative effect has not been elucidated. We recently showed that the opioid peptide beta-casomorphin-7, derived from bovine (bBCM7) milk, decreases cysteine uptake, lowers levels of the antioxidant glutathione (GSH) and decreases the methyl donor S-adenosylmethionine (SAM) in both Caco-2 human GI epithelial cells and SH-SY5Y human neuroblastoma cells. While human breast milk can also release a similar peptide (hBCM-7), the bBCM7 and hBCM-7 vary greatly in potency; as the bBCM-7 is highly potent and similar to morphine in its effects (Fig. 2.7). Since SAM is required for DNA methylation, we wanted to further investigate the epigenetic effects of these food-derived opioid peptides. In the current study the main objective was to characterize functional pathways and key genes responding to DNA methylation effects of food-derived opioid peptides. Casein and gluten-derived opioid peptides decrease excitatory amino acid transporter 3 (EAAT3)-mediated cysteine uptake by human GI epithelial cells and human neuronal cells in a dose dependent manner, resulting in redox and epigenetic consequences via their capacity for  $\mu$ -OR activation (Trivedi *et al.*, 2014). Epigenetic regulation of gene expression is of particular importance during early development when changes in DNA or histone methylation status can exert lifelong and even trans generational effects (Bird *et al.*, 2007). Thus milk derived opioid peptides may exert an important epigenetic influence with extended consequences. It is noteworthy to mention that the human form of BCM-7 was far less potent as compared to the bovine form of BCM-7 in cysteine pathway inhibition and histone methylation.

Inhibition of cysteine uptake, inducing oxidative stress as well as decreased SAM levels. With regard to neural development, epigenetic regulation can influence neural stem cell differentiation as well as neuronal plasticity and/or neuronal maturation, which are particularly prominent during fetal and early postnatal development (LaSalle *et al.*, 2007).

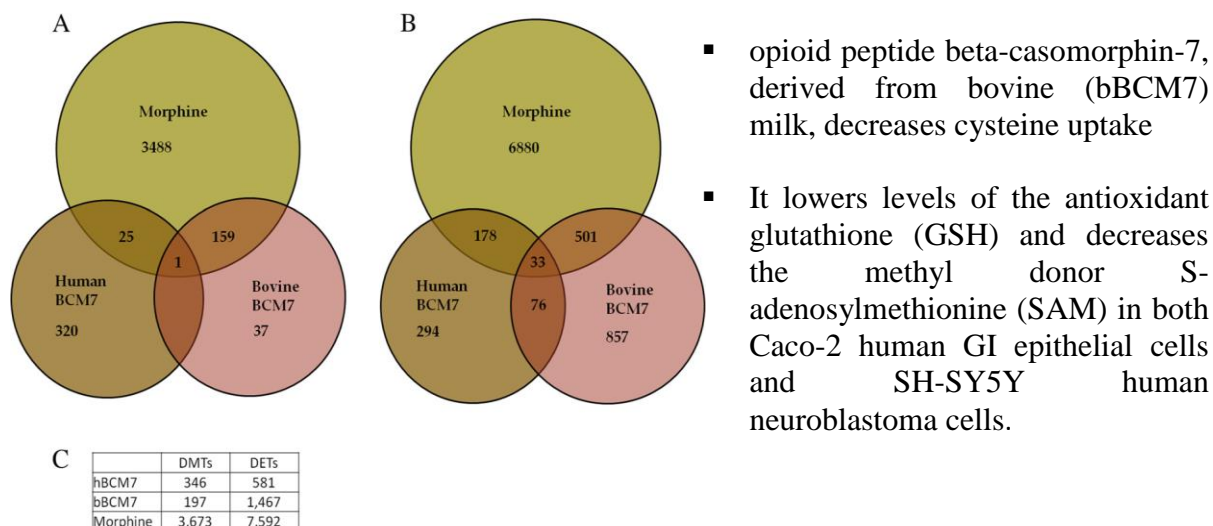


**Fig.2.7** The effects bBCM7, hBCM-7 and morphine vary greatly in DNA methylation

We previously highlighted the critical role of prenatal and postnatal epigenetic programming in the redox-based linkage between GI, brain, and immune systems, which could potentially contribute to the etiology of autism and other disorders (Waly *et al.*, 2012). These redox-based metabolic and epigenetic changes have not only been identified in early developmental and neurological diseases (Morgan *et al.*, 2006), but also characterized in diseases arising across the lifespan, including immunological ((Waly *et al.*, 2012)) and neurodegenerative disorders (Flight *et al.*, 2007). Opioids and their receptors have an important role in analgesia and alcohol and substance use disorders (ASUD). We have identified several naturally occurring amino acid changing variants of the human mu-opioid receptor (MOR), and assessed the functional consequences of these previously undescribed variants in stably expressing cell lines. Several of these variants had altered trafficking and signaling properties. We found that an L85I variant showed significant internalization in response to morphine, in contrast to the WT MOR, which did not internalize in response to morphine. Also, when L85I and WT receptor were expressed, WT MOR internalized with the L85I MOR, suggesting that, in the heterozygous condition, the L85I phenotype would be dominant. This finding is potentially important, because receptor internalization has been associated with development of tolerance to opiate analgesics. In contrast, an R181C variant abolished both signaling and internalization in response to saturating doses of the hydrolysis-resistant enkephalin [D-Ala2, N-MePhe4, Gly5-ol] enkephalin (DAMGO). Co-expression of the R181C and WT receptor led to independent trafficking of the 2 receptors. S42T and C192F variants showed a rightward shift in potency of both morphine and DAMGO, whereas the S147C variant displayed a subtle leftward shift in morphine potency. These data suggest that these and other such variants may have clinical relevance to opioid responsiveness to

both endogenous ligands and exogenous drugs, and could influence a broad range of phenotypes, including ASUD, pain responses, and the development of tolerance to morphine.

## 2.5 Structure and function of MOR agonist

Structurally, these beta casomorphins behave like opioids like morphine. Morphine is primarily an agonist ligand for the  $\mu$ -opioid receptor (Fig. 2.8). Its affinities for  $\delta$  and  $\kappa$  receptors are sufficiently low but its affinity for  $\mu$  –opioid receptor is very high that it is used as a selective  $\mu$ -receptor ligand in pharmacological studies (Takemori *et al.*, 1987). Betacasomorphine are bioactive compound have ability to elicit downstream signaling as like morphine. In betacasomorphine aromatic amino acid provides a pharmecophoric binding residue. The crystal structure of some bioactive peptides including bovine rhodopsin (PDB ID: 1u19), squid rhodopsin (PDB ID: 2z73),  $\beta$ 1- adrenergic receptor (PDB ID: 2vt4), and  $\beta$ 2- adrenergic receptor (PDB ID: 2rhi), and A2A adenosine receptor (PDB ID: 3eml).All the crystal structure of bioactive peptide generally belong to the superfamily of G-protein couple receptors (GPCRs). The quality of the initial models was evaluated using Molprobit (Fig. 2.9), which evaluates the accuracy of macromolecular structures through analysis of contacts and evaluation of dihedral angle combinations (Davis *et al.*, 2007).

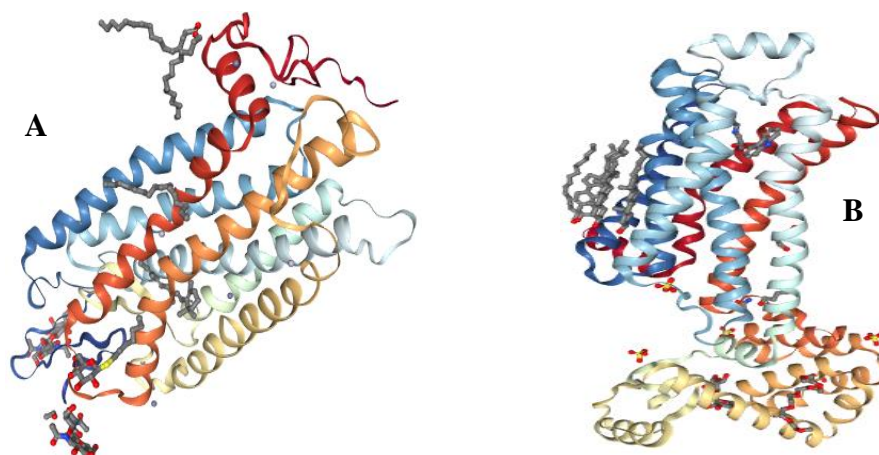


**Fig.2.8** Crystal structure of bioactive peptide. [A] Bovine rhodopsin (PDB ID: 1u19), [B]  $\beta$ 2- adrenergic receptor

## 2.6 Molecular docking

Docking is a very versatile method which predicts the preferred orientation of one molecule with respect to other in a stable complex. Binding affinity and interacting residue strength of the complex can be known from docking. The relations between biological entities like proteins, nucleic acids, carbohydrates and lipids play a key role in signal transduction

process. The relative conformational change of protein and ligands molecules can affect the strength of the signal transduction. Hence molecular docking is used to find both the binding affinity strength and type of the signal produced. Docking plays an important role in drug designing as well drug delivery. It is used to predict the binding orientation, affinity and activity of drugs with respect to their protein targets. The major function of molecular docking in pharmacological study of many drugs. Present days, opioids are generally used to control the pain. There are three subtypes of opioid receptors – mu, delta and kappa. The mu-opioid receptor sare high binding affinity to target protein (BCMs) .Naloxone is a competitive antagonist to mu opioid receptor. Beta-casomorphins especially BCM-7 has highest affinity for MORs opioid receptor and least affinity for kappa 1 opioid receptor. The order of its affinity for opioid receptors is: mu 1 > mu 2 > delta > kappa 1. Docking studies were performed on mice mu-opioid receptor as well human opioid receptor.

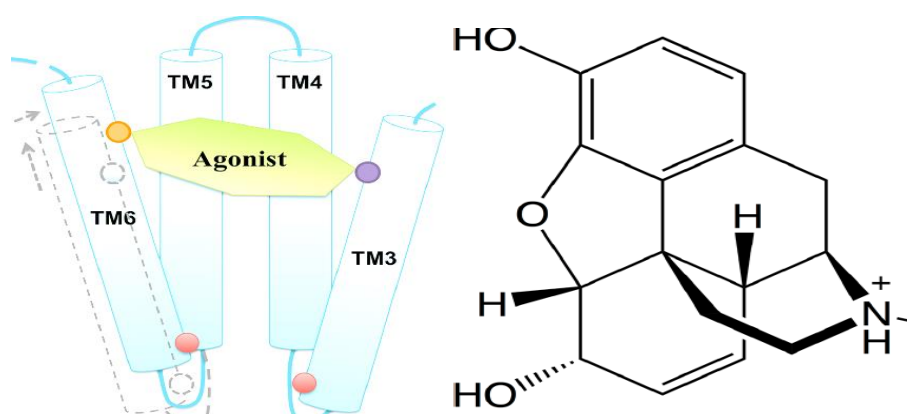


**Fig. 2.9** Molecular structure of morphine (agonist)

Molecular docking of morphine to the model structure and comparing the identified binding-pocket residues with prior mutagenesis and binding studies. To evaluate the structural integrity of the crystal model structure, we performed all-atom molecular dynamics simulation of the model structure in GROMACS (Lindahl *et al.*, 2001) using a modified Gromos96 force field for the protein, lipid, and morphine (Chandrasekhar *et al.*, 2003; Oostenbrink *et al.*, 2005; Schuttelkopf and van Aalten, *et al.*, 2004). The GROMACS software most widely used in study of interaction and energy minimization of crystal model structure. The *in silico* structural model to identify high-affinity ligands using structure-based drug screening methods, it is crucial to accurately model the ligand binding pocket of the receptor. The molecular dynamics simulations of MOR1 receptor with morphine, a widely clinically used opioid agonist.

### 2.6.1 MORs binding and interaction study

Opioid receptors are belong to the large family of 7-transmembrane G protein-coupled receptors and have high sequence homology. Opium is one of the world's oldest drugs, and its derivatives morphine and codeine are among the most used to relieve severe pain. These prototypical opioids produce analgesia as by binding to and activating the G-protein-coupled receptor associated  $\mu$ -opioid receptor ( $\mu$ OR) in the central nervous system. Here we describe the crystal structure of the  $\mu$ OR in complex with an irreversible morphine antagonist. Compared to the binding pocket observed the binding affinity of MOR with morphine agonist and antagonist opioids. These high-resolution insights into opioid receptor structure will enable the application of structure-based approaches to develop better drugs for the management of pain and addiction. There are three major opioid receptors for morphine and related compounds: the  $\mu$ ,  $\delta$  and  $\kappa$  opioid receptors. Out of these, the  $\mu$ -opioid receptor (MOR) is the main site of morphine binding in the brain (Pasternak *et al.*, 2001; Wood and Iyengar, 1988).

The MOR is responsible for morphine-mediated analgesia (spinal and supraspinal), hypothermia, respiratory depression, intestinal motility changes, tolerance and withdrawal (Loh *et al.*, 1998; Matthes *et al.*, 1996; Schuller *et al.*, 1999; Sora *et al.*, 1997; Tian *et al.*, 1997). Most of the MOR splice variants are originated at the downstream of Oprm1 promoter region (Pan *et al.* 2001) recent study reported 8 splice variants originating at the upstream promoter. Three of these new variants (MOR-1H, MOR-1I, MOR-1J) encode the MOR-1 isoform in addition to novel peptides encoded by upstream open reading frames (Pan *et al.*, 2001). The transcript variants of MOR are capable of strongly binding morphine in vitro and are expressed throughout the brain as well as central nervous system (Abbadie *et al.*, 2000; Pan *et al.*, 1999, 2000, 2005). Opioid peptides affect a number of physiological functions including hormone secretion, neurotransmitter release, feeding, gastrointestinal motility, and respiratory activity (Pasternak, 1988). Opioid are also useful in controlling the extensive physiological, behavioral, and pain. MOR display the characteristic binding affinities for various selective ligands (Fig. 2.10). The opioid receptors (MOR) that bind the enkephalin peptides are expressed most predominantly in the basal ganglia, striatum, and cerebral cortex (Mansour *et al.*, 1988; Wood *et al.*, 1988). The major class of opioid binding sites is represented by the  $\mu$  opioid receptor. It functions as the physiological target of such potent exogenous opioid such as morphine and fentanyl, as well as the endogenous opioid peptides  $\beta$ -endorphin, enkephalins, and dynorphins. The  $\mu$  opioid receptor are also effectively

implicated in analgesia (Wood and Iyengar, 1988). Opioid drugs with high abuse liability such as morphine and fentanyl, all bind selectively to the  $\mu$  opioid receptor.

Characterization and interactions of MORs may help to understand the downstream signalling pathway and cause the selective activation of particular signalling and regulatory pathways.

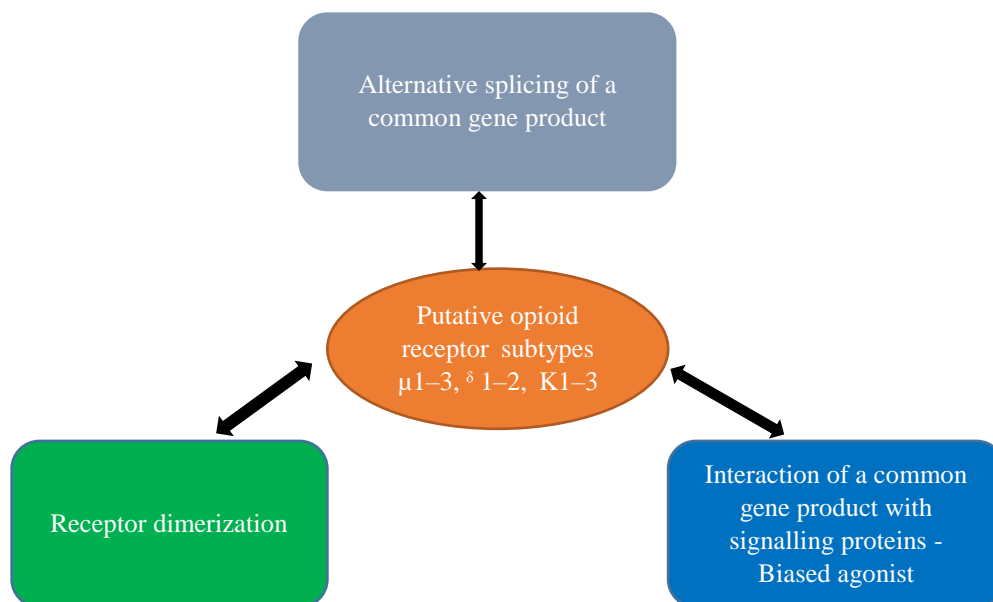


**Fig. 2.10** Schematics of  $\mu$ -opioid receptor interaction

### **2.7 Expression of a Membrane-inserted OPRM in bacterial system (*E.coli*)**

Mu opioid receptor belongs to the super family of G protein-coupled receptors (GPCRs). GPCR represents the largest gene family of mammalian genome which account for up to 50% of all drug targets including cardiovascular and gastrointestinal diseases, central nervous system and immune disorders, cancer and pain (Fredriksson *et al.*, 2003). On present days, there are four major different types of Opioid receptors including mu, kappa, delta, OPR-1 (Singh *et.,al* 1997). Out of four opioid receptors mu opioid receptor is activated by endogenous opioid peptides such as Beta endorphins and exogenous alkaloid such as morphine.

The expression of membrane protein various *E.coli* strains (RP, RIL, C41, and C43) were used to screen for expression of the target protein. At high temperature (37°C), the N-terminal his-tagged OPRM was found to be produced both in inclusion bodies and in membrane-inserted form.it was observed that only C41 cells show a low expression level of the target protein. For other cells OPRM was increased at higher expression levels in

inclusion bodies. In the case of expression in RIL cells 30–50% of OPRM was degraded into a large N-terminal fragment (ca. 18 k Da). It was observed that induction with IPTG at 37°C severe foam formation with loss of cell density. Thus the expression of OPRM was found to be toxic. Very slow growth of culture was observed for induction at 18°C. These results indicated a proper harvesting time and induction period should be optimized at 18°C. The proper induction time of target protein less than 10hrs maximized the cell yield of culture (final OD at 600nm= 225, cell pallet >8g/l in all case. The expression of OPRM was optimized with IPTG concentration (0.2mM-1mM). At 0.4mM IPTG concentration was found to effectively induce the expression of OPRM while increasing the IPTG concentration led to degradation of the protein or to the formation of inclusion bodies. OPRM was obtained in the membrane fraction. The optimal expression level of OPRM was determined to be 0.3–0.5 mg/litre of culture by complete solubilisation of the protein in the membrane fraction under denaturing conditions with 6 M urea and 0.8% laurylsarcocine. Verities of detergents were used for solubilisation and extraction of OPRM from E.coli membrane and as controls: Zwitterion detergents (1% (w/v) LDAO, 1% (w/v) Fos-12), non-ionic detergents (1% (w/v) DDM, 1% (w/v) Cy6) and anionic detergent (1% (w/v) SDS, 0.8% (w/v) laurylsarcocine with/without 6 M urea). Adding Urea with detergent showed very good solubilisation efficiency. Extraction of OPRM with SDS, laurylsarcosine alone, or 6 M urea with 0.8% (w/v) laurylsarcosine proved to be most efficient.

### **2.7.1 Isolation of OPRM**

Isolation of membrane protein OPRM was carried out with several purification processes such as affinity chromatography, ionic exchange chromatography and size exclusion chromatography. Ionic Exchange chromatography was not as good as other chromatography because it was given limited value in purification of the membrane protein especially when solubilised with an ionic or zwitterionic detergent. OPRM extracted from membrane was isolated through metal chelate affinity chromatography (Ni-NTA) two times, followed by size exclusion (Superdex 200) chromatography. In the first isolation step the majority of OPRM can be captured by Ni-NTA. A second Ni-NTA chromatography of the diluted sample improves the purity to ca. 85%. N-terminal his-tag, OPRM protein was found at position of 38 kDa on 12% SDS-PAGE, though the expected Mw is 46kDa. Most of the GPCRs proteins were found to migrate anomalously smaller than expected on SDS-PAGE due to their hydrophobicity and compact structure (Grishammer *et al.*, 1995). Natively purified OPRM receptor was categorized from bacterial membrane by circular dichroism.

The secondary structure of purified target protein after gel filtration was determined by CD data from the far-UV spectrum in the 200-250nm range by K2D convolution. The purified folded protein was characterized to have a secondary structure including 46±5% alpha-helix. The binding of OPRM to natural ligand endomorphine-1 is achieved by Plasmon surface resonance. Initially about 8000Ru of OPRM (46kDa) were bound to the Ni-NTA chip. By increasing the concentration of agonist EM-1 to the immobilized OPRM increase the binding signal which confirms the agonist binding capacity of OPRM. After induction at 37°C for 4h large amounts of OPRM were overproduced in RIL cells. The specific degradation of OPRM 18 kDa of N-terminal was present when expressed with in RP and RIL cells at 37°C. RPIL and RP cells overexpressed after cleaved by protease (18 kDa) where as C41 and C43 cells direct the protein only into Inclusion bodies. The effectiveness of two *E.coli* strain C41 (DE3) and C43 (DE3) in over express in toxic and membrane protein (Miroux *et al.*, 1996). Compare with other *E.coli* strain Rp and RPIL, BL21 (D3), C41 and C43 strain were observed to yield more membrane mass per cell mass. Over expression C41 (DE3) and C43 (DE3) was found to be superior for over expressing toxic and membrane protein. The over expression of OPRM was largely tolerated by C43 with the condition of 0.4 mM IPTG at 18°C for 8-12 hrs. This finding is potentially important, because mu opioid receptor has been associated with development of tolerance to opiate analgesics.

# **CHAPTER –3**

---

---

## **Materials & Methods**

---

---

## MATERIALS AND METHODS

---

To sequence characterize the  $\mu$ -opioid receptor from the mice, the cDNA was amplified from brain and gut tissue samples of C57/bl6 mice. The variant which showed maximum expression was cloned and purified. The information on different transcript variants of  $\mu$ -opioid receptors was also collected from literature. In silico analysis was carried out to understand the structural-functional properties of these receptors and their interaction with different ligands.

### **3.1 To characterize mu opioid receptor (MOR) and its spliced variants in brain and gut tissues of mice**

#### **3.1.1. Chemicals, Enzymes, Solutions, Buffers and Equipments**

All chemicals/ reagents used in the present study were of molecular biology grade. Details of the chemicals, restriction enzymes, buffers and major equipment's used in the present study are listed in Appendix I.

#### **3.1.2 RNA isolation from brain and gut**

I. Tissue samples from brain and gut were collected in Trizol after dissection of mice and RNA was isolated using the following protocol

- The trizolated frozen mice tissue (Brain and gut) were thawed and homogenized w (Cole Parmer, USA).
- Added 1 $\mu$ l of linear acrylamide and vortexedthesample, then centrifugedat 4°Cat 10,000 rpm for 10 min. The acrylamide was added at the rate of 1 $\mu$ l / ml Trizol
- The upperphase was transferred to a fresh 1.5ml microcentifuge tube. Added 200  $\mu$ l chloroform/ml Trizol, mixedvigorously for 30 seconds. The contents were incubated at room temp for 2-3 min.Centrifuged again at 10,000 rpm for 10 min. at 4°C.
- The top layer (containing RNA) was gently aspirated without disturbing the interphase, and transferred to a fresh 1.5ml microcentifuge tube.
- To the aqueous phase, added 600 $\mu$ l acid: phenol: chloroform (5:1) for denaturationand thereafter centrifuged at 13,000 rpm for 15 min under cold conditions (4°C).
- Separated the upper phase and collected in a fresh tube. Added500 $\mu$ l of isopropanol and keptat room temperaturefor 30 minutes. Centrifuged the mixture at 15,000 rpm for 15 min at 4°C.

- Discarded the supernatant, added 1ml of 75% ethanol to the pellet to wash RNA and thereafter vortexed for 1 min. The contents were centrifuged at 15,000g for 5 min at 4°C. Discarded the supernatant and pellet was stored.
- The RNA pellet was kept at 42°C for removal of ethanol for 10-15 min and dissolved in 40-60 µl RNA storage solution (1mM Na-citrate). Measured O.D of RNA using Nanovue plus for quantification and use in further studies.

## II. Purification of RNA

RNeasy Mini Kit column (Qiagen, Germany) was used to remove the traces of genomic DNA followed by on column digestion with RNase free DNase enzyme. The purification of RNA was performed using manufacturer protocol with minor modifications:

- Each sample was adjusted to a volume of 100µl with RNase-free water. Added 350µl of buffer RLT and mixed well. Further, added 250µl ethanol (96-100%) to the diluted RNA, and mixed well by pipetting carefully.
- To RNeasy spin column, 350µl buffer RW1 was added and centrifuged for 15 sec at 10,200 rpm to wash the spin column membrane. The flow-through was discarded.
- Again, 350µl of buffer RW1 was added to the RNeasy spin column and centrifuged for 15sec at 10,200rpm. The flow-through was discarded.
- The samples were then transferred (700µl) to an RNeasy Mini spin column and centrifuged for 15 sec at 10,200 rpm.
- 500µl RPE buffer was added to the RNeasy spin column to wash column membrane and then centrifuged for 15sec at 10,200 rpm. Repeat the washing step once again.
- Elution of RNA: placed spin column membrane in fresh 1.5ml collection tube and added 30µl of RNase free water directly to the column. Centrifuged the contents for 1 min at 10,200 rpm, collected the elute and repeated the same step twice to ensure maximum collection of pure RNA.

## III. Evaluation of RNA quality/integrity

- Measured the concentration and purity of total RNA using a Nanovue plus (GE, Healthcare).
- **Precaution:** All reagents were prepared in 0.1-0.2% DEPC treated sterile water and RNase free glassware. Before the RNA isolation, due care was taken to clean the hands with RNA ZAP.

#### IV. Agarose gel electrophoresis of RNA sample

Integrity of all the extracted RNA was checked on denaturing Agarose gel the extracted RNA was stored at  $-80^{\circ}\text{C}$  till further use.

- The 1.5% Agarose gel was prepared in 1X TAE buffer (pH 8.0), using molecular biology grade Agarose (Sigma Chem. Co., USA) and stained with EtBr.
- The RNA samples mixed with tracking dye and were loaded and Electrophoresis was carried out at 80 V for half an hour.

#### 3.1.3 cDNA Synthesis

From the purified RNA, cDNA was synthesized using RevertAid<sup>TM</sup>FirstStrand cDNA Synthesis Kit (Fermentas, USA). To prepare the cDNA, 2 $\mu\text{l}$  of purified RNA was thawed on ice and 2.0  $\mu\text{l}$  (~200ng) of it was taken in nuclease free PCR tube. Reaction was set using 20  $\mu\text{l}$  master mix1 (prepared using the reagents as mentioned in Table 3.1) for each sample.. After mixing well by pipetting, the samples were incubated at  $65^{\circ}\text{C}$  for 5 min and snap chilled on ice for 5 min.

**Table 3.1 Composition of master mix1 for cDNA synthesis**

S. No.	Constituents	Volume ( $\mu\text{l}$ )
1.	Olio dT <sub>12-18</sub> primer(100 $\mu\text{M}$ )	1.0
2.	Random primers(100 $\mu\text{M}$ )	1.0
3.	dNTPs(10 mM)	1.0
4.	Nuclease free water	17.0
<b>Total volume</b>		<b>20.0</b>

After snap chilling, 18  $\mu\text{L}$  of master mix 2 composed of reagents mentioned in Table 3.2 was added to the each tube. A reaction was performed in an Eppendorf Gradient cyler using the program as  $25^{\circ}\text{C}$  for 5 min,  $50^{\circ}\text{C}$  for 60 min and  $70^{\circ}\text{C}$  for 15 min for cDNA synthesis. Synthesised cDNA was then diluted 1:4 (v:v) with DNase/ RNase free water and a semi-quantitative PCR was performed with  $\beta$ -actin gene in all samples with six standards to check the cDNA integrity.

**Table 3.2: Composition of reagents for preparation of Mix1I for cDNA synthesis**

S. No.	Constituents	Volume ( $\mu\text{l}$ )
1.	5X Buffer	8
2.	RiboLockTMRNase Inhibitor (20 u/ $\mu\text{l}$ )	0.5
3.	M-MuLV Reverse Transcriptase (200u/ $\mu\text{l}$ )	1.0
4.	Nuclease free water	8.5
<b>Total volume</b>		<b>18.0</b>

### 3.1.4 PCR amplification of MOR

For amplification of MORs primers were designed using Primer 5.0 software. Care was taken to design the primers which could amplify maximum number of MOR transcripts. Details of primers are given in (Table 3.3).

**Table 3.3 Primer details of mu-opioid receptor (MOR)**

Primer	Sequence 5' to 3'	Amplicon Length	Annealing Temperature
MOR FP	ATGATGGAAGCTTTCTCTAAGTCTG	25bp	58° C
MOR RP	TCACCTGCCAAGCTGGCCTT	20bp	

PCR amplification was carried out in thermal cycler using the conditions viz., each PCR amplification was carried out in 25µl reaction volume with 20-30 ng cDNA, 2pM of each of forward and reverse primer, 1X reaction buffer, 1.5mM MgCl<sub>2</sub>, 200µM of each dNTPs and 1 unit of Taq DNA polymerase. PCR machine was programmed for the specific condition: an initial denaturation at 94° Taq for 5 min. followed by 35 cycles of 94° C for 60 s; annealing temperature (60° C) for 60 s and 72° C for 60 s with a final extension for 10 min. at 72° C. After completion of cycle, amplification was confirmed by 2% agarose gel electrophoresis..

### 3.1.5 Gel extraction purification

The QIAquick gel extraction kit was used to purify the PCR products from the gel. The steps involved in purification are as follows:

- The amplified products were electrophoresed on 1.5% agarose gel.
- The gel slice containing DNA was weighed in a microcentrifuge tube and 3 volumes of gel binding buffer (QG) was added to 1 volume of gel (100 mg ~ 100 µl).
- The tubes were incubated at 56° C for 10 min to melt the slices of agarose gel completely
- The sample were mixed with one gel volume of isopropanol and passed through the QIAquick column to bind DNA.
- The tube was centrifuged for 1 minute; flow-through discarded and QIAquick column was placed back in the same collection tube.
- To elute DNA, 30 µl of buffer EB (10 mM Tris·Cl, pH 8.5) was added to the centre of the QIAquick membrane and allowed to stand for 1 min, and then centrifuged for 1 min.

- The purified DNA was used for sequencing of transcripts as well as cloning.

### 3.1.6 Sequencing of different transcript variants of MORs

PCR products of specific variants were sequenced using Big Dye terminator kit (Applied Biosystems, USA) in ABI 3100 automated DNA Sequencer. The amplified DNA was purified with exonuclease 1/Antarctic phosphatase (New England Bio lab, Beverly, USA) treatment and then sequenced both directions.

The typical sequencing reaction included the following components:

PCR product (25 ng/μl)	-	3.0 μl
10 x Ready Reaction mix (RR)	-	1.0 μl
10 x Sequencing Buffer (SB) Buffer	-	1.5 μl
Primers (5pM)	-	0.8 μl
PCR grade water	-	3.7 μl
<b>Total</b>	-	<b>10.0 μl</b>

Sequencing reactions were set up on quantitated purified PCR amplified templates of the respective genes using 1/8<sup>th</sup> of the standard volume of ABI Prism BigDye Terminator Sequencing Kits (Applied Biosystems). For sequencing reactions, both forward (5') and reverse (3') primers of specific variants were used. For sequencing, the typical reaction for each clone was set-up. After mixing, the contents were subjected to the thermo-cycling conditions of 96<sup>o</sup>C for 1min and 24 cycles of 94<sup>o</sup>C for 10 sec and 60<sup>o</sup>C for 4.5 min. On completion of PCR cycles, the reaction was immediately terminated by adding 2.0 μl of 125mM EDTA (pH 8.0). The product was precipitated by adding 2.0 μl of 3 M sodium acetate (pH 5.3), 10.0 μl of molecular biology grade H<sub>2</sub>O and 60.0μl of 95% ethanol and incubated for 15 minutes at room temperature. The contents were centrifuged at 1650 x G for 45 minutes and supernatant was removed carefully without disturbing the pellets. The pellet was washed with 200 μl of 75% ethanol and air-dried. Finally, the sequencing reaction product was resuspended in 10.0 μl of HiDi formamide (provided in the kit) and heat denatured at 95<sup>o</sup>C for 5 minutes before analysing on 3100ABI sequencer.

### 3.2. To clone MOR in Pichia/Bacterial expression system for their over expression and purification

To clone and express 6 TM μ-opioid receptor in bacterial system, primers with EcoRI site in the forward and XhoI in reverse primer were designed. The specific cDNA was amplified using the condition as:

The typical polymerase reaction included the following components:

DNA Template (25 ng/μl)	3.0 μl
10 x STB	10 μl
dNTPs	2 μl
Forward Primers (5pM)	3 μl
Reverse Primers (5pM)	3 μl
Taq poly	0.8 μl
dH <sub>2</sub> O	28.2 μl
<b>Total</b>	<b>50 μl</b>

PCR amplification was carried out in thermal cycler using the conditions viz., each PCR amplification was carried out in 25μl reaction volume with 20-30 ng cDNA, 5pM of each of forward and reverse primer, 10X reaction buffer, 1.5mM MgCl<sub>2</sub>, 200μM of each dNTPs and 1 unit of Taq DNA polymerase. PCR machine was programmed for the specific condition: an initial denaturation at 94° Taq for 5 min. followed by 35 cycles of 94° C for 60 s; annealing temperature (60° C) for 60 s and 72° C for 60 s with a final extension for 10 min. at 72° C. Products were resolved on 1% agarose gel, sliced the band and PCR products were purified using QIAquick gel extraction kit (Section 3.1.5).

### 3.2.1 Vector System

For cloning of MOR gene, pET28a vector having T7 lac strong promoter regions as well as shows Kanamycin resistance (Fig. 3.1) was used. Presence of N-terminal 6xHis-tagged protein with a thrombin site provides capability for both constitutive and inducible gene expression. The bacterial strain *E. coli* DH5α™ was used for plasmid propagation, cryo-storage and molecular cloning while the strain *E. coli* Rosetta™ (DE3) was used for recombinant protein expression and purification (Table 3.4).

**Table 3.4 Bacterial strains used for cloning, expression and propagation**

Strain	Sources	Genotype
<i>E. coli</i> DH5α™	MTCC	F- Φ80lacZΔM15 Δ(lacZYA-argF) U169 recA1 endA1 hsdR17 (rK-, mK+) phoA supE44 λ- thi-1 gyrA96 relA1
<i>E. coli</i> Rosetta™ (DE3)	MTCC	F- ompThsdSB(RB- mB-) gal dcm λ(DE3 [lacI lacUV5-T7 gene 1 ind1 sam7 nin5]) pLysS RARE (CamR)
BL 21(DE3)	MTCC	F-, ompT, hsdSB (rB-, mB-), dcm, gal, λ(DE3), pLysS, Cm
BL21(C41)	MTCC	OverExpress C41(DE3)pLysS: F - ompThsdSB (rB - mB -) gal dcm (DE3) pLysS (CmR)

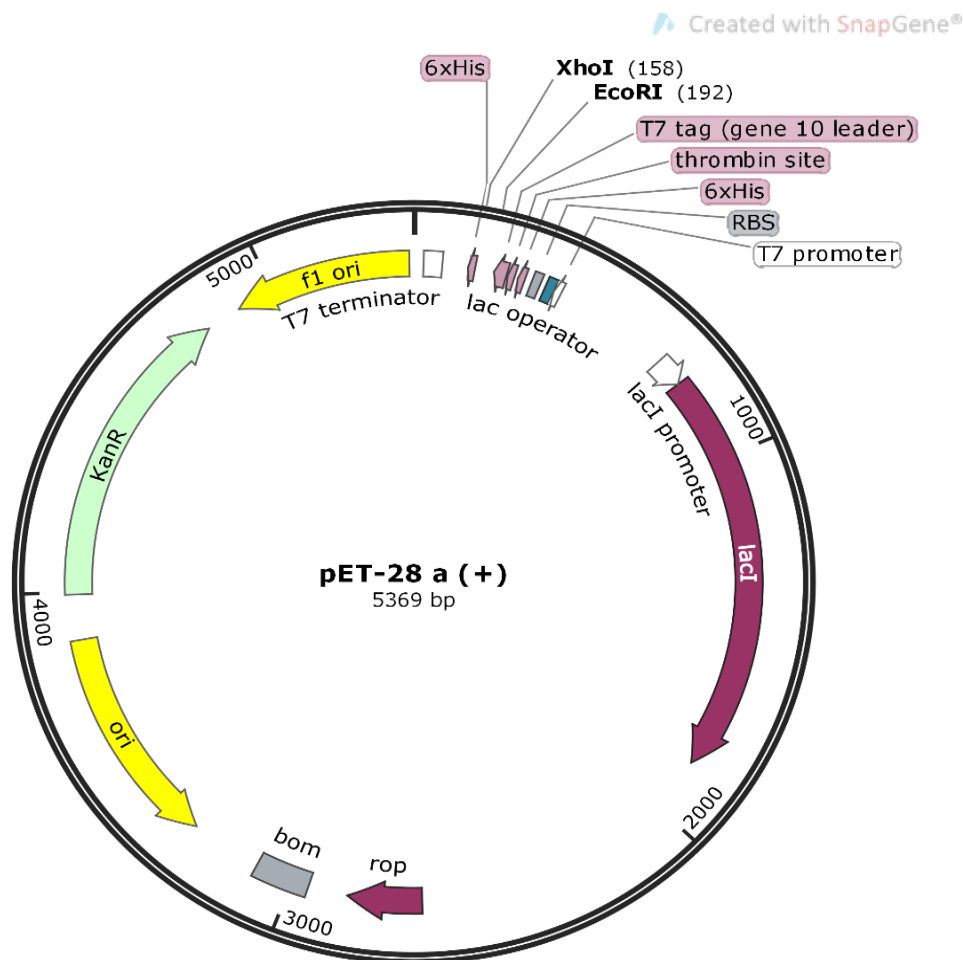


**Fig. 3.1** Vector Map pET28a (+) expression system

### 3.2.2 Restriction digestion of vector and PCR product

For cloning, the amplified product of MOR-1M gene was purified using a PCR Clean-up kit from HiMedia®. The plasmid DNA was isolated using plasmid DNA isolation kit from HiMedia®. Restriction digestion of the insert and vector was carried out with EcoR1 & Xho1 at 37° C for 4 hrs. to overnight depending upon the fidelity of the enzymes. The reaction was stopped by heat inactivation at 65<sup>0</sup>C for 5 min. The size and purity of the vector and insert DNA was checked on low melting agarose gel. Further, these were eluted from the cut gel pieces using Gel Elution kit from HiMedia®.

### 3.2.3 Ligation of digested PCR product of MOR with the digested cloning/expression cloning vector pET28a (+)

The ligation is very sensitive and depends on the appropriate concentration of T4 DNA ligase and ATP. T4 DNA ligase, an enzyme encoded by bacteriophage T4 catalyses the joining reaction between DNA molecule involving 3'-hydroxy and the 5'-phosphate termini. For the

catalytic activity this enzyme require the presence of ATP and  $Mg^{2+}$ . Ligation reactions were set up using the double digested agarose gel extracted products (insert 1.26  $\mu$ l and vector 1  $\mu$ l) in varying insert to vector ratios (depending on insert sizes) and double digested vector. (1  $\mu$ l). Vector alone was also used in one ligation reaction as a self-ligation control. The ligation reactions were carried out at 4 to 8<sup>o</sup>C for 16-18 hrs.

### **3.2.4 Transformation**

Transformation of ligation reaction mixtures was performed using competent cells by heat shock method as well as electroporation.

- An aliquot of 5  $\mu$ l of ligation mixture was added to 100  $\mu$ l of competent cells and mixed gently by pipetting. The mixture was incubated on ice for 10 min.
- The tubes were then transferred to heating block at 42<sup>o</sup>C and held for 90 seconds. The tubes were immediately transferred back on ice and allowed to chill for 5 minutes.
- To the above mixture, 900  $\mu$ l of SOC media was added and mixed. The tubes were incubated at 37<sup>o</sup>C for 1 hr in rotary shaker to allow the bacteria to recover and develop the antibiotic resistance.
- After the recovery period, the samples were removed from the incubator and spin down to collect the cells. The supernatant was discarded in a way that the cell pellet and 100  $\mu$ l of media were retained in the tubes.
- The cell pellet was resuspended in the residual media and plated on LB agar containing appropriate antibiotics. Plates were incubated at 37<sup>o</sup>C for 12-16 hrs.
- After the transformed colonies grew on the LB agar plate, these (individual colonies) were patched onto a fresh antibiotic containing LB agar plate and also inoculated in 10 ml of antibiotic containing LB broth tubes simultaneously. These were allowed to grow for 12-16 hrs at 37<sup>o</sup>C with 200 rpm of agitation. After the growth period the plates and tubes were examined for culture growth. The plate containing the labelled transformed patches was stored at 4<sup>o</sup>C. For clone conformation (Fig. 3.2), the transformed plasmids were isolated from culture using standard alkaline lysis method (Sambrook *et al.*, 1989).
- The transformants were PCR amplified and double digested with their respective restriction enzyme pairs for release of insert. Then the PCR and digestion mixtures were run on an Agarose gel [0.8-1% gel (w/v)] to verify positive clones via insert release and positive PCR amplification. Twenty clones were confirmed by PCR and

restriction digestion. Recombinant Plasmid were custom sequenced directionally using T7 promoter and T7 terminator universal primer. NCBI- BLAST was performed to identify the homology of the MOR sequence.

### 3.2.5 Expression of recombinant MOR

Mice MOR (cloned in pET28a (+) vector with N-terminal His tag) were overexpressed in *E.coli* C41 (DE3). The cells were grown in LB medium at 37°C to O.D<sub>600</sub> of 0.6 and then induced with 0.4 mM IPTG (Approximately 5mg/ml of protein is obtained from 2 lt culture). Induction was carried out at 18°C for 16 hrs followed by harvesting by centrifugation at 5000g. The pellet was resuspended in lysis buffer (20mM Tris-Cl (pH 8.0), 150mM NaCl and 10% glycerol, plus 5mM MgCl<sub>2</sub>, 2mM beta-ME, 1mM EDTA (pH 8.0).

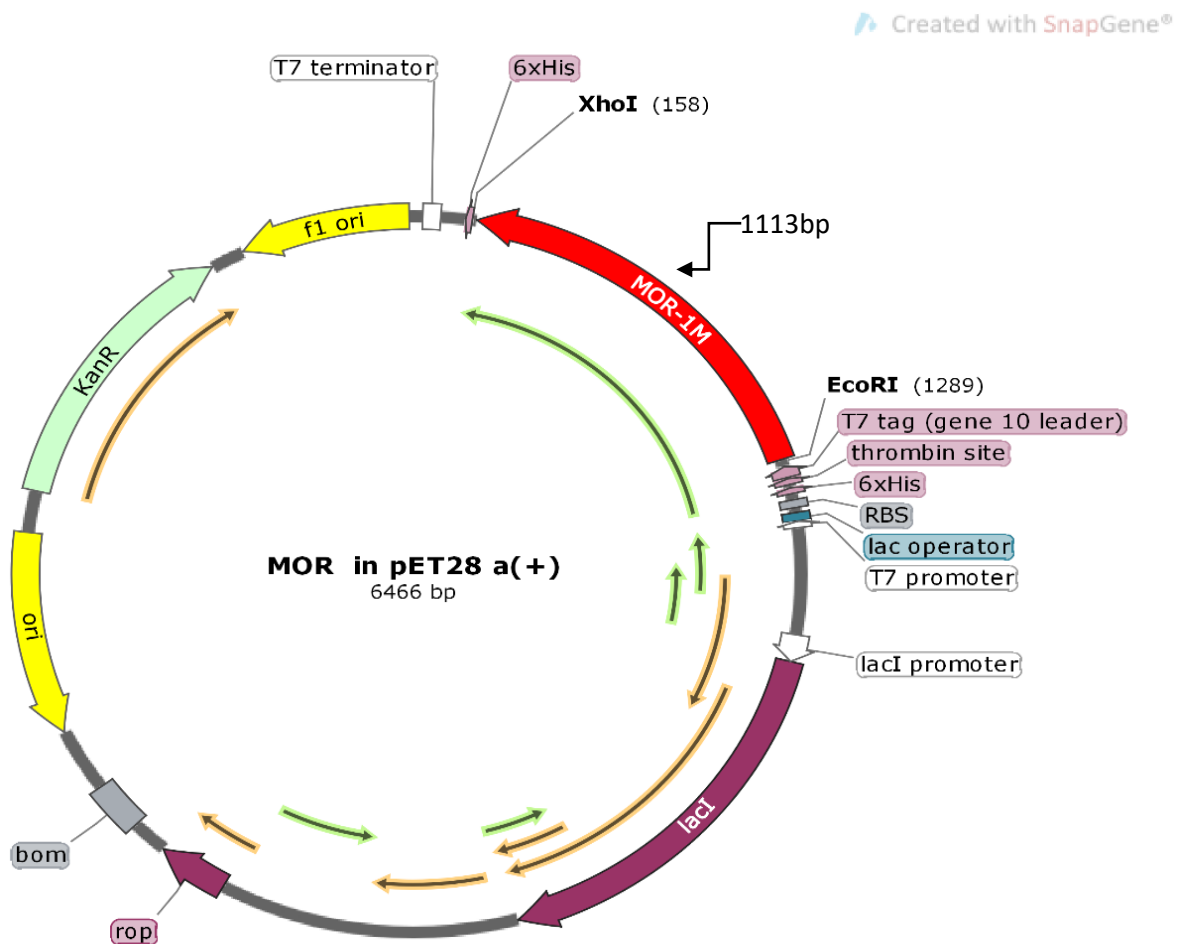


**Fig.3.2** Orientation ofMOR gene cloned in pET28a (+) expression vector

Phenylmethylsulfonyl fluoride (PMSF) was added to a final concentration of 1mM post which cells were sonicated on ice (15'' ON, 30'' OFF, 45% amplitude). The cell lysate was centrifuged at 1000g to remove unbroken cell and cell debris, followed by another centrifugation at 10000g for 40 min to collect white inclusion bodies. The supernatant was further centrifuged at 85,000g for 1h to harvest a membrane fraction. The pellet was flash frozen and stored at -80°C until further used.

### ***3.2.6 Detergent screening and purification***

One gm of the resulting membrane pellet was solubilised in 10–20 ml of solubilisation buffer containing 20mM Tris-Cl (pH 8.0), 300mM NaCl and 10% glycerol, 0.8% L-laurylsarcosine plus 6M urea (pH 8.0) and 5mM imidazole. The solubilisation was allowed to proceed with gentle agitation at 4°C for 2 h. The solubilised supernatant was separated by centrifugation at 20,000 g (4°C, 30min).

### ***3.2.7 Isolation and purification of recombinant MOR***

The clarified supernatant was filtered using 0.22 micron filter and loaded onto a HisTrap™HP 5ml at 1ml/min, washed (for 100 ml) with 20mM Tris-Cl (pH 8.0), 300mM NaCl and 25mM Imidazole (pH 8.0), 10% Glycerol (pH 8.0), 0.8% L-laurylsarcosine plus 6M urea and the protein was eluted using 20 mM Tris-Cl (pH 8.0), 300mM NaCl and 300mM Imidazole (pH 8.0), 10% Glycerol, pH 8.0, 0.8% L-laurylsarcosine plus 6 M urea) using 100% gradient in 30ml with 1.3 ml elution fraction size. The eluted fractions were analyzed on a 12% SDS-PAGE gel. The pooled peak fractions (purest ones) diluted with low salt buffer (25mM Tris-Cl (pH 8.0), 100 mM NaCl, 1mM EDTA) (e.g. 5ml of pooled fractions was diluted upto 50ml with low salt buffer) were loaded on to HiTrap™ Q FF 5ml for anion-exchange and eluted out with 25mM Tris-Cl (pH 8.0), 1M NaCl, 1mM EDTA using 100% gradient in 30 ml with 1.3 ml elution fraction size. The purified protein was separated by PAGE (12% SDS–PAGE) according to Laemmli (.1970).

### ***3.2.8 Ammonium sulphate precipitation of MOR Protein***

Ammonium sulphate is commonly used for protein purification and protein separation by changing the solubility based on salt concentration. It is a simple and effective means of fractionating proteins. The cell lysate was centrifuged at 1000g to remove unbroken cells and cell debris, followed by another centrifugation at 10000g for 40 min to collect white inclusion bodies. The supernatant was further centrifuged at 100,000g for 1hr to harvest the membrane fraction. The solubilisation was allowed to proceed with gentle agitation at 4°C for 2 hr. The

solubilised supernatant was separated by centrifugation at 20,000g (4°C, 30 min) and filtered through 0.22µ filter. On-line calculators (<http://www.encorbio.com/protocols/AM-SO4.htm>) were accessed to determine the amounts of solid ammonium sulfate required to reach a given saturation. Ammonium sulphate was added to protein lysate at 4°C for 30 min. on a magnetic stirrer. The saturated protein was centrifuged at 25,000 rpm for 20 minutes at 4°C, to pellet out protein. More saturated ammonium sulfate or solid ammonium sulfate was added to make next concentration, repeat stirring and centrifugation at same temperature. Ammonium salt concentration (0-100%) used for MOR protein precipitation is given in Table 3.5. All gradient pellets were solubilised in lysis buffer and analysed on 12% SDS PAGE gel. 60-80 % gradients were collected and dialyzed in low salt buffer. Q-Sepharose low salt buffer used (25mM Tris-Cl, pH 7, and 75mM NaCl) was exchanged after 45 minute and dialyzed for a total of 1h 30 minutes. After dialysis, it was passed it through Mono Q columns but due to high pI (9.68), the protein did not bind to columns and come out in flow –through. So, considering that MOR recombinant protein is a DNA binding protein Mono Q columns was replaced with Heparin high affinity columns, the recombinant protein was loaded onto column at appropriate conditions, collected the fractions (F2-F8) and were analysed on 12% SDS PAGE gel.

**Table 3.5 Ammonium sulphate precipitation of MOR protein**

Conc. Gradients	Initial Volume	Final Volume	Req.(NH <sub>4</sub> ) <sub>2</sub> SO <sub>4</sub>	Saturation Buffer
0-20	50	52.92	5.49 g	20 %
20-40	52.92	56.20	6.18 g	40 %
40-60	56.20	59.91	6.99 g	60 %
60-80	59.91	64.15	7.98 g	80 %
80-100	64.15	69.04	9.20 g	100 %

### 3.2.9 SDS-PAGE analysis

MOR protein was separated on 12% resolving and 5% stacking SDS-PAGE as follows:

- First of all resolving gel was prepared, and casting frames were set on the casting stands. Appropriate amount of resolving gel solution was pipetted and filled into the gap between the glass plates.
- Then SDS-PAGE gel was allowed to solidify for 20-30 min.

- Then the stacking gel was prepared and poured into the top of the resolving gel and well forming comb was inserted properly without trapping any air.
- After ensuring complete gelation of the stacking gel, comb was inserted into the gel. Finally glass plates were taken out from casting frame and set the cell buffer dam. Running buffer was poured (electrophoresis buffer) into the inner chamber, the buffer surface reached the required level in the outer chamber.
- Preparation of the samples: About 100µg of each sample was prepared. Samples were mixed with 5X protein loading dye, and heated in water bath for 5-10 min.
- Prepared samples were loaded into wells, followed by covering the whole assembly and then connected with anodes.
- Appropriate voltage (90v) was set to run electrophoresis and was run till it reaches the end.
- Visualization of separated protein following the electrophoresis was achieved by Coomassie staining. Following SDS-PAGE, the polyacrylamide gels were immersed in Coomassie blue staining solution, heated for 30 s in a microwave and incubated at room temperature with gentle agitation for 15-60 minutes.
- After staining, gels were rinsed with dH<sub>2</sub>O and incubated 45 minutes in Coomassie de-staining solution with gentle agitation. The stained protein bands were observed using a white light Tran- illuminator.
- All reagent recipes are mentioned in Table 3.6, Table 3.7 and Table 3.8.

**Table 3.6 Composition of SDS-PAGE running buffer and protein loading dye**

<b>10X SDS-PAGE Running Buffer</b>		<b>5X Protein Gel Loading Dye</b>	
<b>Reagent</b>	<b>Concentration</b>	<b>Reagent</b>	<b>Concentration</b>
Tris Base	250 mM	Bromophenol Blue	0.5 % (w/v)
Glycine	2.5 M	Glycerol	50% (v/v)
SDS	1 % (w/v)	SDS	10% (w/v)
Added DTT or β-ME fresh from stocks (kept the prepared stocks of 5X dye at -20°C for long term storage).		Tris-Cl (pH 6.8)	250 mM
		DTT/β-ME	500 mM/5 % (v/v)

**Table 3.7 Composition of resolving and stacking gel**

Resolving Gel (10 ml)			5 % Stacking Gel (3 ml)	
Reagent	10%	15%	Reagent	Volume
	Volume			
Acrylamide/Bis-Acrylamide (mix ratio 29:1 and 30% w/v)	3.3 ml	5 ml	Acrylamide/Bis-Acrylamide (mix ratio 29:1 and 30% w/v)	0.5 ml
1.5 M Tris-Cl (pH 8.8)	2.5 ml	2.5 ml	1 M Tris-Cl (pH 6.8)	0.38 ml
SDS (10 % w/v)	100 µl	100 µl	SDS (10 % w/v)	30 µl
APS (10 % w/v)	100 µl	100 µl	APS (10 % w/v)	30 µl
TEMED (100 %)	4 µl	4 µl	TEMED (100 %)	3 µl
dH <sub>2</sub> O	4 ml	2.3 ml	dH <sub>2</sub> O	2.1 ml

**Table 3.8 Protein staining and de-staining solutions (1L)**

Solution Reagent	Staining		Destaining	
	Concentration (%)	Amount	Concentration (%)	Amount
Methanol	50	500 ml	50	500 ml
Acetic Acid	10	100 ml	10	100 ml
dH <sub>2</sub> O	40	400 ml	40	400 ml
Brilliant Blue (R250)	0.25	2.5 g	-	

### 3.3 To undertake interaction studies of MOR with BCM7/9 by *in silico* approach

#### 3.3.1 Mice $\mu$ -opioid receptor gene

Nineteen distinct transcript variants of MORs sequences selected from a much larger pool of sequences available in public databases were used as reference sequences. Further, using the sequence data from objective 1, and from the databases, 34 genes were identified as representative of MORs gene family of mice. For sequence analysis and further characterization resources like NCBI (<https://www.ncbi.nlm.nih.gov/>), UniProt (<https://www.uniprot.org>) and conserved domain database (<https://www.ncbi.nlm.nih.gov/cdd/>) were utilized. The DNA strand and chromosomal location of all selected sequences were recorded as per the UCSC genomic browser (<http://genome.ucsc.edu/>). Various biochemical parameters of MOR such as molecular weight, theoretical pI, instability index, aliphatic index and grand average of hydropathicity (GRAVY) were predicted by ProtParam Server (<https://web.expasy.org/protparam/>). These

biochemical parameter have changed according to sequence difference (<http://web.expasy.org/protparam/>). SOPMA(<https://npsa-prabi.ibcp.fr/cgi-sopma.html>) and PSIPRED (<http://web.expasy.org/protparam/>) web server where been used for the prediction of secondary structures.

### **3.3.2 Homology modelling of receptor and ligands**

As the crystal structure for mice mu receptors as well as ligands (BCM7/9) were unavailable in the PDB databank, the strategy of homology modelling was utilized to generate their 3D structure. For structure prediction, mice mu receptor protein sequence (NC\_000076) was retrieved from the NCBI database and four templates were selected using homology search from NCBI and PDB databases. The  $\mu$  opioid receptor (MORs) seven trans membrane GPCR protein 3D structure prediction was conducted using I-TASSER server (<http://zhanglab.ccmb.med.umich.edu/I-TASSER/>) online database and the best models were selected based on their C-values. The amino acid sequences were submitted to the online server of the I-TASSER and the result generated in PDB format. The three templates (4n6hA, 5zbh, 4dk1A) were used for homology modelling using I-TASSER., out of the 10 top templates chosen from the LOMETS threading programs based on the highest significance in the threading alignments of the template with the query protein by Z-score; (the difference between the average and raw scores in the unit of standard deviation). The generated model of mu receptor was visualized using UCSC Chimera (<https://www.cgl.ucsf.edu/chimera>).and PyMole Server (<http://www.pymol.org/>). The ligand structures of BCM7 and BCM9/ was modelled by MODELLER server (<https://bioinformatictools.wordpress.com/tag/modeller/>) that displayed DOPE score of 0.97 and 0.98 respectively which is a reliable statistical potential to assess quality of homology model in ligand structure prediction.

### **3.3.3. Active Site Analysis and Residues Recognition**

Active sites and ligand binding sites were generated using a meta-server approach to protein-ligand binding site prediction (<http://zhanglab.ccmb.med.umich.edu/COACH/>). The complementary ligand binding site was predicted using COACH by matching (4n6hA, 5zbh, and 4dk1A) I-TASSER generated with protein in the BioLiP protein function database. The functional templates were detected and ranked by COACH using composite scoring function that is based on structure and sequence profile comparisons.

### 3.3.4 3D model validation

Validation of the structural quality of the generated models were done using the programs: PROCHECK, (Laskowski *et al.*, 1993) PROSA (Wiederstein *et al.*, 2007), FT SITE, PROSA (<https://prosa.services.came.sbg.ac.at/prosa.php>) uses knowledge based potentials of mean force to evaluate model accuracy and it shows local model quality by plotting energies as a function of amino acid sequence position. SOPMA (<https://npsa-prabi.ibcp.fr/cgi-sopma.html>) and PSIPRED (<http://web.expasy.org/protparam/>) web server were used for the prediction of secondary structures. The percentage of residues in the favoured region of Ramachandran plot was calculated using RAMEPAGE server (<http://mordred.bioc.cam.ac.uk/~rapper/rampage.php>).

### 3.3.5 In Silico Protein-Protein Interaction Study

Eleven selective transcript variants of MORs, namely MOR-1, MOR-1A, MOR-1B1, MOR-1B2, MOR-1C, MOR-1D, MOR-1G, MOR-1M, MOR-1N, MOR-1U, and MOR-1mRNA, and were selected for docking studies. Two selective ligands, BCM-7 and BCM-9 for different transcript variants of MORs were docked to homology models based on both the templates. The PDB files of ligand and target receptor were uploaded to Patch Dock server (<https://bioinfo3d.cs.tau.ac.il/PatchDock/>) for docking, using cluster RMSD at default value of 4Å°. This server depends on shape complementarity of software results molecular surfaces to generate the best starting candidate solution (Schneidman-Duhovny *et al.*, 2005). The Connolly dot surface representation of the molecules into different component such as convex, concave, and flat patches were generated through PatchDock algorithm. Thereafter, the complementary patches were harmonized to form transformation candidates, which were later refined using FireDock server (<http://bioinfo3d.cs.tau.ac.il/FireDock/>), and rescored the side chains interface of the top 10 candidate solutions. It also amends the orientation of the relative molecules by confining the flexibility to the side-chains of the interacting surface and allow the movements of small rigid-body (Duhovny, D., 2002) Thereafter, the interactions and binding observed in the docked conformations in PDB format were visually using the PyMol software (DeLano, W.L *et al.*, 2002). The interacting amino acidic residues, were identified defined by PDBsum server and prominent binding sites were predicted by LIGPLOT server (<https://www.ebi.ac.uk/thornton-srv/software/LigPlus/>). The comparative energy minimization of docked model for MOR-BCM7 and for MOR-BCM9 was calculated by YASARA server (<http://www.yasara.org/minimizationserver.htm>)

# **CHAPTER -4**

---

---

## **Results and Discussion**

---

---

## RESULTS AND DISCUSSION

The present study was undertaken for characterization of mu receptors of mice distributed across different cell surfaces of various cells and tissue types. The present study describes the characterization of mice mu opioid receptors including the identification of different transcript variants, generation of their homology models, their stability and validation of 3D structures. One of the mu receptor MOR-1M was also cloned in pET28A for its expression and purification so as to generate the resource for in vivo studies as well. . In most of the cases, to conduct the animal trials related to effect of BCM7/BCM9 from A1 or A2 type milk respectively, on human health mice is the most preferred animal model. Hence, to gain insight into the structure-function relationships of the opioid receptors with the bioactive peptides (beta casomorphins-BCMs) generated from cow milk beta casein, the interaction studies with BCM7 as well as BCM9 and comparative stability of the docked structure was also studied. The results with respect to specific objectives are presented here.

### **4.1: To characterize mu opioid receptor (MOR) and its splice variants in brain and gut tissues of mice**

#### **4.1.1: Sampling details, RNA isolation and cDNA synthesis**

Male C57BL/6 mice purchased from Indian Institute of Integrated Medicine, Jammu and maintained at ICAR-NDRI, animal house were used as resource for tissue samples. These mice were also used to establish experimental evidence for the cause and effect relationship of A1/A2 milk with disease progression. RNA was extracted from the brain and gut tissues exhibited high quality as determined by  $A_{260/280}$  ratio. The OD ratio ( $A_{260/280}$ ) of extracted RNA samples was in the range of 2.10 to 2.15 indicating purity of the RNA sample, free from DNA and protein (Table 4.1). 1.5 % denaturing Agarose gel showed intact 28S rRNA and 18S rRNA bands indicating the integrity of extracted RNA (Fig.4.1).

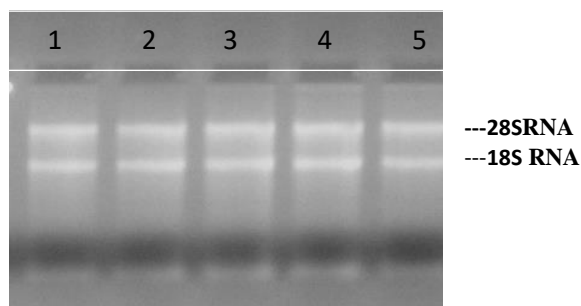


**Fig. 4.1** Representative gel picture of isolated RNA from brain and gut tissue

*Lane 1, 2, 3: RNA from brain tissue; 4, 5: RNA from Gut tissue*

**Table 4.1: Purity and quantity of RNA from brain and gut tissue of mice**

S.No.	Tissue ID	O.D 260/280	Conc. ng/ $\mu$ l
1	Br 1	2.11	478
2	Br 2	2.12	1126
3	Br 3	2.15	173.6
4	Br 4	1.99	339.6
5	Br 5	2.13	144
6	Gt 1	2.13	1338
7	Gt 2	1.99	339.6
8	Gt 3	2.1	413
9	Gt 4	2.0	812
10	Gt 5	2.1	155

Further, semi-quantitative analysis of primers using the freshly synthesized cDNA showed the specificity of primer pairs as well as the quality of cDNA synthesized. ACTB primer pair was used to amplify the representative cDNA samples. The representative gel picture for ACTB gene amplified in brain and gut cDNA samples is shown in (Fig 4.2). The presence of specific amplification product corresponding to the expected size for ACTB gene reflected the specific amplification. The accuracy of ACTB primers pair was also ensured by the presence of a unique peak during the dissociation step (melt curve) at the end of qPCR reaction.



**Fig. 4.2** Amplified products of ACTB on 2% agarose gel indicating quality of cDNA prepared from Brain and Gut derived RNA samples Lane 1, DNA marker (100bp), and 2-6, amplified cDNA from Brain; 7-9, amplified cDNA from Gut

#### **4.1.2. PCR amplification of $\mu$ opioid receptor (MOR)**

Each of the first strand cDNA made from brain tissue was amplified using gene specific primers. Primer set were designed to amplify cDNAs that encoded the complete ORF of MORs. The transcripts/ spliced variants of mu receptors (MOR-1M (1113 bp), MOR-G (990 bp), MOR-1K (250 bp) and MOR-1L (250 bp) from mice brain are shown in (Fig 4.3). The

specific amplification products corresponded to expected product size for major transcript variants MORs, as reflected by specific band. Sequences of these splice variants derived using ABI 3100 automated DNA sequencer were compared with those available at NCBI data base (<https://www.ncbi.nlm.nih.gov/>), using BLAST (<https://blast.ncbi.nlm.nih.gov/Blast.cgi>). One of these sequences that is MOR-1M was used for cloning, expression and purification.

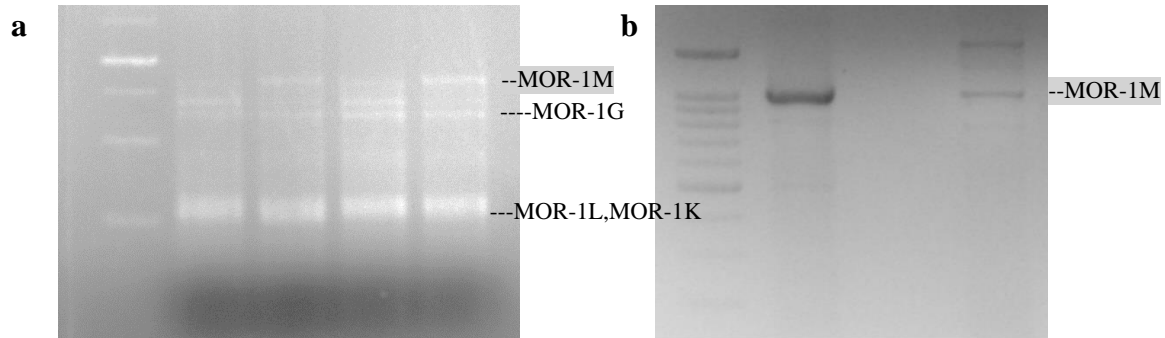


**Fig. 4.3** Amplified MOR transcript variants on 2 % Agarose gel, Lane 1, DNA marker (100bp) 2 &4: MOR-1M (1113) Lane 2, 3, 4: MOR-G (990 bp); Lane 5: MOR-1K (250 bp) and lane .5MOR-1L (250 bp).

#### **4.1.3 Identification and retrieval of $\mu$ -opioid receptor gene**

The information on transcript variants of mu-opioid receptor collected using extensive literature and database resources like NCBI (<https://www.ncbi.nlm.nih.gov/>), UniProt (<https://www.uniprot.org>) and conserved domain database (<https://www.ncbi.nlm.nih.gov/cdd/>) resulted in identification of 31 MORs transcript. Among 31 transcript variants of mu-opioid receptor gene, 17 were categorised as protein coding, 11 as non-mediated decay (NMD) and 3 as processed transcript. Due to alternative splicing of OPRM-1 gene 11 transcript variants contained a premature termination codon (Table 4.2) and were degraded by Nonsense-mediated mRNA decay (NMD) which selectively degrades such mRNAs (Hug *et al.*, 2016). NMD operates in the cytoplasm and is a post-transcriptional mRNA quality control mechanism to remove mRNAs containing premature termination codons (Kervestinet *et al.*, 2012 and Jacobson *et al.*, 2012).

The mRNAs harboring a termination codon 50 to 55 nucleotides upstream of the final exon-exon junction are efficiently degraded by NMD. The process is signalled by the presence of the exon junction complex and a multi-subunit protein complex, located 20 to 24 nucleotides upstream of an exon-exon junction (Nagy and Maquat 1998; Andersen *et al.* 2001). This acts as a quality control process to maintain the quality of gene expression and deletes the aberrant mRNA which otherwise might lead to production of truncated proteins with predicted deleterious effects for the organism (Schweiggruber *et al.*, 2013; Panet *et al.*, 2011,

2005b).The 11 OPRM1 gene splice transcript variants regulated by region-specific NMD include MOR-1E,MOR-1L,MOR-1Eiii,MOR-1EiV,MOR-1K,MOR-1W, MOR-1Ja, MOR-1Ha,MOR-1T1, MOR-1T2 and MOR-1Vii.

**Table 4.2: Characteristics of Mice mu opioid receptor (MOR) transcript variants**

Name	Transcript ID ( ENSMUST)	Transcriptio n length (nt)	Amino Acid (aa)	Biotype	Total Exon	Coding Exons
Oprm1-201	0000000783.12	1500	425	PC	4	4
Oprm1-202	00000052751.13	1334	393	PC	5	4
Oprm1-203	00000056385.13	1440	398	PC	5	4
Oprm1-204	00000063036.13	1427	325	PC	5	4
Oprm1-205	00000078634.11	1695	456	PC	4	4
Oprm1-206	00000092729.10	1422	388	NMD	5	4
Oprm1-207	00000092731.10	1332	392	PC	4	4
Oprm1-208	00000092734.10	1569	398	PC	6	4
Oprm1-209	00000105597.7	1133	39	NMD	5	2
Oprm1-210	00000105601.8	1161	222	NMD	5	2
Oprm1-211	00000105602.7	1366	390	PC	3	3
Oprm1-212	00000105603.1	2053	389	PC	4	4
Oprm1-213	00000105604.7	1616	393	PC	4	4
Oprm1-214	00000105605.7	1503	391	PC	4	4
Oprm1-215	00000105607.7	2369	398	PC	5	4
Oprm1-216	00000105611.7	2420	438	PC	6	6
Oprm1-217	00000105615.8	1258	370	PC	6	6
Oprm1-218	00000123861.7	1020	222	NMD	3	2
Oprm1-219	00000129221.7	2205	356	NMD	8	4
Oprm1-220	00000129954.7	1706	448	NMD	8	5
Oprm1-221	00000133486.1	256	No protein	Processed transcript	3	0
Oprm1-222	00000135502.7	1363	416	PC	4	4
Oprm1-223	00000141897.1	1939	No protein	Processed transcript	7	0
Oprm1-224	00000143875.1	696	84	NMD	4	2
Oprm1-225	00000144264.7	2120	399	NMD	8	4
Oprm1-226	00000147171.7	1570	330	NMD	6	4
Oprm1-227	00000148625.1	242	No protein	Processed transcript	2	0
Oprm1-228	00000150374.7	1174	41	NMD	5	2
Oprm1-229	00000152674.1	1179	104	PC	3	2
Oprm1-230	00000154906.7	2039	409	PC	4	4
Oprm1-231	00000154941.7	1540	337	NMD	7	4

**Abbreviation:** *oprm-1*: mu-opioid Receptor, *nt* : number of nucleotides between start and end; *AA*: length in amino acid of the protein products; *PC*: protein coding, *NMD*: non mediated decay.

#### 4.1.4 Domain structure of MOR-1 gene

The information on structural domains and other features of the mu opioid receptor transcript variants revealed the presence of G\_PROTEIN\_RECEP\_F1\_1, PS00237; G-protein coupled receptors family 1 signature (PATTERN) and “G\_PROTEIN\_RECEP\_F1\_2, PS50262; G-protein coupled receptors family 1 profile” (matrix) in 16 transcript variants. The Prosite pattern GPCRs family\_1(PS00237) corresponded to 17 amino acid positions (153-169) covering from the second half of the TM III for 14 variants (Table 4.3) while for two variants (Oprm1-204 and Oprm1-217) though it corresponded to 17 amino acids, the position varied to 85-101 amino acids. Similarly, Prosite profile GPCRs F1\_2 (PS50262) corresponded to similar 252 amino acid position in all the 14 transcript variants (85-336) while in Oprm1-204 and Oprm1-217, it corresponded to 249 amino acids with position 18-268. For one of the transcript variant oprm1-206, oprm1-206, oprm1-206, oprm1-209, oprm1-218, oprm1-219, oprm1-220, oprm1-221, oprm1-223, oprm1-224, oprm1-225, oprm1-226, oprm1-22, oprm1-228 and oprm1-231 7TM, these GPCRs family patterns were not identified. Another highly conserved sequence observed in these splice variants was NPxxY (AsparagineProline xx Tyrosine) motif located at the cytosolic end of seventh trans-membrane domain. This motif is generally considered as the characteristic of most GPCRs (Probst *et al.*, 1992) and contributes to G protein-coupled receptor internalization and signal transduction (Hausdorff *et al.*, 1991; Robinson 1994). Marin *et al.*, 2000, also reported that cytoplasmic part of the NPxxY region contributes to a binding site for the G protein as well as very crucial for hydrophobic interaction in ligand affinity, receptor sequestration, heterotrimeric G protein coupling (Barak *et al.*, 1995). The positions of Asn, Pro, and Tyr residues in these variants were constant within the motif whereas x is any amino acid. The inner two residues are generally hydrophobic in nature, while the residues that flank Tyr and Asn may vary. The position for this motif was same for 16 variants that is 332-336 (Fig.4.4). On comparison of MOR transcript variants and isoforms of mice, it was observed that motif, NPVLY (NPXXY) corresponding to 5 amino acid residue (332-336) was homologous across all the 7TM variants but absent in MOR-1K, MOR-1L, MOR-1Ja, MOR-1Ha belonging to the category of 6TM variants MOR-1K, MOR-1L and MOR-1Ia, MOR-1Ja, MOR-1Ha which is 1TM variant. Similarly these variants lacked DRY (Fig.4.5) motif (165-167 amino acids). The hundred percent homology was observed for the helical trans-membrane domain (TM) TM1 (67-91), TM2 (105-129), TM3 (141-163), TM4 (184-205) TM5 (229-253) TM6 (278-304) and TM7 (313-336) sequences for the 7TM transcript variants including some 6TM

**Table 4.3 Structural domain groups of mice mu opioid receptor transcripts**

Protein	RefSeq ID	Structural domains and their amino acid position				
		Family AGPCR-like	PFAM 7TM PF00001	Prosite pattern GPCRs family_1 (PS00237)	Prosite profileGPCRs F1_2 (PS50262)	Motif (NPxxY)
Oprm1-201	-	39-363	85-336	153-169	85-336	332-336
Oprm1-202	NM_001304950 NP_001291879	39-363	85-336	153-169	85-336	332-336
Oprm1-203	NM_001304950	39-363	85-336	153-169	85-336	332-336
Oprm1-204	NM_001302796 NP_001289725	24-296	26-268	85-101	18-268	332-336
Oprm1-205	NM_001302796	39-363	85-336	153-169	85-336	85-336
Oprm1-206	-	-	-	-	-	332-336
Oprm1-207	-	39-363	85-336	153-169	85-336	332-336
Oprm1-208	-	39-363	85-336	153-169	85-336	332-336
Oprm1-209	-	-	-	-	-	-
Oprm1-210	-	-	-	-	-	-
Oprm1-211	NM_001304937 NP_001291866	39-363	85-336	153-169	85-336	332-336
Oprm1-212	NM_001304937	39-363	85-336	153-169	85-336	85-336
Oprm1-213	-	39-363	85-336	153-169	85-336	85-336
Oprm1-214	NM_001304938 NP_001291867	39-363	85-336	153-169	85-336	332-336
Oprm1-215	NM_001302793 NP_001289722	39-363	85-336	153-169	85-336	332-336
Oprm1-216	NM_001039652 NM_001304955 NP_001034741 NP_001291884	39-363	85-336	153-167	85-336	332-336
Oprm1-217	NM_001302795 NP_001289724	26-295	26-268	85-101	18-268	332-336
Oprm1-218	NM_001302795	-	-	-	-	-
Oprm1-219	-	-	-	-	-	21-272
Oprm1-220	-	-	-	-	-	85-336
Oprm1-221	-	-	-	-	-	-
Oprm1-222	-	39-363	85-336	153-169	85-336	332-336
Oprm1-223	-	-	-	-	-	-
Oprm1-224	-	-	-	-	-	-
Oprm1-225	-	-	-	-	-	332-336
Oprm1-226	NM_001302794 NP_001289723	-	-	-	-	332-336
Oprm1-227	NM_001302794	-	-	-	-	-
Oprm1-228	-	-	-	-	-	-
Oprm1-229	-	38-95	-	-	-	-
Oprm1-230	NM_001304948 NP_001291877	39-363	85-336	153-169	85-336	332-336
Oprm1-231	NM_001304948	-	-	-	-	21-272

**Abbreviation :** *OPRM-1*, Mu-opioid receptor, *PFAM*, Pfam is a database of protein families that includes their annotations and multiple sequence alignments generated using hidden Markov models; *GPCR*, G-protein couple receptor, *PROSITE* protein database, It consists of entries describing the protein families, domains and functional sites as well as amino acid patterns and profiles in them, The *NPXXY* motif (X represents any amino acid) in the seventh transmembrane (7TM) domain of the highly conserved among G protein-coupled receptors.

such as MOR-1M and MOR-1G variants but absent in 1TM. The variations were observed in the sequence for TM4, and TM5 for the variants MOR-1L, MOR-1Ha and MOR-1Ia

respectively. The glycosylation of asparagine (GlcNac) is considered essential for determinant of protein structure and function. These were observed at position 9, 31, and 46 amino acid residue in all the 7TM transcript variants but absent in 6TM and 1TM variants (MOR-1M, MOR-1N, MOR-1G, MOR-1K, MOR-1L, MOR-1Ja, MOR-1Ha and MOR-1Ia). In addition homology for one N-linked glycosylation site (GlcNac) (38 amino acid) was observed in all transcript variants of transcript variants of OPRM1 gene. The chromosome 10 is considered essential for determinant of transcript variants protein structure and function. The cellular location of all OPRM-1 transcript variants on plasma membrane and endosome given in (Table 4.4). The agonists, such as morphine, and bioactive peptides influence the MOR location within membrane domains and endosome responsible for activating signalling pathway (Zheng *et al.*, 2008).

**Table 4.4 Characterization and localization of OPRM-1 transcript variants/isoforms**

Name	UniProt	CCDS	Chr. Location	Position	Localization
Oprm1-201	P42866	-	-	6,788,809-6,838,680	PM & E
Oprm1-202	P42866	CCDS78788	10	6,788,809-7,037,201	PM & E
Oprm1-203	P42866	CCDS78787		6,758,593-6,849,858	PM & E
Oprm1-204	P42866	CCDS78785	10	6,758,593-7,037,546	PM & E
Oprm1-205	A0A0R4J0Z2	-	-	6,788,809-6,832,987	PM & E
Oprm1-206	P42866	-	-	6,788,809-6,841,362	PM & E
Oprm1-207	P42866	-	-	6,788,809-6,839,919	PM & E
Oprm1-208	P42866	CCDS78787		6,758,593-6,849,858	PM & E
Oprm1-209	Q4U2P0	-	-	6,758,593-6,849,858	PM & E
Oprm1-210	A1KZZ4	-	-	6,788,694-7,037,177	PM & E
Oprm1-211	P42866	CCDS83674	10	6,788,809-6,830,639	PM & E
Oprm1-212	E9Q7D4	-	-	6,788,837-6,832,793	PM & E
Oprm1-213	E9Q7D3	-	-	6,788,837-6,839,954	PM & E
Oprm1-214	P42866	CCDS83673	10	6,788,809-6,841,537	PM & E
Oprm1-215	P42866	CCDS78787	10	6,758,593-6,850,613	PM & E
Oprm1-216	P42866	CCDS56687	10	6,788,809-7,038,198	PM & E
Oprm1-217	P42866	CCDS78784	10	6,758,506-7,037,201	PM & E
Oprm1-218	A1KZZ4	-	-	6,788,809-6,979,764	PM & E
Oprm1-219	E9PVC1	-	-	6,788,809-7,037,462	PM & E
Oprm1-220	E9QAQ1	-	-	6,788,809-7,037,177	PM & E
Oprm1-221	-	-	-	6,789,025-6,828,911	PM & E
Oprm1-222	P42866	-	-	6,788,809-6,979,754	PM & E
Oprm1-223	-	-	-	6,788,975-7,037,482	PM & E
Oprm1-224	Q4U2P9	-	-	6,758,593-6,828,964	PM & E
Oprm1-225	P42866	-	-	6,788,809-7,037,482	PM & E
Oprm1-226	P42866	CCDS78783	10	6,758,506-6,979,704	PM & E
Oprm1-227	-	-	-	6,789,099-6,849,987	PM & E
Oprm1-228	Q4U2P1	-	-	6,758,593-6,849,858	PM & E
Oprm1-229	E9Q270	-	-	6,788,601-6,850,348	PM & E
Oprm1-230	P42866	CCDS83672	10	6,788,809-6,841,380	PM & E
Oprm1-231	E9Q2X5	-	-	6,788,809-7,037,198	PM & E

**Abbreviation and symbols:** CDD, conserved domain database of NCBI, Location, chromosomal location of the genes; Position, chromosome positions comprising the coding region for start and end positions; PM: plasma membrane, E: endosome.

#### 4.1.5 Splicing and generation of different variants

Different transcript variants of mu receptors are generated by splicing of different exons. In all there are 16 exons in OPRM1 and 31 splice variants are generated from splicing of various exons as depicted in (Fig. 4.6). In mice OPRM-1 transcript variants the amino acid length varies from 39 (MOR-1K) to 474 (MOR-1U) with molecular weight of 52 kDA and 37 kDA respectively. The position of variants for splicing varies in between 387 to 398 at 3' end and 1 to 94 at 5' end (Table 4.5). Among the different exons in mice MOR-1 gene, exon 11 is the major exon associated with 5' p splicing and is located approximately 30 kb upstream of exon 1 (Pan *et al.*, 2001). Exon 11 contains its own promoter distinct from the promoter of exon 1. The majority of exon 1-associated variants undergo alternative 3' splicing at tip of C-terminal in which exon 4 is replaced by a series of alternative exons. Based on splicing at particular exons the different transcript variants can be categorised in three groups.

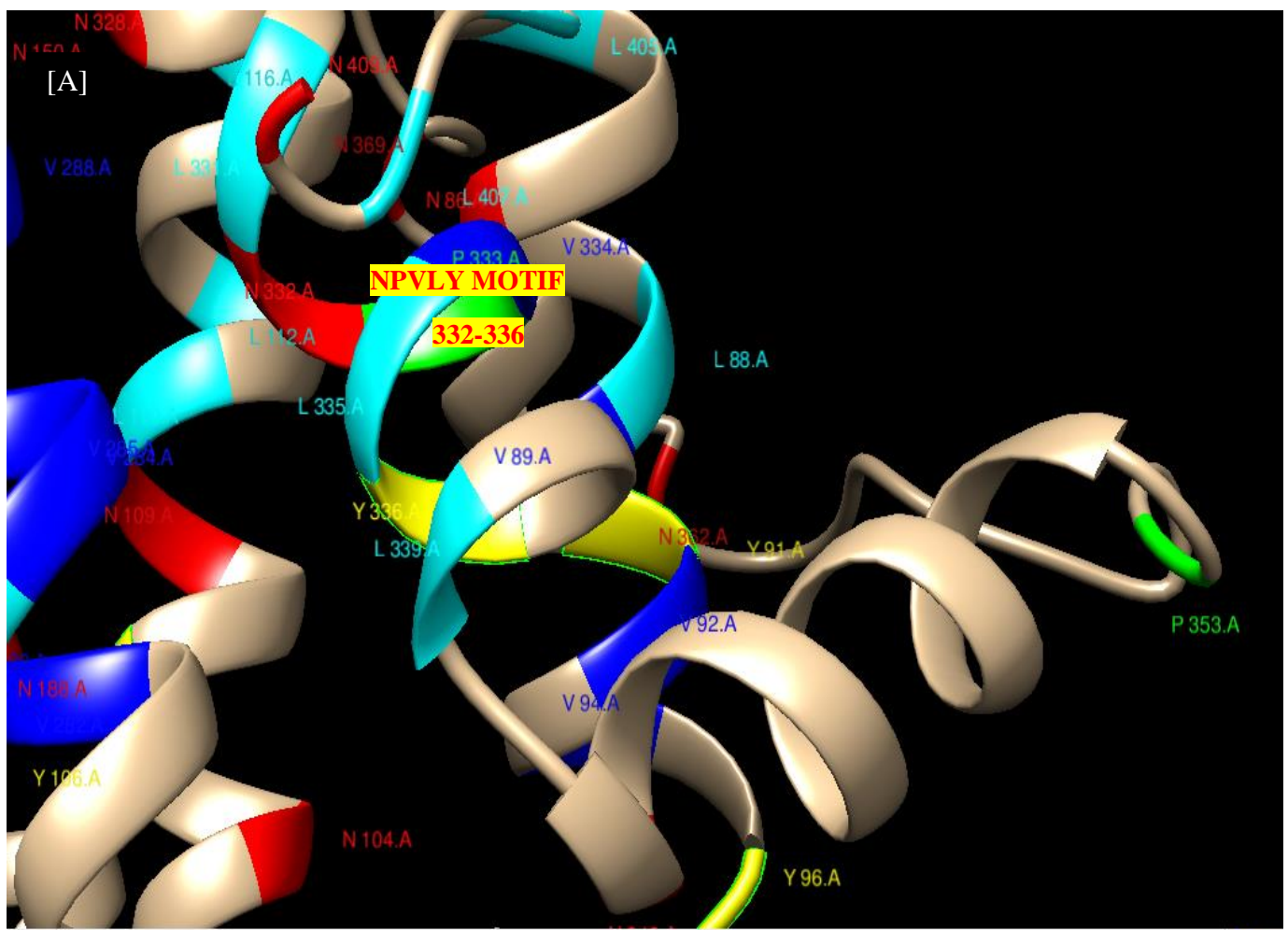
Group 1 consisted of 7TM transcript variants (MOR-1, MOR-1A, MOR-1B1-1B2, 1B3, 1B4 & 1B5, MOR-1C, MOR-1D, MOR-1F, MOR-1Ei, MOR-1Eii, MOR-1Eiii, MOR-1Eiv MOR-1V, MOR-1W, MOR-1P, MOR-1O, MOR-1I, MOR-1J and MOR-1H) resulting from splicing of exon 1. All the full length 7TM transcript variants contain exon 1, 2 and 3 which encodes the entire MOR-1 receptor except for the tip of C-terminal 12 amino acid. Due to this sequence similarity, MOR-1 transcript variants share, identical binding pockets as well as intra- and extracellular loops ((Bare, *et al.*, 1994, Zimprich, *et al.*, 1995, Pan *et al.*, 1999, 2005b; Pan, 2005). The mouse OPRM-1 transcript variants also contain an exon 5, alternative splicing in exon 5 generates five different transcript variants in the mouse (MOR-1B1 through MOR-1B5) with different C-terminal amino acid sequences (Pan, 2005; Pan *et al.*, 2005b). The mice transcript variants MOR-1A, and MOR-1O are intron retention variants with silent donor splice sites in exons 3a and 7a, respectively. Alternative Splicing at exon 18 at 3' splice site that generate two different C terminal transcript variants, MOR-1V and MOR-1W (Doyle *et al.*, 2007a). In addition to exons 1, 2 and 3 which were present uniformly, additional exons were also observed in some of the 7 Tm transcript variants of OPRM1 gene such as exon 4 (MOR-1, 1I, 1J and 1T), exon 3b (MOR-1C), exon 5a (MOR-1B1, 1B2, 1B3 and 1B4), 5b (MOR-1B2, 1B3 and 1B4), and 5c (MOR-1B3 and 1B4), 5d and 5e (MOR-1B4), exon 6 (MOR-1Es, 1F, 1V and 1W), exon 7 (MOR-1C, 1Es, 1F MOR-1V, 1U and 1W), exon 7a and 7b (MOR-1O), exon 8 (MOR-1C, 1D, 1Es, 1F 1V, 1U and 1W), exon 9 (MOR-1C, 1D, 1F, MOR-1V and 1U), exon 10 (MOR-1F), exon 15 (MOR-1P), exon 18 (MOR-1W) and exon 19 (MOR-1U).

**Table 4.5 MOR transcript variants and its canonical sequence position for alternate splicing**

MOR transcript variant	Gene Name	UniProt	Length (L)	Position of variants for splicing	Mass (Da)	Residues different from Canonical sequence
MOR-1, MOR-1J, MOR-H, MOR-T	Oprm1-201, Oprm1-203, OPRM-208, Oprm1-215	P42866-1	398	387-398	44,421	LENLEAETAPLP
MOR-1A	Oprm1-211	P42866-2	390	387-398	43,563	LENLEAETAPLP → VCAF
MOR-1B1	Oprm1-214	P42866-3	391	387-398	43,759	LENLEAETAPLP → KIDLF
MOR-1B2	Oprm1-230	P42866-4	409	387-398	45,911	LENLEAETAPLP → KLLMWRAMP TFKRHLAIMLSLDN
MOR-1B3, MOR-1Q	Oprm1-207	P42866-5	392	387-398	43,786	LENLEAETAPLP → TSLTLQ
MOR-1B4, MOR-1R	Oprm1-201	P42866-6	425	387-398	47,752	LENLEAETAPLP → AHQKPQECL KCRCLSLTILVICLHFQHQFFIMIK KNVS
MOR-1B5, MOR-1P	Oprm1-206	P42866-7	388	387-398	43,345	LENLEAETAPLP → CV
MOR-1C	Oprm1-216	P42866-8	438	387-398	48,753	LENLEAETAPLP → PTLAVSVAQIF TGYPSPHVEKPKCKSCMDRGMNRN LLPDDGPRQESGEGQLGR
MOR-1D	Oprm1-213	P42866-9	393	387-398	43,942	LENLEAETAPLP → RNEEPSS
MOR-1E, MOR-1Eiii, MOR-1iv	Oprm1-210	P42866-10	401	387-398	44,848	LENLEAETAPLP → KKKLDSQRG CVQHPV
MOR-1F	Oprm1-211	P42866-11	444	387-398	49,094	LENLEAETAPLP → APCACVPGAN RGQTKASDLLDLELETVGSQAD AETNPGPYEGSKCAEPLAISLVPLY
MOR-1O	Oprm1-222	P42866-12	416	387-398	46,388	LENLEAETAPLP → PTLAVSVAQIF TGYPSPHVEKPKCKSCMDR
MOR-1P, MOR-1R	Oprm1-213, Oprm1-218	P42866-13	453	387-398	50,715	LENLEAETAPLP → IMKFEAIYPKL RHMGPSYPS
MOR-1G	Oprm1-226	P42866-14	330	1-94	37,958	MDSSAGPGNIGNFLVMYVIV → M MEAFSKSAFQKLRQRDGNQEGKS YL
MOR-1M	Oprm1-217	P42866-15	370	1-94	42,290	MDSSAGPGNIGNFLVMYVIV → M MEAFSKSAFQKLRQRDGNQEGKS YL
				387-398		LENLEAETAPLP → PTLAVSVAQIF TGYPSPHVEKPKCKSCMDRGMNRN LLPDDGPRQESGEGQLGR
MOR-1N	Oprm1-204	P42866-16	325	1-94	37,479	MDSSAGPGNIGNFLVMYVIV → M MEAFSKSAFQKLRQRDGNQEGKS YL
				387-398		LENLEAETAPLP → RNEEPSS
MOR-1U	Oprm1-217	P42866-17	474	387-398	52,982	LENLEAETAPLP → PTLAVSVAQI QESGEGQLGR
MOR-1V	OPRM-218	P42866-18	420	387-398	47,197	LENLEAETAPLP → KQEKTKTKSA WEIWEQKEHTLLGETHLTIQHLS
MOR-1W	Oprm1-225	P42866-19	399	388-398	44,654	ENLEAETAPLP → AFGCCNEHHDQ R
MOR-1K	Oprm1-209	Q4U2PO	39		4562,28	
MOR-1L	Oprm1-228	Q4U2P1	41		4936,86	
MOR-1Ha	Oprm1-224	Q4U2P9	84		4936,86	
M-OR-1	OPRM1-205	A0A0R4J0Z2	456		51,022.88	

The composition of exon in transcript variants MOR-1Eii, MOR-1Eiii and MOR-1Eiv is identical to that of MOR-1E, except for an insertion of exon 19 between exons 7 and 8. In addition to some of 7 TM transcript variants of mu-opioid receptor gene with predicted protein sequences identical to MOR-1 (MOR-1H, MOR-1i and MOR-1J).

Group 2 (Six trans-membrane domain variants) consisted of truncated 6TM transcript variants (MOR-1G1, MOR-1M, MOR-1N, MOR-1L, MOR-1K) resulting from splicing of exon 11 and due to skipping of exon 1, these are categorised as 6TM transcript variants. The most of the truncated 6 TM transcript variants of OPRM1 gene also contain additional exon such as mice MOR-1G has a terminal exon 4, MOR-1M has exons 7/8/9, the same 3' composition as MOR-1C, and MOR-1N has exons 8/9, the same 3' composition as MOR-1D (Pan *et al.*, 2001, 2005b). Although MOR-1K and MOR-1L also lack exon 1, some additional exon in between exon 11 and 2 (exon 13 (MOR-1K) and exon 14 (MOR-1L) were also observed.



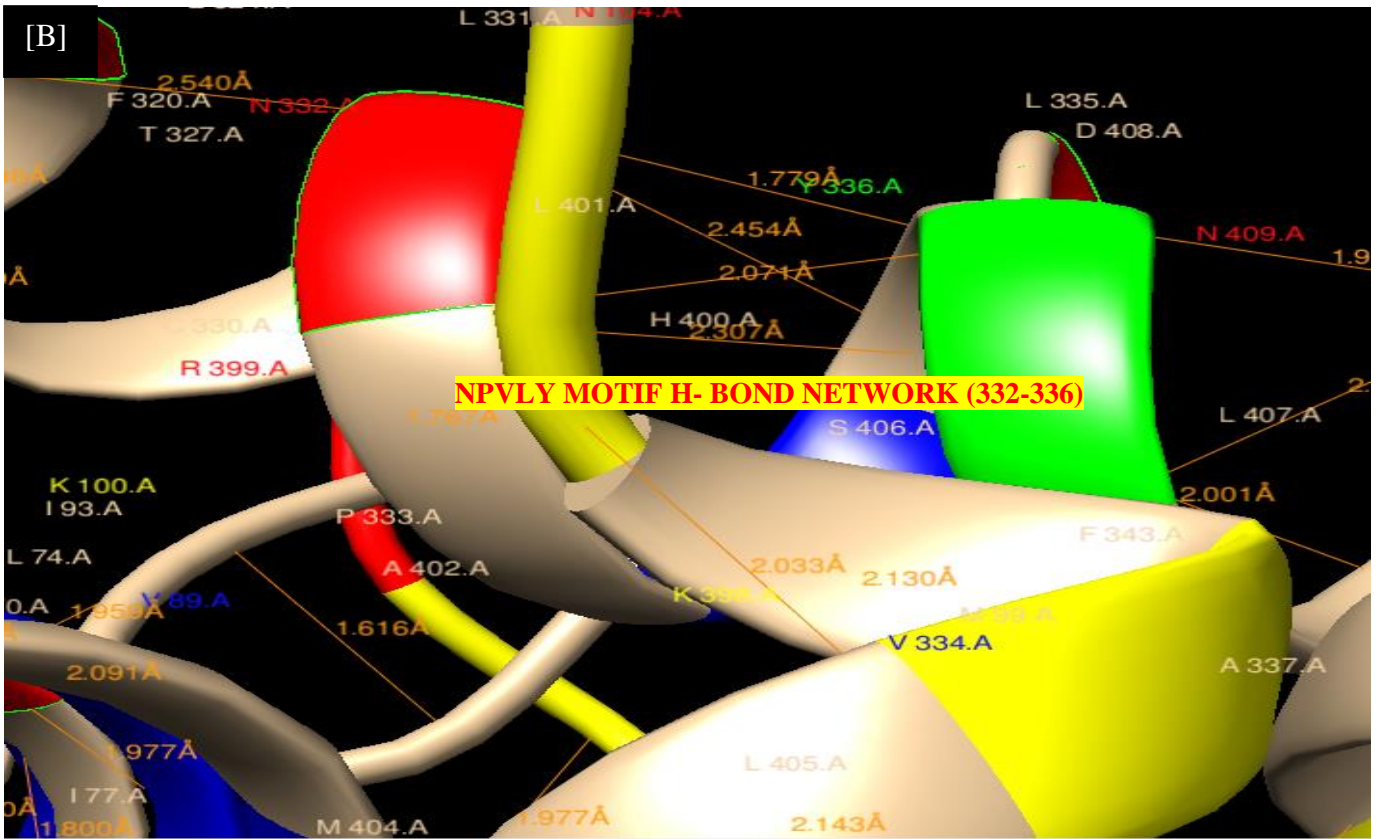


**Fig.4.4 [A &B] Interaction near the NPxxY motif.** The polar network ends at the cytoplasmic surface with a web of interactions involving the conserved NPxxY sequence

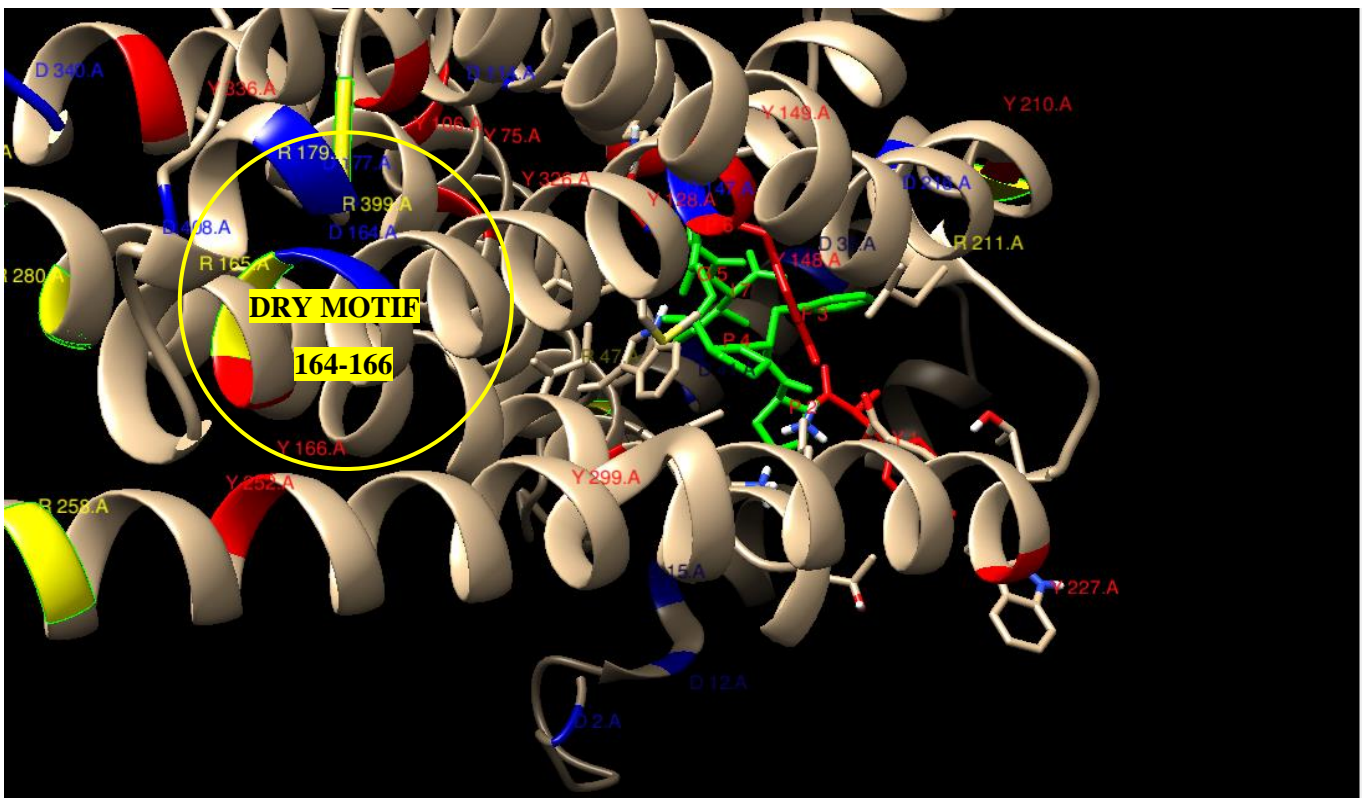


**Fig.4.5 G-protein couple receptor (GPCRs) DRY motif**

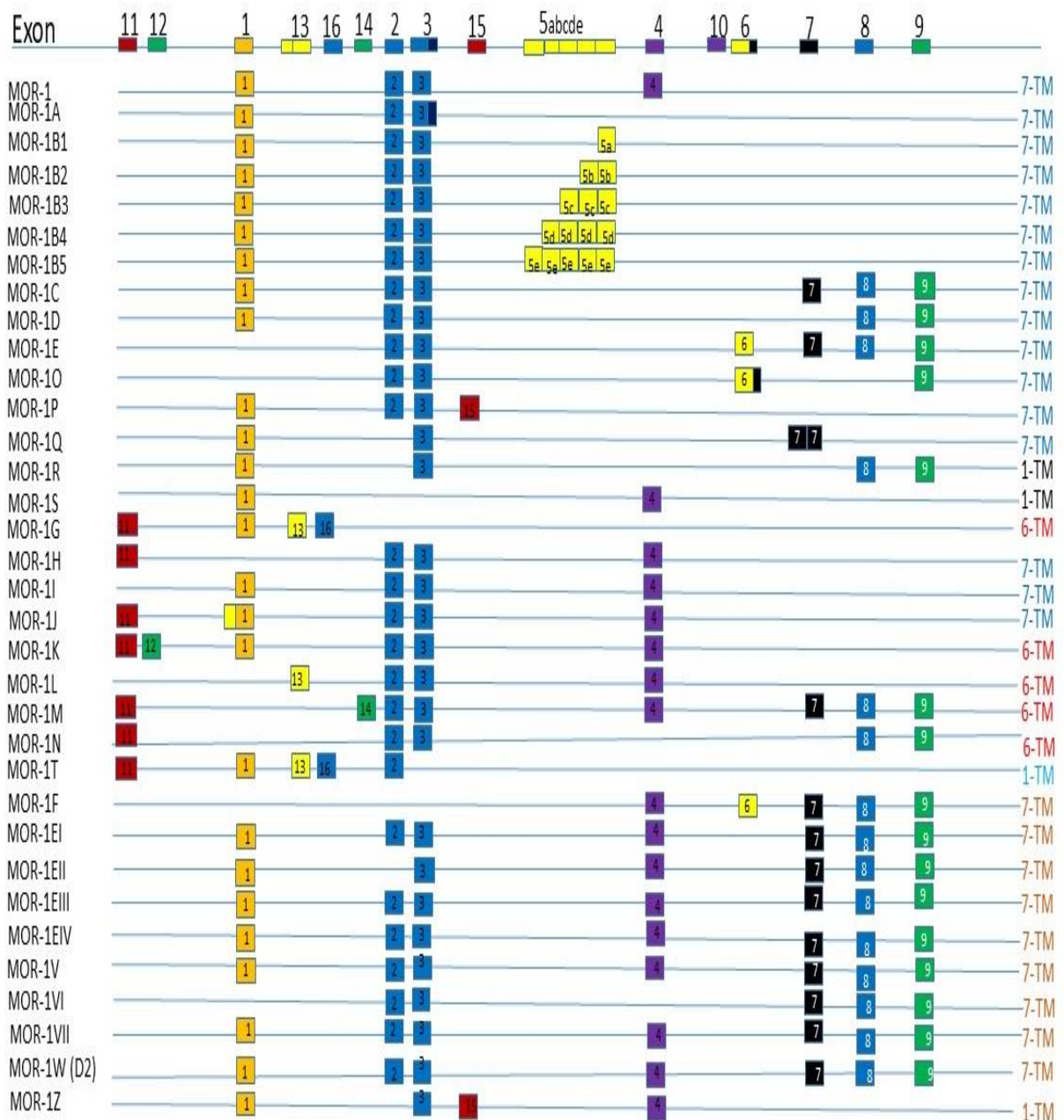


**Fig.4.6:** Splice variants of OPRM-1 gene generated from splicing at different exons

Group 3 (Single trans-membrane domain variants) consisted of transcript variants with one trans-membrane domain (1TM) have been identified in mice rats and humans, which is encoded by exon 1 (Du *et al.*, 1996, 1997; Kvam *et al.*, 2004; Pan, 2005; Pan and Pasternak, 2011; Xu *et al.*, 2013). The 1TM mouse transcript variants of OPRM-1 gene have been identified, which are generated by exon skipping and are associated with the exon 1 promoter (Pan and Pasternak, 2011; Xu *et al.*, 2013). Five single TM mouse variants such as (MOR-1S, MOR-1R MOR-1Q, MOR-1T and MOR-1Z) that result from the splicing at exon 1 but unlike group 1, these lack exons 2 and 3. The most of the truncated 1Tm transcript variants of

OPRM1 gene contain additional exon including exon 1a (MOR-1H), exon 1b (MOR-1i) and exon 12 (MOR-1j).

#### **4.1.6 Sequence homology of OPRM-1 across and within species**

ClustalW alignment of the opioid receptors across different species that is mice, rat, human and cow, showed a high degree of sequence similarity. Mice MORs shared 97.7% homology with rat MOR followed by 93.8% and 91.5 % homology with human and cow MOR respectively (Fig. 4.7). Key residues like DRY motif at alignment positions 189–191 (Minami and Satoh *et al.*, 1995; Gether *et al.*, 2000) and the conserved Cys-Cys bridge between EL1 and EL2 provided by residues at 165 and 245 (Palczewskiet *al.*, 2000), which are crucial for the functioning of opioid receptors, were homologous across species. The agonist binding of GPCRs is regulated by sodium ions, which binds at Asp in the TM2 domain (Christopoulos and Kenakin *et al.*, 2002). This particular binding site for Na<sup>+</sup> site was found to be conserved across the species. Further, among these MOR proteins from four species, trans-membrane domains and the three intracellular loops, important for MORs ligand binding and G protein coupling showed highest homology. The most divergent region was N-terminus, followed by the C-terminus and second/third extracellular loop domains. Pasternak and Pan (2013) have also reported 60–70% homology of MOR-1 with other opioid receptor families, particularly at trans- membrane and intracellular loop regions at the amino acid level.

Mammalian MORs contains the extended eleven amino acid sequence (C-terminus extension; alignment positions 419–429), as compared to the non-mammalian species. Phosphorylation of Thr at position 425 in this extended sequence is considered essential for internalization and desensitization (Wang *et al.*, 2002). This ‘add-on’ piece of protein represents translation of exon 4 and was observed only in of rat mu opioid receptors and was lacking in hMOR and mMOR splice variants. Similar results have also been reported by other workers (Pan *et al.*, 2003 and 2005).

ClustalW alignment of the different splice variants of mice OPRM-1 was also carried out (Fig 4.8). The homology search revealed that amongst the 19 splice variants, (MOR-1, MOR-1A, MOR-1B1-1B2, 1B3, 1B4 & 1B5, MOR-1C, MOR-1D, MOR-1F, MOR-1Ei, MOR-1Eii MOR-1Eiii, MOR-1Eiv, MOR-1Q, MOR-1V, MOR-1W, MOR-1P, MOR-1O) have sequence homology from amino acid position 1-360 that is the region including exon 1-3. Variations

across these receptors were observed at exon 4, however, sequence for Motifs NPXXY (NPVLY) and DRY was conserved in all the 7 transmembrane domains.

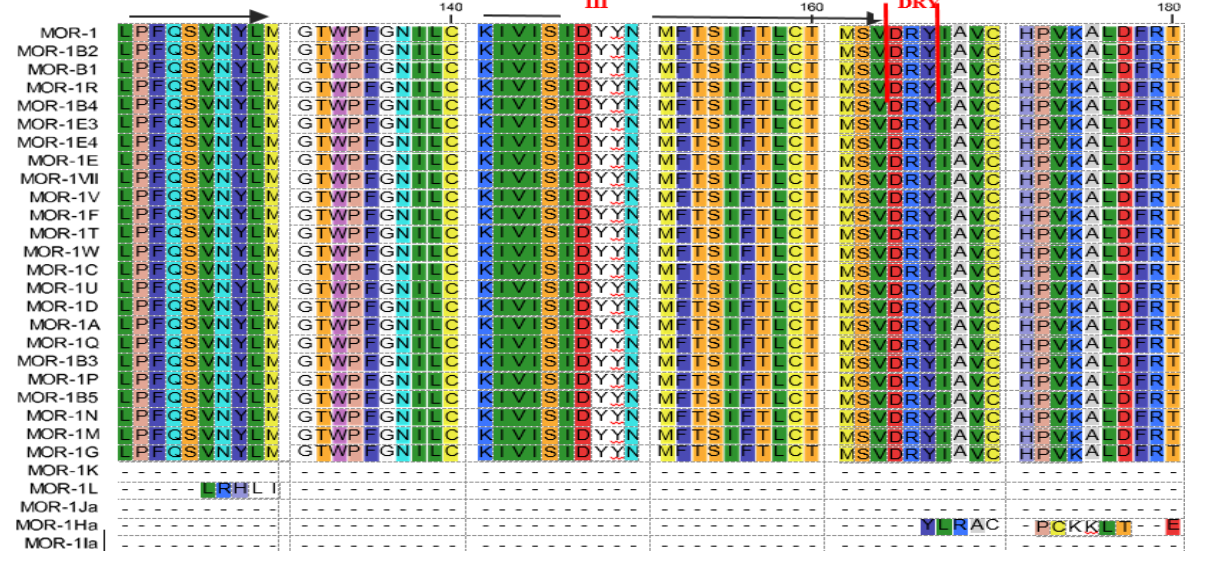
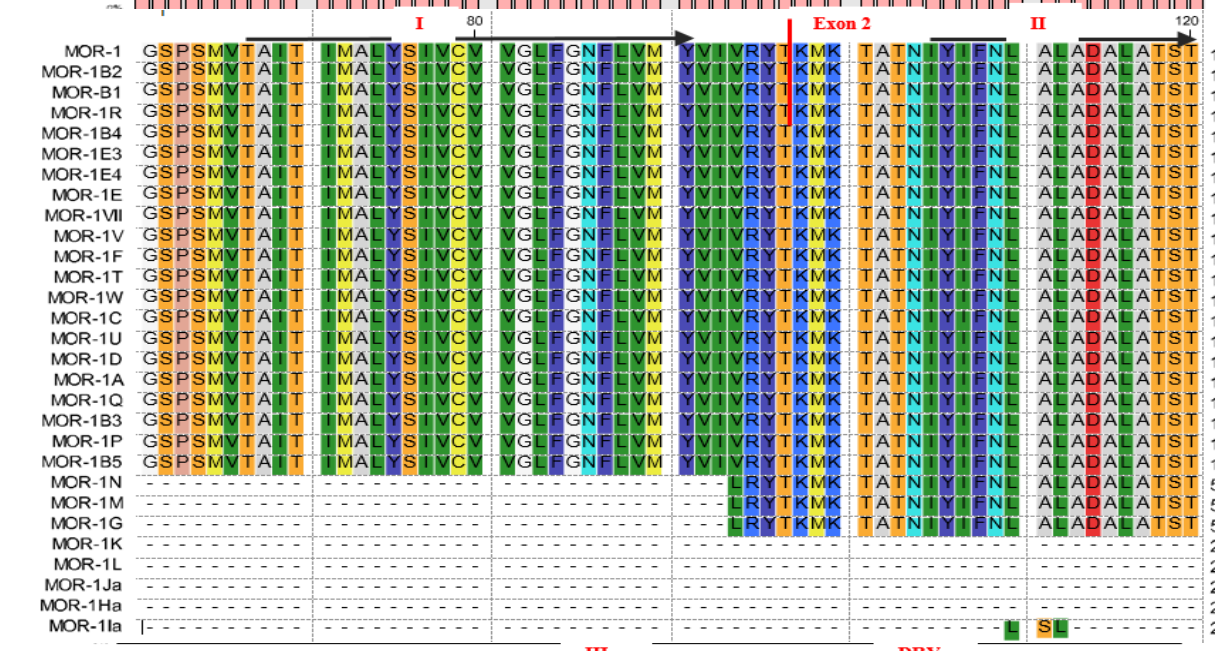
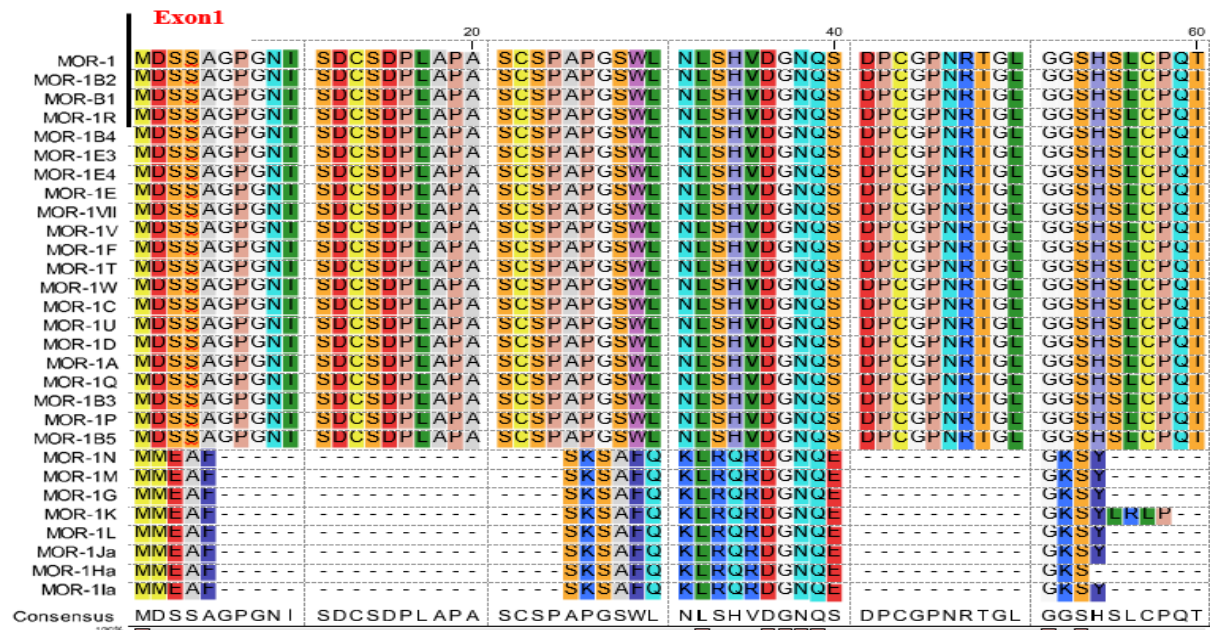
The transcript variants; MOR-1G1, MOR-1M and MOR-1N, had sequence similarity from amino acid position 1 to 386. Within mice splice variants, maximum homology was observed between MOR-1 and MOR-B1 (98%). Similar to across species results, trans-membrane domains and the three intracellular loops showed highest homology while N-terminus, followed by the C-terminus and second/third extracellular loop domains were the most divergent regions within mice transcript variants as well.

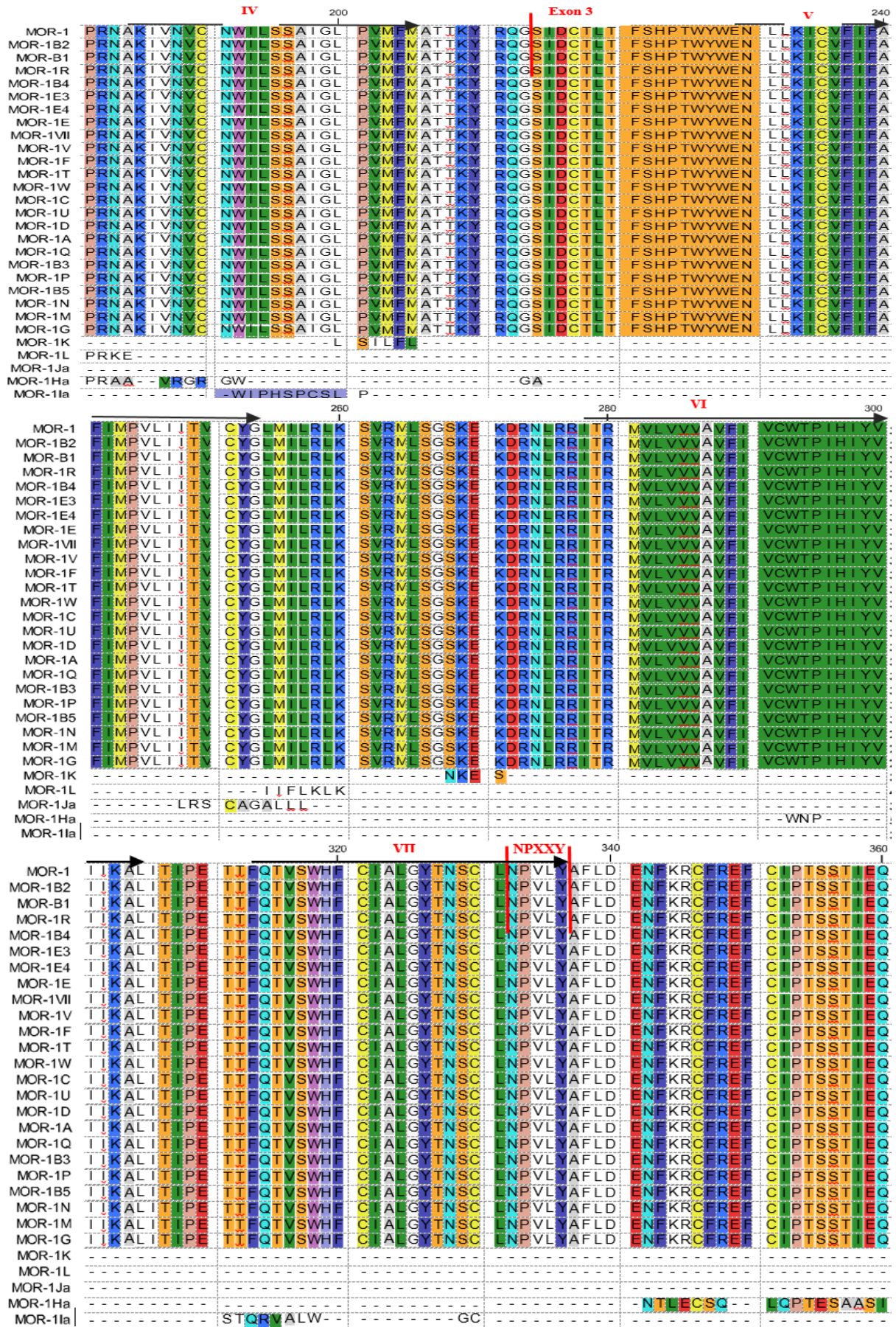
#### **4.1.7 Phylogenetic analysis**

The phylogenetic trees were constructed using the Neighbour-Joining (NJ) methods of distance procedure to find the branching pattern among the identified  $\mu$ -opioid receptor gene (Fig 4.8). The phylogenetic trees obtained using nucleotide and amino acid sequences showed the same grouping pattern with three major groups. Group I consisted to 7TM receptors (MOR-1W, MOR-1F, MOR-1P, MOR-1B5, MOR-1Q, MOR-1B3, MOR-1R, MOR-1B4, MOR-1B2, MOR-1VII, MOR-1V and MOR-1B1) while group II had receptor 1E and its isoforms (MOR-1E, MOR-1E3 and MOR-1E4).

Group III was the most divergent group consisting of receptors belonging to different categories that 7TM, 6TM as well as 1TM (MOR-1A, MOR-1U, MOR-1C, MOR-1, MOR-1T, MOR-1G, MOR-1M, MOR-1Ia, MOR-1K, MOR-1L, MOR-1Ja, MOR-1Ha, MOR-1N and MOR-1D). It might be due to their similar exonic structure. Similarly, the placement of MOR1E<sub>(s)</sub> in one group could be explained as these are the only variants which have exon 19.

The distance matrix revealed the maximum divergence (0.180) between MOR1F and MOR1M; while MOR1 and MOR1D showed least distance (Table 4.6). Overall, the receptors within 7TM group showed least divergence whereas maximum distance was observed between receptors belonging to group 1 that is 7TM and group 2 consisting of 6TM receptors.





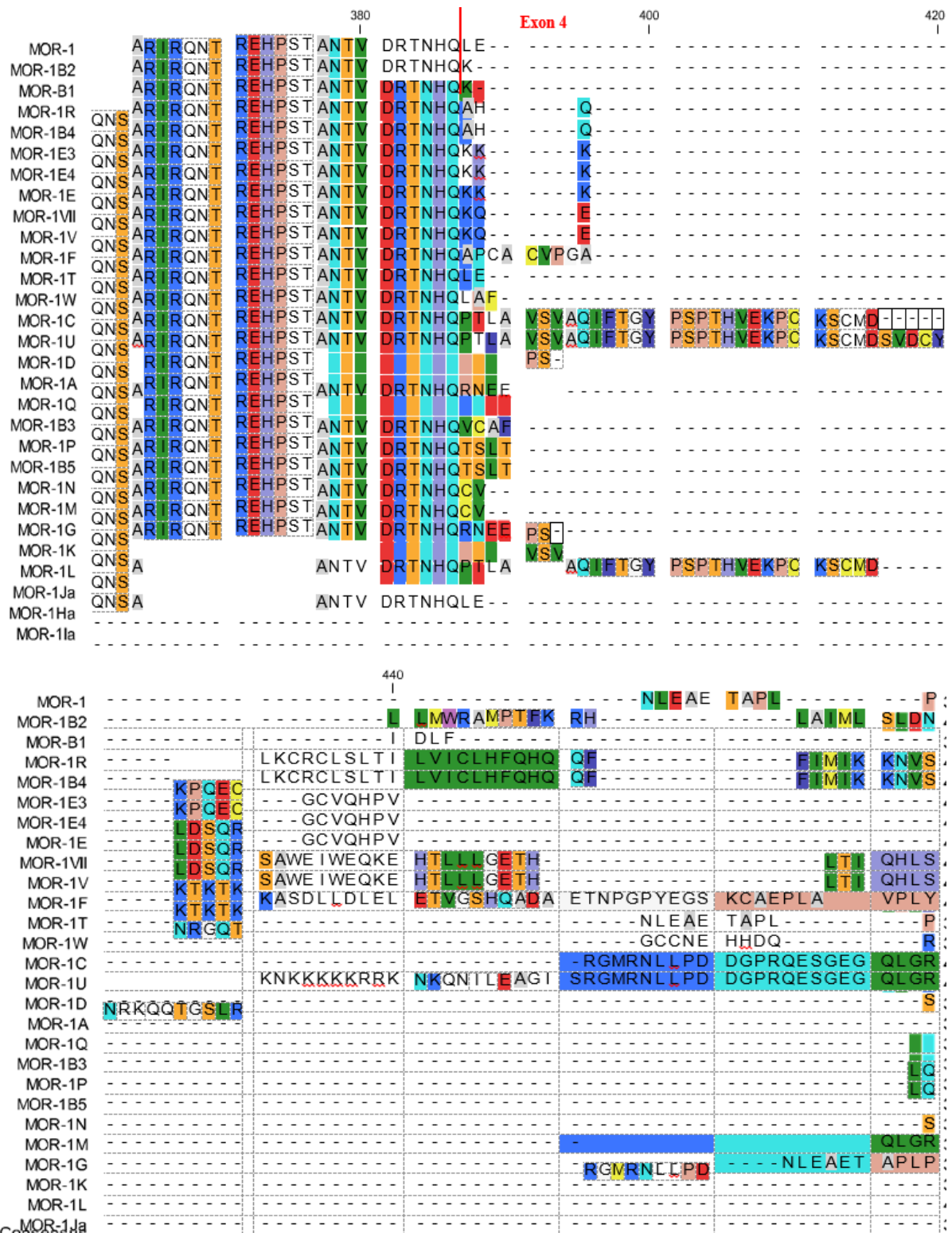


**Fig. 4.7** Alignment of OPRM-1 gene transcripts based on amino acid sequences. *The trans- membrane domains are shown by the underlined regions.*

**Table 4.6 Estimates of evolutionary divergence between amino acid sequences of different MOR receptors**

	1	2	3	4	5	6	7	8	9	10	11	12	13	14	15	16	17	18	19	20
1]																				
2]	0.058																			
3]	0.070	0.028																		
4]	0.055	0.008	0.010																	
5]	0.058	0.000	0.028	0.008																
6]	0.055	0.003	0.010	0.003	0.003															
7]	0.082	0.031	0.050	0.013	0.031	0.018														
8]	0.028	0.092	0.115	0.071	0.092	0.077	0.047													
9]	0.055	0.005	0.010	0.008	0.005	0.003	0.008	0.064												
10]	0.016	0.058	0.071	0.055	0.058	0.055	0.067	0.012	0.055											
11]	0.067	0.023	0.038	0.003	0.023	0.015	0.072	0.141	0.003	0.064										
12]	0.055	0.005	0.023	0.013	0.005	0.013	0.033	0.095	0.010	0.055	0.018									
13]	0.067	0.028	0.050	0.010	0.028	0.018	0.079	0.150	0.010	0.067	0.050	0.033								
14]	0.085	0.025	0.053	0.013	0.025	0.018	0.105	0.180	0.005	0.077	0.086	0.028	0.070							
15]	0.071	0.028	0.036	0.005	0.028	0.003	0.038	0.101	0.005	0.067	0.028	0.008	0.028	0.030						
16]	0.071	0.028	0.036	0.005	0.028	0.003	0.038	0.101	0.005	0.067	0.028	0.008	0.028	0.030	0.000					
17]	0.058	0.000	0.028	0.008	0.000	0.003	0.031	0.092	0.005	0.058	0.023	0.005	0.028	0.025	0.028	0.028				
18]	0.082	0.031	0.050	0.013	0.031	0.018	0.000	0.047	0.008	0.067	0.072	0.033	0.079	0.105	0.038	0.038	0.031			
19]	0.082	0.031	0.050	0.013	0.031	0.018	0.000	0.047	0.008	0.067	0.072	0.033	0.079	0.105	0.038	0.038	0.031	0.000		
20]	0.067	0.028	0.050	0.010	0.028	0.018	0.079	0.150	0.010	0.067	0.050	0.033	0.000	0.070	0.028	0.028	0.028	0.079	0.079	

1: MORIG, 2: MORIVII, 3: MORIB2, 4: MORB1, 5: MORI, 6: MORID, 7: MORIU, 8: MORIM, 9: MORIA, 10: MORIN, 11: MORIR, 12: MORIW, 13: MORIV, 14: MORIF, 15: MORIE3, 16: MORIE4, 17: MORIT, 18: MORIP, 19: MORC, 20: MORI-K

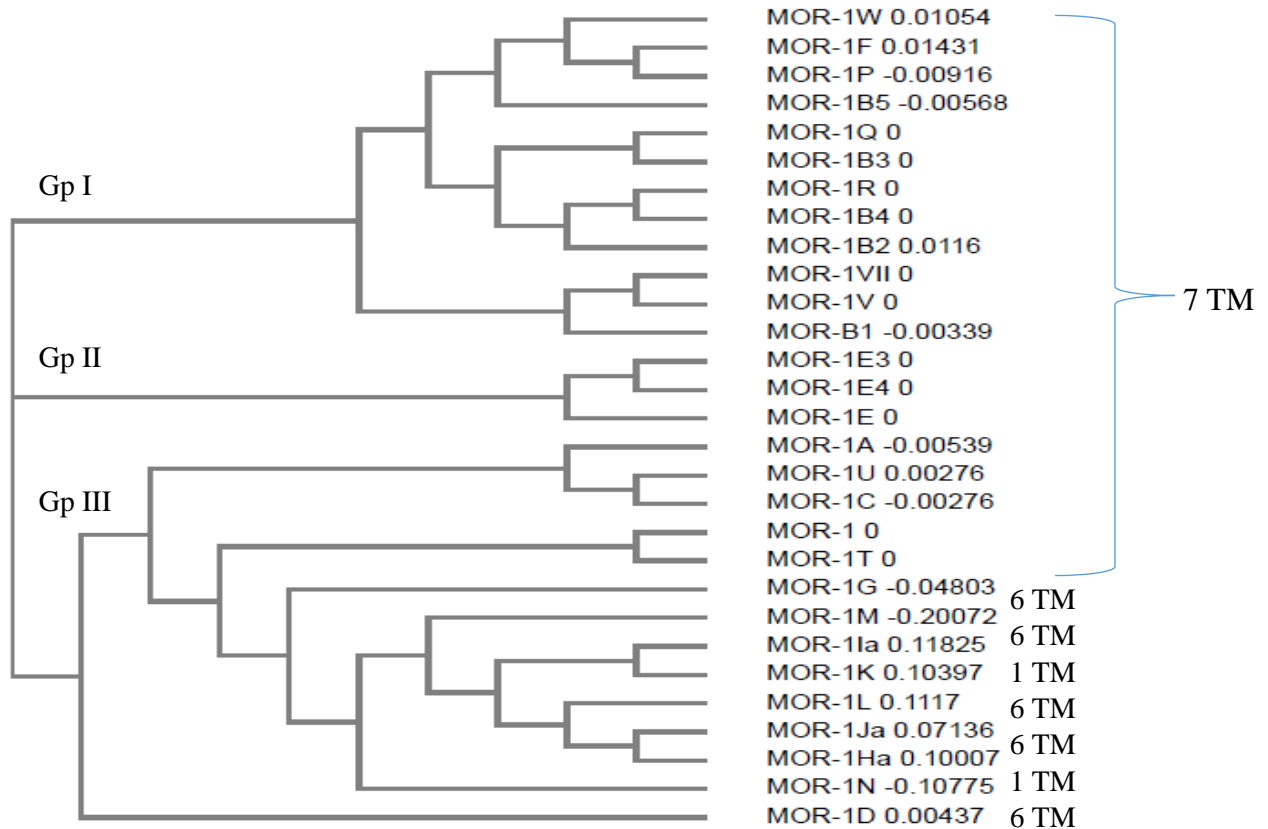


**Fig.4.8** Amino acid based phylogenetic analysis of OPRM-1 transcript variants

#### 4.1.8. Physicochemical properties and the abundance of amino acids in MORs transcript variants protein

Various physiological parameters of MOR-1 protein were predicted by ProtPram Server. The *Mus musculus* reference amino acid sequence consisted of 398 amino acids with 44420.98 Dalton molecular weight and theoretical pI value of 8.62. The speculated formula for the protein is C<sub>2005</sub>H<sub>3139</sub>N<sub>519</sub>O<sub>557</sub>S<sub>31</sub> and their half-life is 30 hours (mammalian reticulocytes, *in vitro*). Total numbers of positive and negative residues were 30 and 23, respectively. Leucine was the most abundant amino acids (9.0 %) in predicted structure of mice MOR-1, followed by isoleucine, threonine and serine with a percentage of 8.8, 8.5, and 8.0, respectively. Tryptophan (1.8 %) and histidine (2 %) were the least abundant residues with and followed by glutamate, asparagine, lysine and glutamine, which contributed 2.5, 2.5 and 3.3 percent to MOR-1 structure, respectively. The physicochemical parameters predicted the protein to be a charged protein as a result of high number of positively charged residues (arginine /lysine= 30) and negatively charged residues (aspartic acid and glutamic acids=23). Overall the the protein was observed to be acidic as indicated by the isoelectric point value of 8.62. Also, the instability index of 36.42 indicated the stability of identified model of MOR-1 as proteins with instability index of < 40 regarded are considered as stable proteins.

**Table 4.7 Physicochemical properties of  $\mu$ -opioid receptor transcript variants.**

MORs	Amino acid	Mol. wt	Theoretical P.I	Instability index	Aliphatic index	GRAVY
MOR-1	398	44420.98	8.62	36.42	97.71	0.318
MOR-1A	390	43563.08	8.84	35.78	97.21	0.361
MOR-1B2	409	45911.00	9.06	36.83	97.95	0.328
MOR-1C	438	48752.91	8.80	37.03	92.56	0.216
MOR-1M	370	42289.54	9.33	34.64	90.62	0.085
MOR-1N	325	37478.98	9.38	35.95	93.88	0.149
MOR-1U	474	52981.85	9.31	41.32	89.64	0.063
MOR-1D	393	43942.35	8.79	38.39	95.47	0.283
MOR-1mRNA	398	44420.98	8.62	36.42	97.71	0.318
MOR-1B1	391	43759.32	8.86	35.69	97.95	0.341
MOR-1G	330	37957.61	9.25	33.61	96.61	0.193

The aliphatic index (97.71), and grand average of hydropathicity (GRAVY=-0.318) also indicated the stable (Table 4.7) nature of derived protein. These properties for the other splice

variants were in similar in range as discussed for MOR-1 except MOR-1U(41.32).The hydrophobic value for all the transcript variants was >30 but varied across the variants ranging from (33.61) to ( 41.32 ). The variation in the hydrophobic values might be responsible for the differential binding affinity of the MORs to their ligands (BCM7/9) (Giuliani *et al.*, 2007).

#### 4.2:To clone MOR in Bacterial expression system for their over expression and purification

##### 4.2.1 Molecular cloning

Three proteins, mMOR-1G, mMOR-1M, and mMOR-1N, having exon 11 spliced directly to exon 2 but with differences at C termini (Bare, *et al.*, 1994, Zimprich, *et al.*, 1995, Panet *al.*,1999, 2005b; Pan, 2005)) are the major transcript variants of OPRM-1 gene. These transcript variants are spliced at both 5' and 3' end to produce pharmacologically active targets through heterodimerisation (Panet *al.*,2001). The cloning and expression of miceMOR-1M was attempted in bacterial system. To facilitate cloning, taq primers used to amplify the target gene, EcoRI site was incorporated in the forward and XhoI in the reverse primer. The amplicon was run on 1.5% percent agarose gel (Fig 4.9).

MOR FP EcoR I      GGGGAATTCATGATGGAAGCTTTCTCT  
MOR- RP Xho I      AATCTCGAGTCACCTGCCAAGCTGGCC

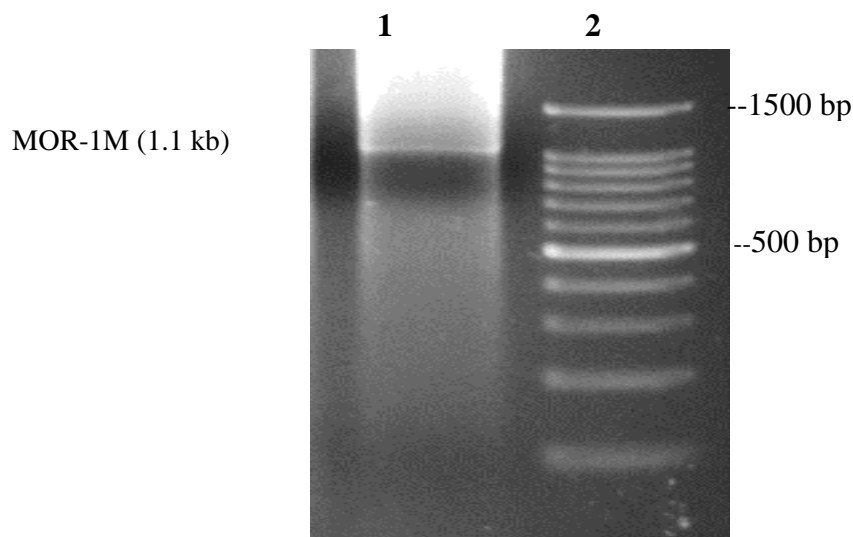


**Fig. 4.9** Electrophoresis of amplified MOR transcript variant MOR-1M (1.1 kb) on 1.5 % Agarose gel. Lane 1, MOR-1M Insert, Lane 2, DNA marker (100bp)

The single amplicon was cut from the gel and target gene DNA was purified. The final concentration of purified amplicon (MOR-1M) was 50 ng/ µl. For cloning pET 28a (+) vector system was used.It has T7 promoter and a His-tag sequence that facilitated the recombinant

protein purification using affinity chromatography. The T7 promoter is very strong promoter induced by IPTG (Sorensen HP *et al.*, 2005). The vectors (pET28a) as well as MOR-M insert were linearized after digestion with restriction enzyme EcoR I and Xho I (Fig 4.10). Ligation reaction was performed with 100 ng/ $\mu$ l linearized vector and 45ng of target gene along with ligation control at 4°C for 16hrs.

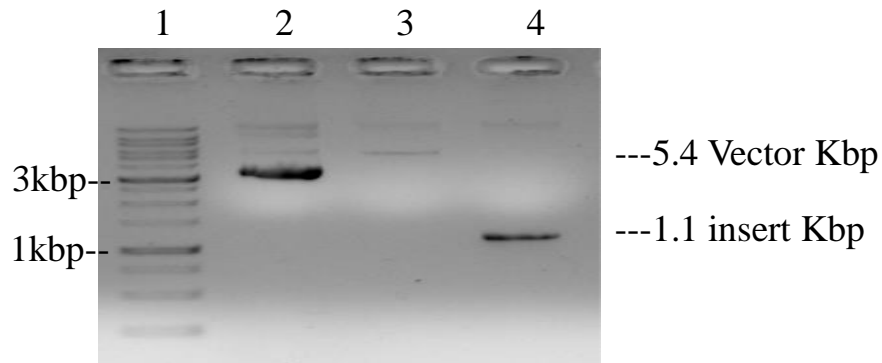


**Fig. 4.10** Preparation of Vector pET28a (+) and MOR insert after digestion with EcoR I and Xho I restriction enzyme. Lane 1, DNA Ladder (1kb), Lane 2, Uncut pET28a (+), Lane 3, pET28a Double digest (EcoR I, Xho I), Lane 4, MOR-M Insert

#### 4.2.2 Transformation of *Escherichia coli* (DH5a) with pET28a (+) containing insert

The ligation mix (vector and MOR-1M) was transformed by standard heat shock procedure. After transformation a large no. of colonies were observed on Kanamycin resistance LB plate (Fig.4.11). The cloned colonies were purified by using plasmid isolation mini kit. The purified recombinant plasmid run on 1.5 % Agarose gel is shown in (fig 4.12). The size of the recombinant plasmid was in the expected range that is ~6.5Kb.

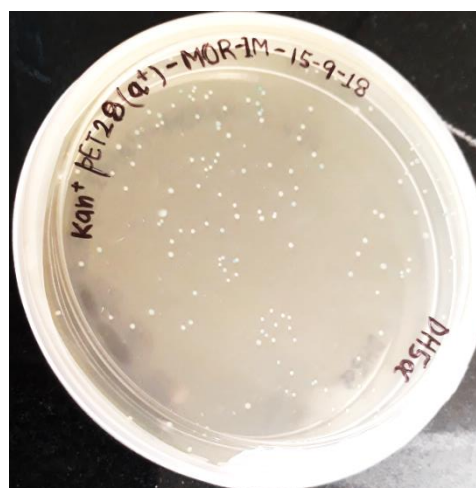


**Fig.4.11** pET 28 (a+)-MOR-1M recombinant Lb plate

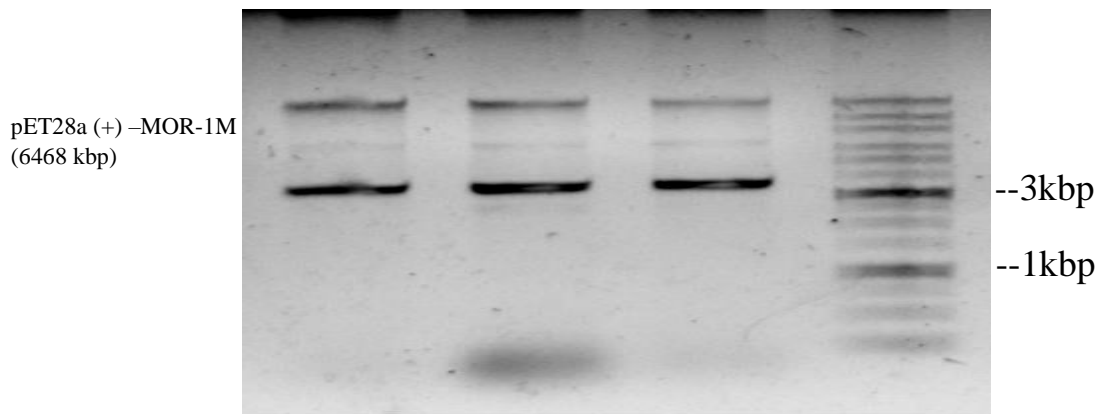


**Fig. 4.12** Electrophoresis of Cloned plasmid on 1.5% Agarose gel. Lane 1, 2 and 3, clone plasmid, Lane 4, DNA ladder (1kb).

#### 4.2.3 Analysis of pET28a (+) containing insert by restriction enzyme

Presence of insert in the recombinant clone was confirmed by double digestion with restriction enzyme EcoR I and Xho I. After restriction digestion the digested products were electrophoresed on 1.5% Agarose gel. Two intact bands of vector pET28a (+) and MOR with size 5369 and 1113 respectively (Fig. 4.13) were observed on the gel confirming the cloning of desired insert.

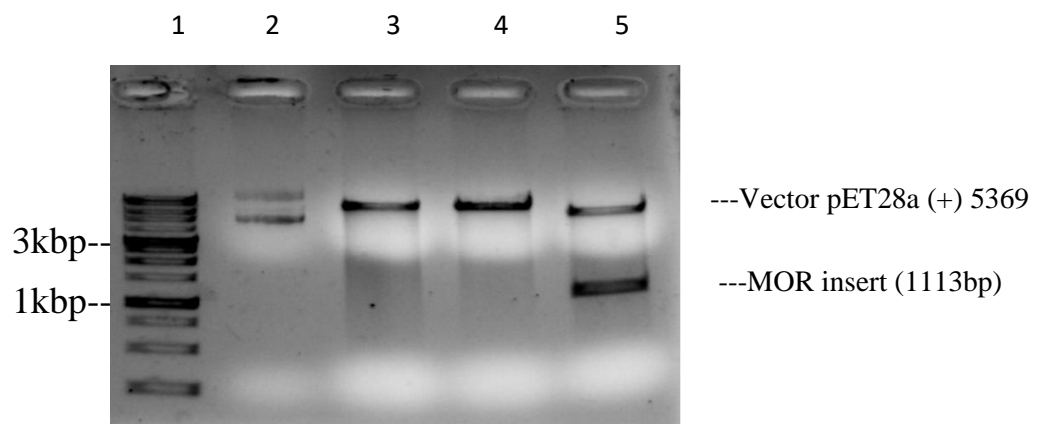


**Fig. 4.13** Electrophoresis of cloned plasmid after double digestion on 1.5% agarose gel for release of insert. Lane 1: Ladder (1Kb), Lane 2: Undigested pET28a (+)-MOR clone, Lane 3: pET28a -MOR single digested (EcoR I), Lane 4: pET28a -MOR single digested (Xho I), Lane 5: pET28a-MOR Double digest (EcoR I, Xho I).

#### 4.2.4 Expression of mice MOR in E.coli

Expression of cloned MOR-1M was checked in different host systems that is *E.coli* C41(DE3), Rosetta and BL21(DE3) cells by growing the cells in LB medium at 37°C to O.D<sub>600</sub> 0.6. The overexpression was achieved by induction with 0.4mM IPTG and cells grown at 18°C for 12-16hrs. The overexpression was achieved by induction with 0.4mM IPTG and

cells grown at 18°C for 12-16 hrs. Similar conditions have also been used in a study by (Stanisila *et al.*, 1991) wherein human  $\mu$ -receptor expression was achieved at 20°C in *E.coli* by using 0.5 mM IPTG. The N-terminal his-tagged MOR-1M was found to be produced both in inclusion bodies and in membrane-inserted form. Across the three host systems, expression of the target protein was observed in *E.coli* C41 cells only, though the level of expression was low. Similar to our findings, Ma et al (2013) tried five different host systems for over expression of human OPRM, however, low level of expression was observed in *E.coli* C41 cells both in inclusion bodies as well as membrane-inserted form. The protein as analysed on a 12% SDS-PAGE gel (Fig. 4.14) showed the correct molecular weight indicating the expression of desired induced protein.

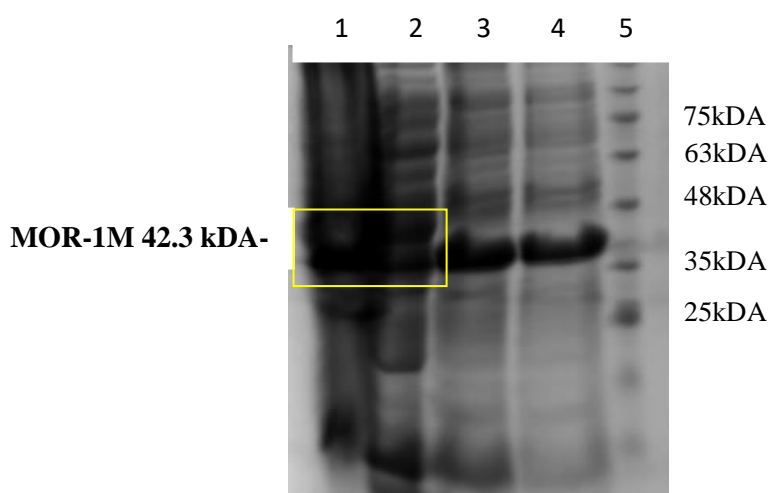


**Fig.4.14** SDS-PAGE analysis for expression of MOR protein from *E.coli* strain C41 (DE3). Lane 1, Uninduced C41 (DE3), Lane 2, Induced C41 (DE3), Lane 3, Pellet, Lane 4, Supernatant and Lane 5, protein ladder.

#### **4.2.5 MOR-1M Solubilisation and purification**

In the purification of recombinant protein, solubilisation of membrane protein is very crucial step and previous study by Grisshammer et al (1995) has indicated that addition of urea with detergent (L- laurylsarcosine) results in best solubilisation of membrane protein (Grisshammer *et al.*, 1995). After normal lysis the recombinant protein was observed in the pellet form. This pellet was solubilised using 6 M urea with 0.8% (w/v) laurylsarcosine detergents and the final concentration of mMOR-1M was observed to be ~0.2–0.3 mg/litre of culture after complete solubilisation of the protein in the membrane fraction under denaturing conditions with 6 M urea and 0.8% laurylsarcosine. The purification of MOR-1M was carried out using chelate affinity chromatography (Ni-NTA) purification process. Majority of MOR-1M was captured by Ni-NTA as revealed by Chromatogram representation of purified MOR-1 (Fig. 4.15).

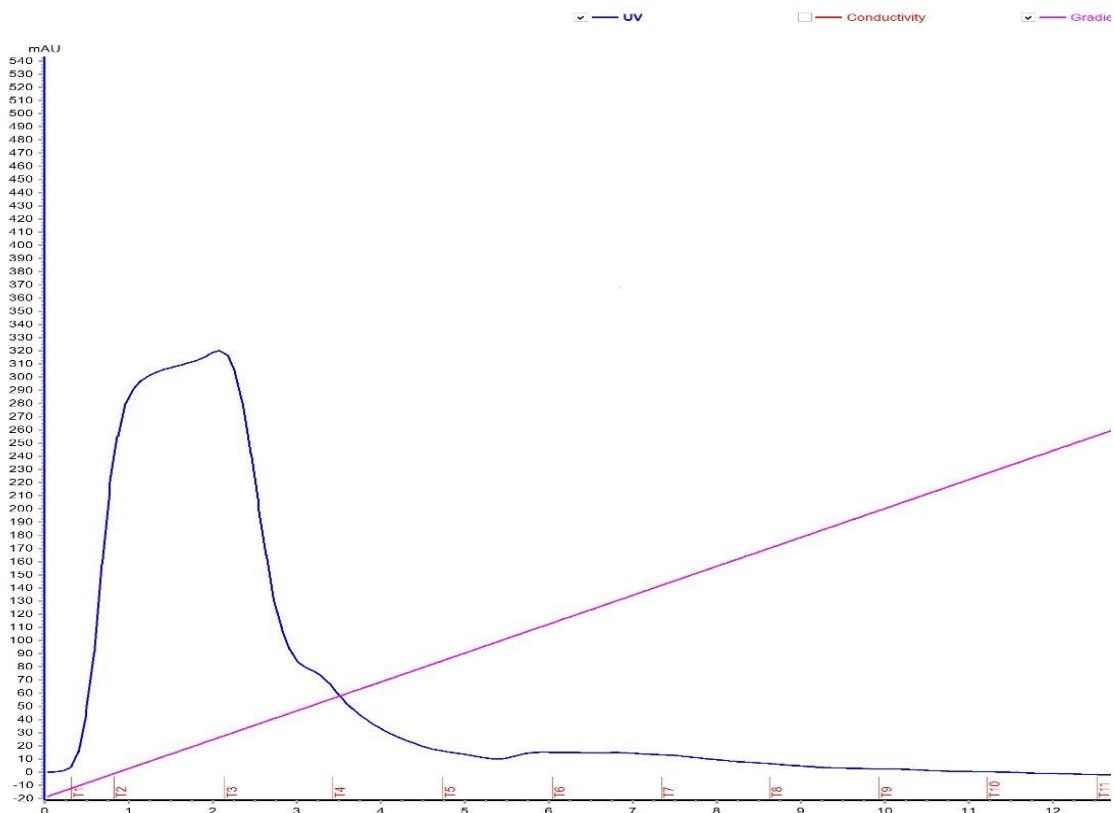


**Fig. 4.15** Chromatogram representation of purified MOR-1 protein through Hi-Trap Ni-NTA column from *E. coli* C41 (DE3)

The purified protein from fraction showing maximum abundance of the protein was run on SDS-PAGE. The size of MOR-1M receptor protein with N-terminal his-tag, was expected as 46 kDA, however the purified MOR-1M receptor protein showed a peak with molecular weight 42.3 kDA (Fig 4.16). This might be attributed to hydrophobicity and compact structure of MOR-1M. Previously, in a study on cloning and expression of human OPRM-1 with the N-terminal his-tag, the observed size of protein was 38 kDA on 12% SDS-PAGE whereas the expected size was 46 kDA (Ma *et al.*, 2013). Also, slight discrepancy between the theoretical MW and the MW observed during SDS-PAGE for the membrane protein including GPCRs is common. It might either be due to incomplete unfolding influencing electrophoretic mobility or differential binding to SDS. The observed MW of a protein might differ from the theoretical value when the protein binds more or less SDS than it should on average due to amino acid composition resulting in size range either large or small than expected (Rathet *al.*, 2009). For the MOR-1M, either of the situation might be true and hence there is a need to sequence the purified protein before using it in future for different analysis.

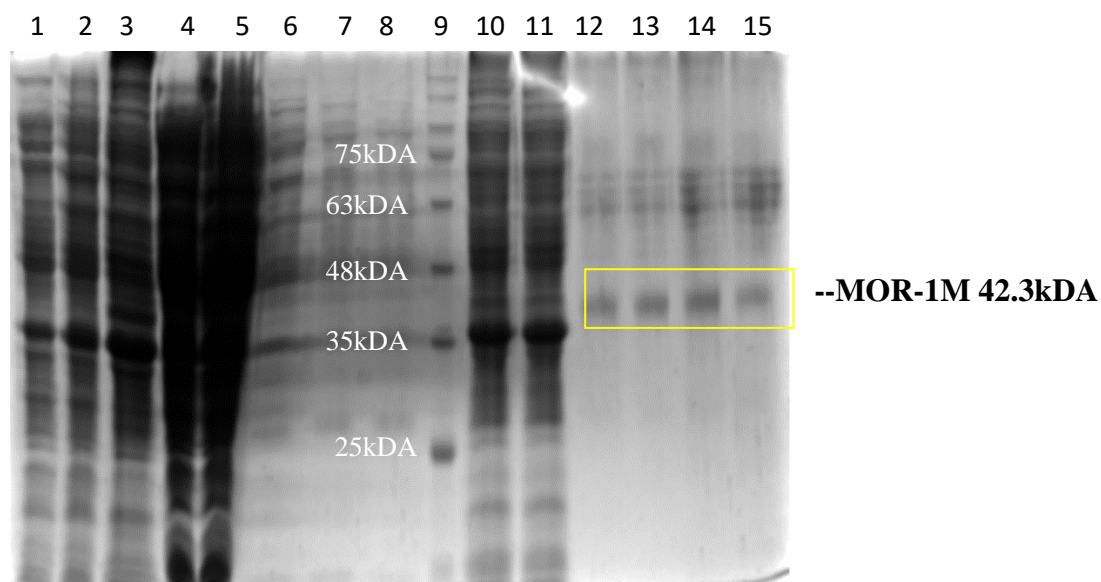


**Fig. 4.16** SDS-PAGE analysis for purified MOR protein from *E.coli* strain C41 (DE3). Lane 1, Uninduced C41 (DE3), Lane 2, Induced C41 (DE3), Lane 3, Induced Pallet C41 (DE3), Lane 4, Flow through, Lane 5, Load, Lane 6, Supernatant Fraction 2, Lane 7, Supernatant Fraction 3, Lane 8, Supernatant Fraction 4, Lane 9, Protein ladder, Lane 10, Detergent solubilized pallet flow through (FT), Lane 11, Detergent solubilized pallet load, Lane 12, Detergent solubilized fraction 3, Lane 13, Detergent solubilized fraction 4, Lane 14, Detergent solubilized fraction 5 and Lane 15, Detergent solubilized fraction 6.

#### 4.2.6 Confirmation for the binding properties of purified receptor protein

The purified protein was precipitated with Ammonium sulphate, which is commonly used for protein purification and protein separation by changing the solubility based on salt concentration. Higher concentration of protein was obtained at 40-60% ammonium salt concentration (fig.4.17), hence we did post dialysis of this particular fraction carried out in presence of low salt buffer. For purification, HiTrap Heparin HP column-strong cation exchanger for high resolution protein was used. The highest Peak was observed at 300 AU (fig.4.18) with 100% gradient. Further, the elute was run on SDS-PAGE and presence of MOR-1M protein band confirmed its binding to heparin and thus DNA binding nature (Fig. 4.19).

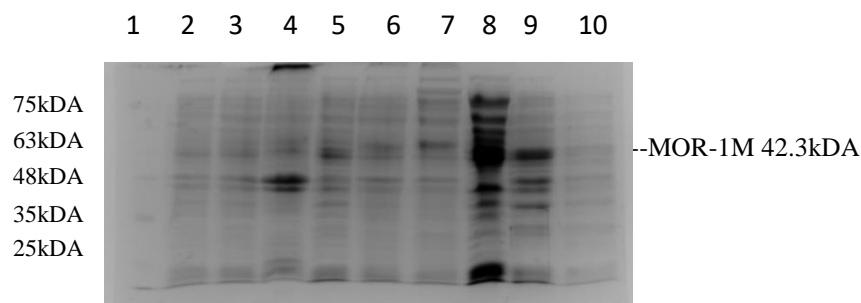


**Fig. 4.17** SDS-PAGE analysis for MOR protein precipitation from *E.coli* strain C41 (DE3). Lane 1, Uninduced C41 (DE3), Lane 2, Induced C41 (DE3), Lane 3, Induced Pallet C41 (DE3), Lane 4, Flow through, Lane 5, 0-20 % gradients, Lane 6, 20-40 % gradients, Lane 7, 40-60 % gradients, Lane 8, 60-80 % gradients, Lane: 9, 80-100 % gradients, Lane 10, Protein ladder

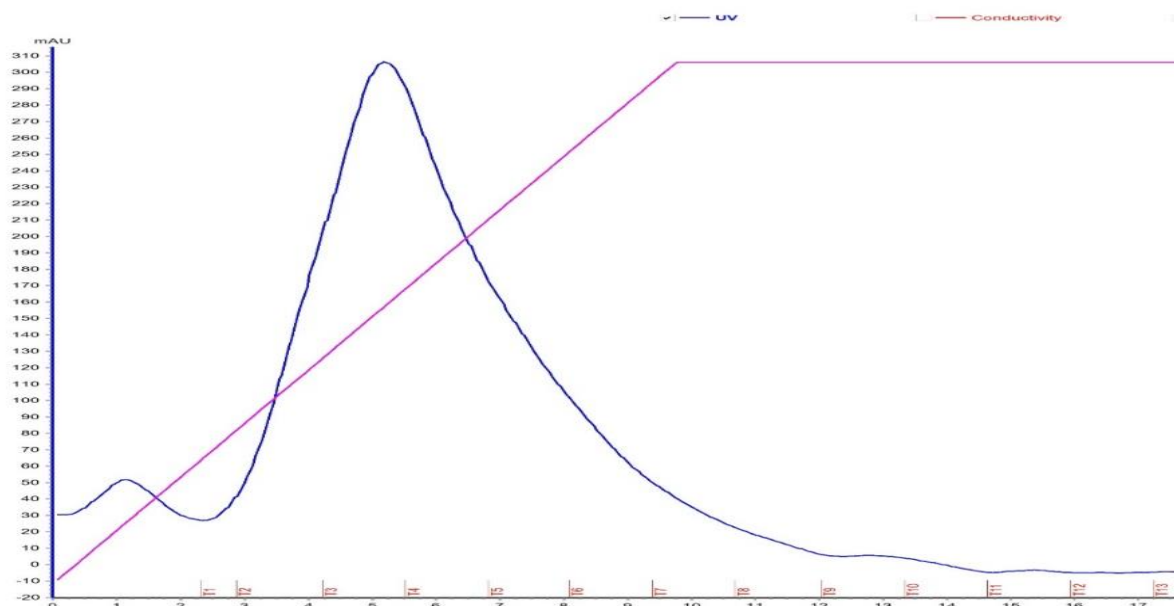


**Fig. 4.18** Hi-Trap Heparin column from *E. coli* C41 (DE3)

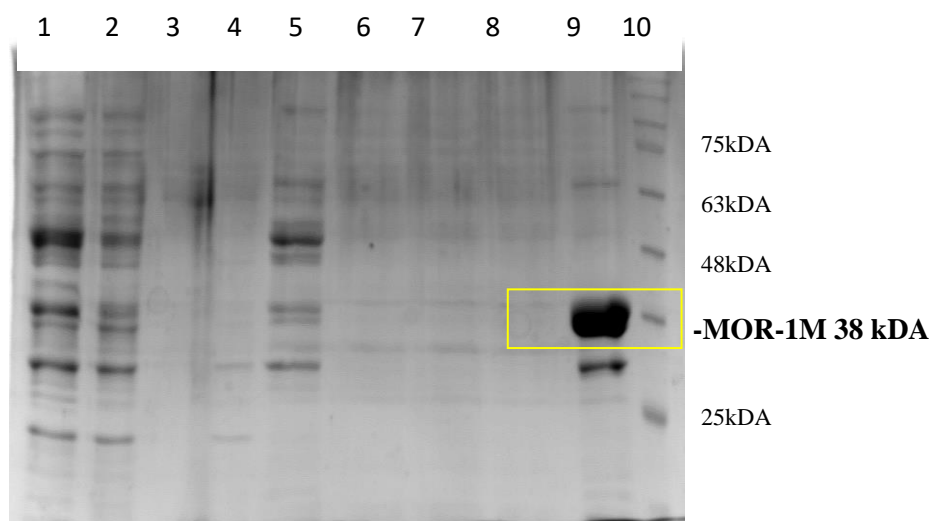


**Fig. 4.19** SDS-PAGE analysis of post dialysis purified MOR protein from *E. coli* strain C41 **Lane 1** Pre-Ammonium sulphate precipitation, **Lane 2**, Post Dialysis Load Ammonium Sulphate Precipitation **Lane 3**, Flow through Dialysis Ammonium Sulphate Precipitation **Lane 4**, Wash **Lane 5-8**, Mono Q Column Fraction **Lane 9**, Fraction number F-5 Heparin column **Lane 10**, Protein ladder

#### 4.3. To undertake interaction studies of MOR with BCM7/9 by Insilco approach

In-silico analysis was carried out to assess the binding efficacy of BCM7/9 with mu-opioid receptor and ascertain the stability of docked molecules. As the crystal structure of mice mu receptors was unavailable in the PDB databank, homology modelling approach was utilized to generate their 3D structure. Homology modelling was performed for 7TM mu-opioid receptor proteins and BCMs. The receptor/ligand interaction was studied using YASARA software.

### 4.3.1 Homology modelling of the 3D Structure of 7TM mu-opioid receptor protein

The 3D structure prediction for mu receptors was carried out using I-TASSER server (<http://zhanglab.ccmb.med.umich.edu/I-TASSER/>). I-TASSER is a preferred tool for homology modelling (Zhanget *al.*, 2009) as herein, the structure templates from PDB library are identified by LOMETS, which is a meta-server threading approach. Each threading program generates tens of thousands of template alignments. I-TASSER uses the templates showing highest significance in the threading alignments as measured by the Z-score, *i.e.* the difference between the raw and average scores in the unit of standard deviation. Finally models are selected utilizing SPICKER program which clusters all the decoys based on the pair-wise structure similarity, and report models corresponding to largest structure clusters. In Monte Carlo theory, the largest clusters correspond to the states of the largest partition function (or lowest free energy) and therefore have the highest confidence. For the selected 11 MORs, three templates 4n6hA, 5zbh and 4dklA showed highest Z score as well confidence score and were used for 3D homology modelling. To understand the stability of the protein structure as well as protein-ligand docking, the comparison of different parameters including C-score, RMSD value and TM-score are essential (Murzin *et al.*, 1995 and Zhang *et al.*, 2009). Hence, for the studied homology models for 11 MORs, the best model was selected on the basis of these three parameters (Table 4.8). The C-score indicated the global accuracy of the model, and was measured based on the significance of the threading alignments and the convergence of the I-TASSER simulations. Models with C-scores ranging from -5 to +2 (Yang *et al.*, 2015 and Zhanget *al.*, 2008) are considered good models. For the studied isoforms, all the models showed C-score values within this range and varied from -0.42 (MOR-1A) to -2.20 (MOR-1U). Amongst the models predicted for different MORs, the MOR-1 model showed least negative value (-0.42) for C-score and hence was considered as best model.

The other parameter that is root mean squared deviation (RMSD) value was also within the expected range ( $>5$ ) for all the predicted models and ranged from MOR-1N ( $7.6 \pm 4.3$  Å) to MOR-1M ( $10.9 \pm 4.6$  Å) (Table 4.9) RMSD value is calculated for all the equivalent atom pairs after the optimal superposition of the native and predicted structures and is one of the criterion for selection of stable structure (Kabschet *al.*, 1978). For RMSD value calculation, all atoms in the structures are equally weighted and if RMSD values are very high, these can be the only criterion as in that case sensitivity to the local structure deviation is more as compared to the global topology. For the predicted models this criterion can very well

implied as all RMSD values are  $>6$ . Another important criterion, template modelling score (TM-score) which counts all residue pairs using the Levitt–Gerstein weight (Levitt and Gerstein, 1998) was also calculated. As the short distance in the Levitt–Gerstein matrix is weighted stronger than the long distance, unlike RMSD value, the TM-score is more sensitive to the global topology than local variations (Zhang *et al.*, 2009 and Skolnick *et al.*, 2004). Additionally, because it adopts a protein size-dependent scale to normalize the residue distances, the magnitude of the TM-score for random protein pairs is protein size independent (Zhang and Skolnick, 2004). For all the 12 MORs, the calculated TM-score was  $>0.50$  except for  $0.45\pm 0.15$  (MOR-U) and  $0.49\pm 0.15$  (MOR-1M). This clearly indicated correct topology of the model implying high structural similarity between the predicted model and the native or experimentally determined structure. Thus all the predicted models satisfied the three basic criteria (C-score, RMSD value and TM-score) and were selected for further analysis.

**Table: 4.8 Quality estimation scores of the predicted 3D structures by I-TASSER.**

Model Name	C-score	Exp.TM-Score	Exp. RMSD	No.of decoys	Cluster density
MOR-1mRNA	-0.46	$0.65\pm 0.13$	$7.8\pm 4.4 \text{ \AA}$	2096	0.1516
MOR-1M	-1.84	$0.49\pm 0.15$	$10.9\pm 4.6 \text{ \AA}$	533	0.0402
MOR-1U	-2.21	$0.45\pm 0.15$	$12.5\pm 4.3 \text{ \AA}$	454	0.0277
MOR-1	-0.46	$0.65\pm 0.13$	$7.8\pm 4.4 \text{ \AA}$	2096	0.1516
MOR-1B2	-0.95	$0.59\pm 0.14$	$9.0\pm 4.6 \text{ \AA}$	1398	0.0945
MOR-1A	-0.42	$0.66\pm 0.13$	$7.7\pm 4.3 \text{ \AA}$	2098	0.1597
MOR-1D	-0.55	$0.64\pm 0.13$	$8.0\pm 4.4 \text{ \AA}$	2080	0.1395
MOR-1C	-1.62	$0.52\pm 0.15$	$10.8\pm 4.6 \text{ \AA}$	772	0.0486
MOR-1N	-0.58	$0.64\pm 0.13$	$7.6\pm 4.3 \text{ \AA}$	7019	0.1371
M-OR-1	-0.46	$0.65\pm 0.13$	$7.8\pm 4.4 \text{ \AA}$	2096	0.1516
MOR-1G	-0.73	$0.62\pm 0.14$	$8.0\pm 4.4 \text{ \AA}$	5769	0.1181
MOR-1B1	-0.48	$0.65\pm 0.13$	$7.8\pm 4.4 \text{ \AA}$	2067	0.1501

#### 4.3.2 Active site analysis and residues recognition

The models generated in PDB format were visualized using PyMole and Chimera server (Fig 4.20). The biological functions of the predicted models were calculated and probable ligands were checked for prediction of active site analysis and residue recognition. The models with high confidence score were submitted to COACH server (<http://zhanglab.ccmb.med.umich.edu/COACH/>) to predict its biological function, including

ligand-binding site, EC number and GO terms. As the template proteins may have additional functional domains, the most frequently-occurring GO terms in each of the three functional aspects (molecular function, biological process and cellular component) was reconciled to generate consensus GO terms. For the homology models generated in the present study the details of the EC number and GO terms are provided in (Table 4.9 and 4.10).

**Table 4.9 Enzyme Commission (EC) and number of active site of MORs**

Name	C-score <sup>EC</sup>	TM-Score	RMSD <sup>a</sup>	Active site
MOR-1mRNA	0.235	0.629	2.83	NA
MOR-1M	0.181	0.666	2.89	216,221
MOR-1U	0.131	0.534	2.74	329
MOR-1	0.235	0.629	2.83	NA
MOR-1B2	0.208	0.613	2.78	285,288,401
MOR-1A	0.242	0.641	2.81	78,116
MOR-1D	0.234	0.635	2.85	364
MOR-1C	0.166	0.576	2.76	364
MOR-1N	0.273	0.752	2.92	261
M-OR-1	0.235	0.629	2.83	NA
MOR-1G	0.261	0.740	2.87	261

For identification of ligand binding sites also, COACH server was used. It is based on the approach of binding-specific substructure comparison (TM-SITE) and sequence profile alignment (S-SITE) combined with ConCavity (Yang *et al.*, 2013b) and FINDSITE, for predictions of complementary binding sites. This approach is considered as one of the best approach and has been used across different studies (Brylinski *et al.*, 2008, Skolnick *et al.*, 2008 and Capra *et al.*, 2009). The complementary ligand binding sites were predicted by matching the MOR I-TASSER generated model with proteins in the BioLiP protein function database (Yang *et al.*, 2013a). The functional templates were detected and ranked using composite scoring function that is based on structure and sequence profile. The probable protein residues involved in the formation of active binding site pockets for ligands as predicted by COACH server is given (Table 4.11) MOR-1mRNA, MOR-1B1, MOR-1, MOR-1D and M-OR-1 reflected the presence of similar binding sites for ligand XTK. For MOR-1N and MOR-1G, though the ligand was same, the predicted sites were different but shared amongst these two receptors. Similarly, MOR-1U and MOR-1C also shared the ligand (ONN) as well as binding sites. MOR B2 and MOR-1M shared the ligand (ONN) but active sites were different. For receptor MOR-1A, the ligand (CVD) as well the predicted sites for ligand binding were also different from the other receptors. The C-score value which is a indicator of reliability of the ligand binding site ranged from 0.20 (MOR-1U) to 0.51 (MOR-

1B1). As C-score value for most of the predicted ligand binding sites was more than 0.40 (except for MOR-1U and MOR-1C), these can be considered as reliable sites (Roche *et al.*,2015). Similarly cluster size value of more than 50 for most of the predicted ligand binding also indicated the reliability of predicted ligand binding sites.

**Table 4.10 Gene ontology term of MOR**

$\mu$ -Opioid receptor (MOR)	Cscore <sub>GO</sub>	TM-score	Associated GO Terms	
			RMSD <sup>a</sup>	
MOR-1	0.47	0.6315	2.65	<u>GO:0019835</u> , <u>GO:0016998</u> , <u>GO:0003796</u> , <u>GO:0016798</u> , <u>GO:0008152</u> , <u>GO:0042742</u> , <u>GO:0016787</u> , <u>GO:0003824</u> , <u>GO:0009253</u> , <u>GO:0007186</u> , <u>GO:0016021</u>
MOR-1A	0.38	0.6432	2.83	<u>GO:0004935</u> , <u>GO:0007186</u> , <u>GO:0016021</u> , <u>GO:0071875</u> , <u>GO:0004940</u>
MOR-1B2	0.40	0.6117	2.67	<u>GO:0019835</u> , <u>GO:0016998</u> , <u>GO:0003796</u> , <u>GO:0016798</u> , <u>GO:0008152</u> , <u>GO:0042742</u> , <u>GO:0016787</u> , <u>GO:0003824</u> , <u>GO:0009253</u> , <u>GO:0007186</u> , <u>GO:0016021</u>
MOR-1C	0.33	0.5751	2.62	<u>GO:0019835</u> , <u>GO:0016998</u> , <u>GO:0003796</u> , <u>GO:0016798</u> , <u>GO:0008152</u> , <u>GO:0042742</u> , <u>GO:0016787</u> , <u>GO:0003824</u> , <u>GO:0009253</u> , <u>GO:0007186</u> , <u>GO:0016021</u>
MOR-1D	0.37	0.6387	3.01	<u>GO:0004935</u> , <u>GO:0007186</u> , <u>GO:0016021</u> , <u>GO:0071875</u> , <u>GO:0004940</u>
MOR-1M	0.27	0.6650	2.63	<u>GO:0004935</u> , <u>GO:0007186</u> , <u>GO:0016021</u> , <u>GO:0071875</u> , <u>GO:0004940</u>
MOR-1mRNA	0.47	0.6315	2.65	<u>GO:0019835</u> , <u>GO:0016998</u> , <u>GO:0003796</u> , <u>GO:0016798</u> , <u>GO:0008152</u> , <u>GO:0042742</u> , <u>GO:0016787</u> , <u>GO:0003824</u> , <u>GO:0009253</u> , <u>GO:0007186</u> , <u>GO:0016021</u>
MOR-1N	0.38	0.6001	2.46	<u>GO:0004935</u> , <u>GO:0004941</u> , <u>GO:0007186</u> , <u>GO:0016021</u> , <u>GO:0071875</u>
MOR-1U	0.27	0.5312	2.77	<u>GO:0019835</u> , <u>GO:0016998</u> , <u>GO:0003796</u> , <u>GO:0016798</u> , <u>GO:0008152</u> , <u>GO:0042742</u> , <u>GO:0016787</u> , <u>GO:0003824</u> , <u>GO:0009253</u> , <u>GO:0007186</u> , <u>GO:0016021</u>
MOR-1B1	0.38	0.6017	2.67	<u>GO:0019835</u> , <u>GO:0016998</u> , <u>GO:0003796</u> , <u>GO:0016798</u> , <u>GO:0008152</u> , <u>GO:0042742</u> , <u>GO:0016787</u> , <u>GO:0003824</u> , <u>GO:0009253</u> , <u>GO:0007186</u> , <u>GO:0016021</u>
MOR-1G	0.36	0.7383	2.63	<u>GO:0004935</u> , <u>GO:0007186</u> , <u>GO:0016021</u> , <u>GO:0071875</u> , <u>GO:0004940</u>

### 4.3.3 3D modelling of beta-casomorphins

To understand the interaction of modelled receptors with betacasomorphine (BCM) ligands, the structure of BCM7 and BCM 9 was deduced and modelled using MODELLER software. I-TASSER could not be used for structural prediction of these small bioactive peptides as the lower acceptable size range of the targets is 10 residues in I-TASSER. The Modeller is a preferred software for homology modelling of small bioactive peptides. Herein, the structure

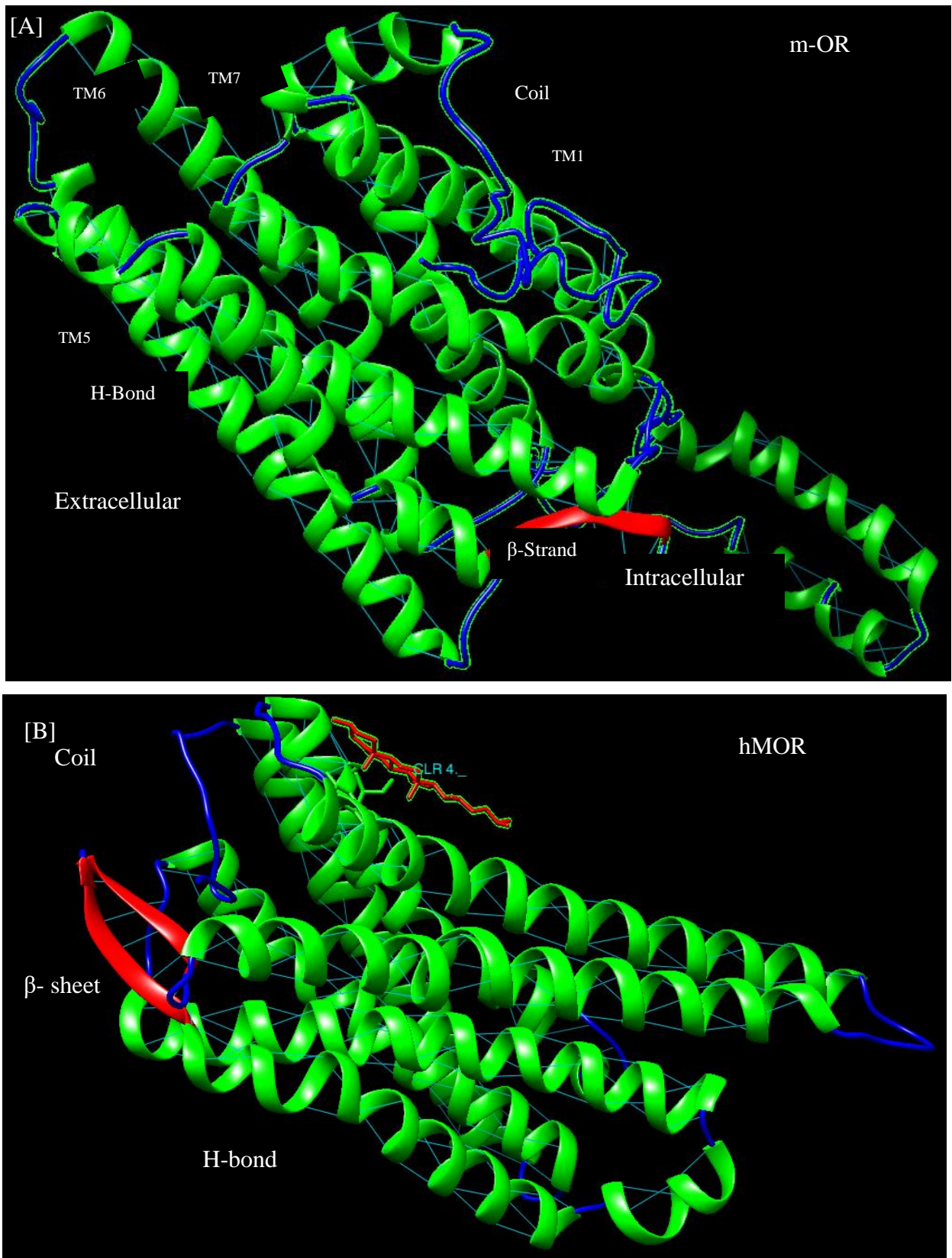


**Fig. 4.20** Homology Model of MOR gene. [A] Mice mMOR, [B] HumanhOPRM-1:Helix is represented by blue coils,  $\beta$ -sheet as red and H-bond as blue line

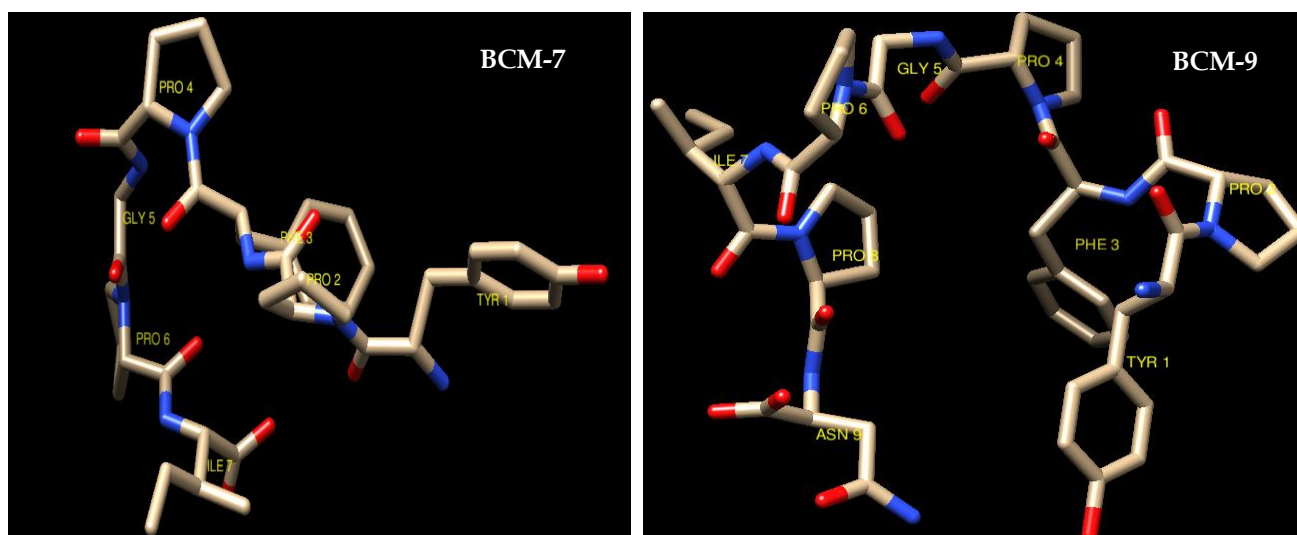


**Fig. 4.21** 3D Modelled structure of  $\beta$ -casomorphine ligands

#### 4.3.4 Secondary structure prediction and 3D Structure validation

SOPMA (Self-Optimized Prediction Method with Alignment) based on the homologue method of (Levin *et al.*, 1986). That takes into account information from an alignment of sequences belonging to the same family was used to draw secondary structures for the 12 MORs. This method can correctly predict 69.5% of amino acids for a three-state description of the secondary structure (alpha-helix, beta-sheet and coil) in a whole database containing 126 chains of non-homologous (less than 25% identity) proteins.

**Table 4.11** Predicted ligand binding sites in the MOR isoforms using the homologue model generated by I-TASSER.

Name	C-score	Cluster size	Ligand name	Ligand binding site
MOR-1 mRNA	0.49	120	XTK	143,144,147,148,232,233,236,240,293,296,297,300,322,326
MOR-1B1	0.51	122	XTK	143,144,147,148,232,233,236,240,293,296,297,300,322,326
MOR-1	0.49	120	XTK	143,144,147,148,232,233,236,240,293,296,297,300,322,326
MOR-1D	0.50	119	XTK	143,144,147,148,232,233,236,240,293,296,297,300,322,326
MOR-1N	0.53	115	XTK	75,76,79,80,164,165,168,172,225,228,229,232,254,258
M-OR-1	0.49	120	XTK	143,144,147,149,232,233,236,240,293,296,297,300,322,326
MOR-1G	0.49	105	XTK	75,76,79,80,164,165,168,172,225,228,229,232,254,258
MOR-1M	0.46	100	0NN	76,76,79,80,83,84,150,168,172,225,229,232,254,258
MOR-1U	0.20	40	0NN	124,127,144,147,148,151,152,217,236,240,293,297,300,322,326
MOR-1B2	0.40	68	0NN	124,144,147,148,151,152,218,236,240,293,297,300,322,326
MOR-1C	0.24	34	0NN	124,127,144,147,148,151,152,217,236,240,293,297,300,322,326
MOR-1A	0.48	118	CVD	127,143,147,148,151,232,,240,293,296,297,300,322,323,326

The PDB files generated by I-TASSER server were used as input for SOPMA server for the prediction of secondary structure. Secondary structure prediction for MORs is represented as alpha helix as 'Hh', extended strand as 'Ee'; beta turn as 'Tt' and random coil as 'Cc'. The number of aminoacids contributing for alpha helix, extended strand, beta turn and random coil are presented in (Table 4.12) and. As is evident from the table, maximum number and percent of residue contribute for alpha helix and random coil followed by extended strand and beta turn. For example in the secondary structure of MOR-1 sequence 168 (42.2%) and 173 (43.47%) residues contributed towards alpha helices and random coil respectively while for extended strands and beta turn the contribution was by 48 (12.06%) and 9 (2.26%) residues respectively. In the (Fig.4.22) alpha helix is represented by blue color, extended strand by red, beta turn by green and random coil by yellow. The predicted homology models for the proteins are generally error prone and needs validation. The predicted structures for the MORs were validated using three software namely, PROSA, RAMPAGE and WHAT IF web server.

**Table 4.12 Calculated alpha helix, extended strand, beta turn and random coil for the secondary structures predicted for  $\mu$ -opioid receptor isoforms by SOPMA**

MORs	Sequence length	Alpha helix (Hh)	Extended strand (Ee)	Beta turn (Tt)	Random coil (Cc)
MOR-1	398	168 (42.2%)	48 (12.06%)	9 (2.26%)	173 (43.47%)
MOR-1A	390	145 (37.18%)	54 (13.85%)	13 (3.33%)	178 (45.64%)
MOR-1B2	409	147 (35.94%)	67 (16.38%)	11 (2.69%)	184 (44.99%)
MOR-1C	438	155(35.39%)	69 (15.75%)	13 (2.97%)	201 (45.89%)
MOR-1M	370	173 (46.76%)	44 (11.89%)	16 (4.32%)	137 (37.03%)
MOR-1N	325	156 (48.00%)	45 (13.85%)	12 (3.69%)	112 (34.46%)
MOR-1U	474	165 (34.81%)	70 (14.77%)	19 (4.01%)	220 (46.41%)
MOR-1D	393	138 (35.11%)	67 (17.05%)	10 (2.54%)	178 (45.29%)
MOR1mRNA	398	168 (42.21%)	48 (12.06%)	9 (2.26%)	173 (43.47%)
MOR-1B1	391	148 (37.85%)	63 (16.11%)	9(2.230%)	171 (43.73%)
MOR-1G	330	165 (50.00%)	44 (13.33%)	12 (3.64%)	109 (33.03%)

**Table 4.13 PROSA Z-score for homology model structure**

<b>μ-Opioid receptor (MOR)</b>	<b>Amino acid</b>	<b>PROSA Z-score</b>
<b>MOR-1</b>	398	-0.34
<b>MOR-1A</b>	390	-1.23
<b>MOR-1B2</b>	409	-2.04
<b>MOR-1C</b>	438	-1.72
<b>MOR-1M</b>	370	-1.05
<b>MOR-1N</b>	325	-1.36
<b>MOR-1U</b>	474	-1.62
<b>MOR-1D</b>	393	-0.65
<b>MOR-1mRNA</b>	398	-0.34
<b>MOR-1B1</b>	391	-0.45
<b>MOR-1G</b>	330	-1.22

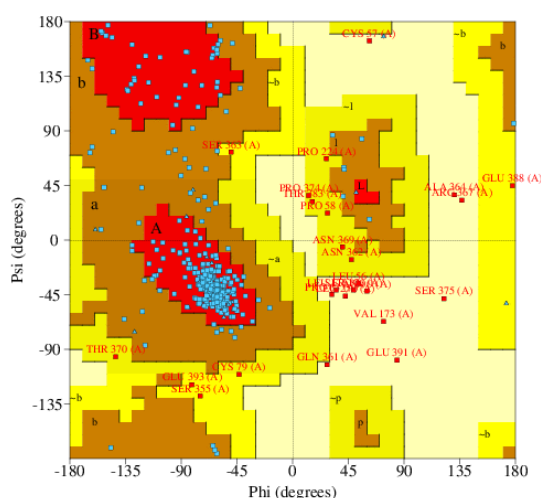
In ProSA web, the overall quality score (Z score) is calculated for a specific input structure. The advantage of ProSA program (Wiederstein *et al.*, 2007, and Sippl *et al.*, 1993) is that it requires only C $\alpha$  atoms so that low-resolution structures and approximate models obtained early in the structure determination process can be evaluated and compared against high-resolution structures. The Z score is displayed in a plot that shows the scores of all experimentally determined protein chains currently available in the Protein Data Bank (Berman *et al.*, 2000). Thus it relates the score of a specific model to the scores computed from all experimental structures deposited in PDB. Problematic parts of a model are identified by a plot of local quality scores and the same scores are mapped on a display of the 3D structure using colour codes. The colour codes can be used to check whether the z-score of the input structure is within the range of scores typically found for native proteins of similar size. Overall, all the models showed negative Z score value (Table 4.13) indicating the stability of deduced structures. The z-score indicated overall model quality and measured the deviation of the total energy of the structure with respect to an energy distribution derived from random conformations (Wiederstein *et al.*, 2007, and Sippl *et al.*, 1993). For all the models of MORs, green coloured plots were obtained and representative plots are shown in (Fig.4.23 a&b). Model quality was also evaluated by RAMPAGE server wherein Ramachandran plot is drawn to show the residues in the favoured region. The Ramachandran



(Table 4.14) indicating that all the modelled 3D structure of MOR proteins have acceptable stability and it conforms to the rule of stereochemistry. Amongst all the homology models, the protein stability check for model generated for MOR-1 revealed 334 residues (83.3%) residues in favoured region,(2.0%) in expected, 37 (9.2%) in allowed region and 30 (7.5%) residues in outlier region and hence a stable structure.

**Table 4.14 Ramachandran plot analysis of molecular docking results of mu-opioid receptor**

MORs	Assessment of the Ramachandran Plot (RAMPAGE)		
	No. of residues in favoured region	No. of residues in allowed region	No. of residues in outlier region
MOR-1A	~98.0% expected: 343 (87.3%)	~2.0% expected: 34 (2.7%)	16 (4.1%)
MOR-1D	(~98.0% expected): 330 (83.3%)	(~2.0% expected): 37 (9.3%)	27 (5.4)
MOR-1U	(~98.0% expected): 379 (79.5%)	(~2.0% expected): 62 (13.0%)	36 (7.5%)
MOR-1G	(~98.0% expected): 292 (87.4%)	(~2.0% expected): 20 (6.0%)	22 (6.6%)
MOR-1M	(~98.0% expected): 338 (90.6%)	(~2.0% expected): 24 (6.4%)	11 (2.9%)
MOR-1mRNA	(~98.0% expected): 334 (83.3%)	(~2.0% expected): 37 (9.2%)	30 (7.5%)
MOR-1N	(~98.0% expected): 283 (86.3%)	(~2.0% expected): 27 (8.2%)	18 (5.5%)
MOR-1	(~98.0% expected):334 (83.3%)	(~2.0% expected): 37 (9.2%)	30 (7.5%)
MOR-1B2	(~98.0% expected): 345 (83.7%)	(~2.0% expected): 51 (12.4%)	16 (3.9%)
MOR-1C	(~98.0% expected): 353 (80.0%)	(~2.0% expected): 56 (12.7%)	32 (7.3%)
MOR-1B1	(~98.0% expected):324 (82.2%)	(~2.0% expected): 44 (11.2%)	26 (6.6%)



[A]

**Fig.4.23** Ramachandran plot of mu opioid receptor by PROCHECK server

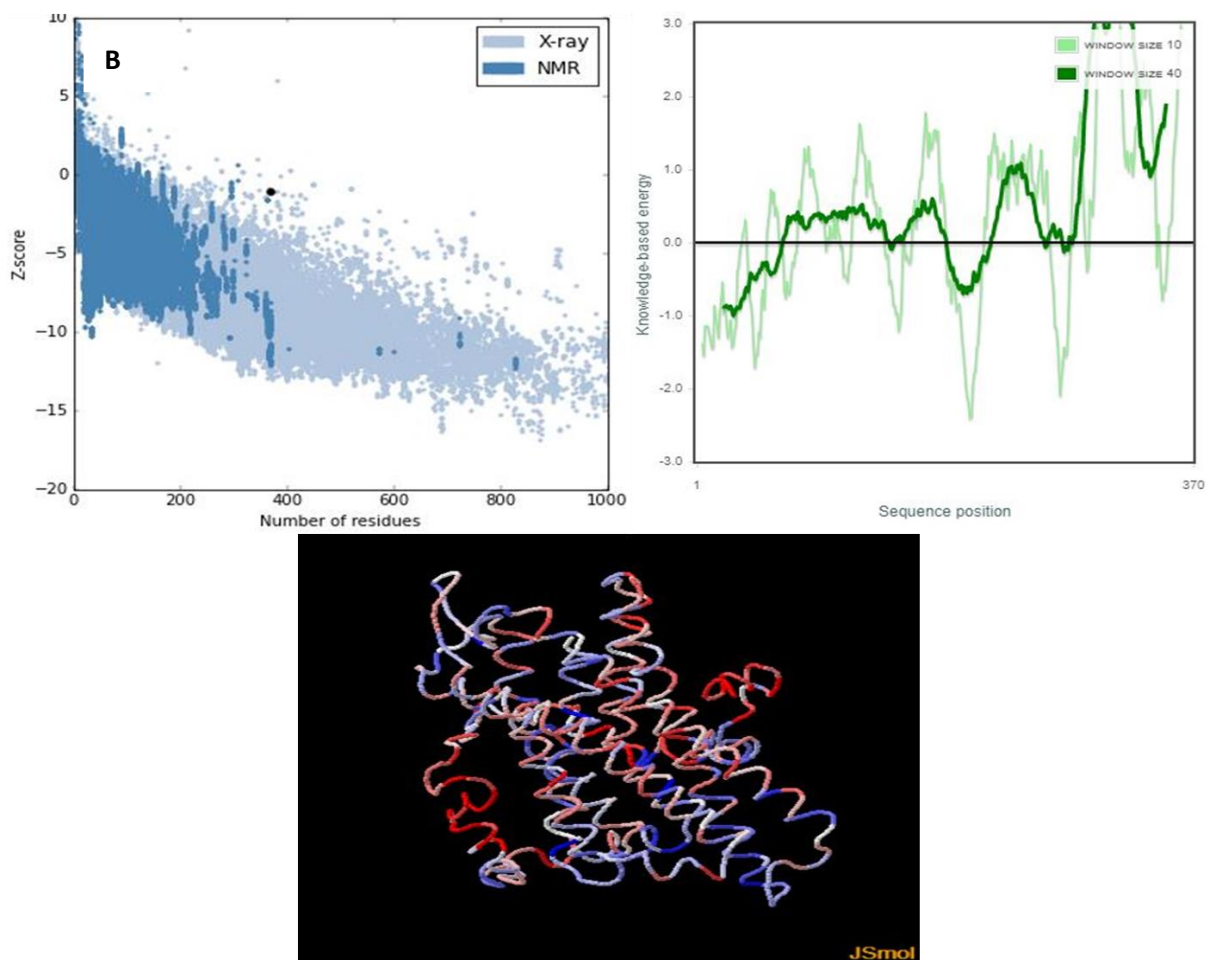


**Fig.4.24** MOR 3D model validation: Residue interaction energy profile for the MOR drawn with PROSA. Residues are coloured from blue to red in the order of increasing residue energy.

#### 4.3.5 Molecular docking and receptor protein interaction study

In order to understand the stability of docked or interacting residues, docking study of MORs and bioactive peptide ligands (BCM7/9) was carried out using the fast docking algorithm PatchDock, which identifies shape complementary interactions between binding partners that is receptor and ligand (Duhovny *et al.*, 2002). The docking results of the structural complex between the MORs and the BCM7/9 were downloaded as PDB files, and they were all visualized using PyMole and chimera software (Fig. 4.24 [A&B]). The docking runs for each of the parameter (MORs and BCM7/9) were done using PatchDock server and all the results generated by this server showed a very high binding energy. This indicates good binding solution for all the transcript variants of (MOR) with BCM7 having the highest binding energy. Further, the generated docking with BCM 7 results were refined using FireDock server. The global energy values for MOR-1, MOR-1A, MOR-1B2, MOR-1D, MOR-1G,

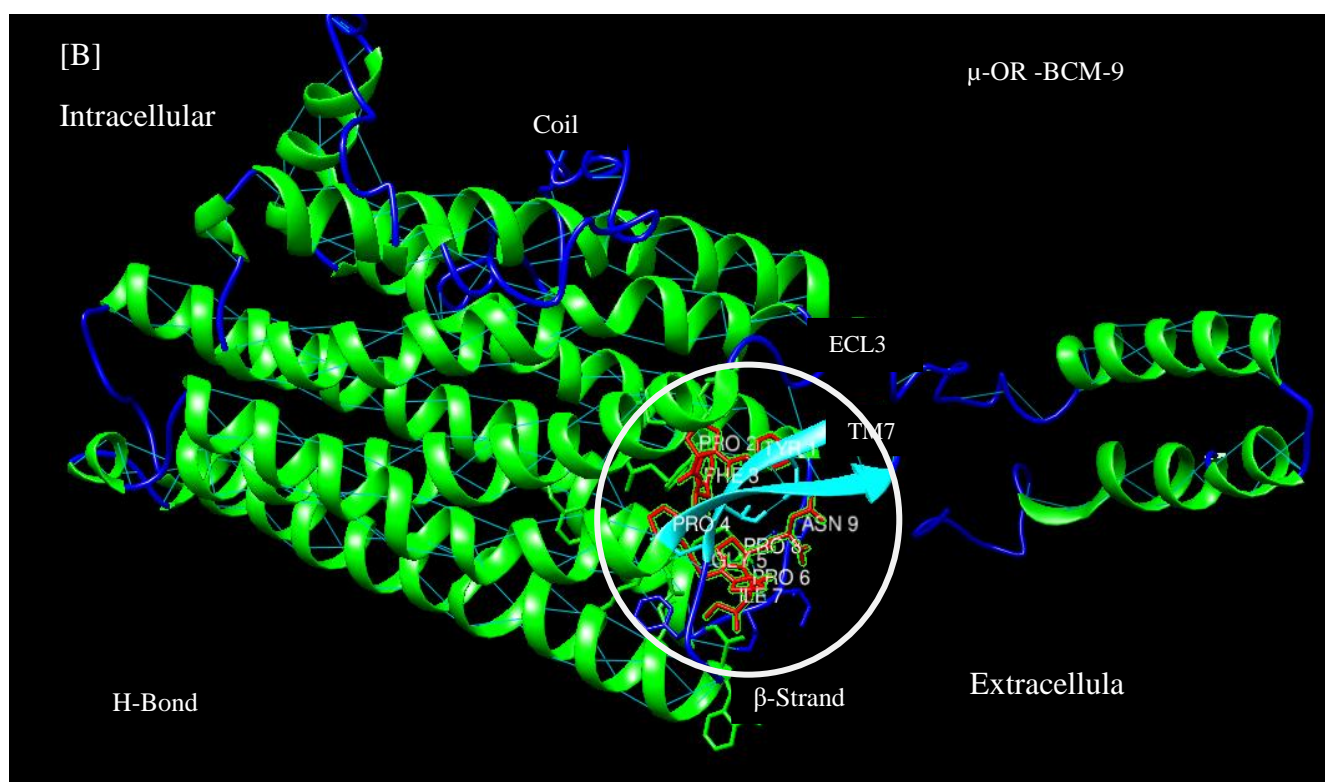
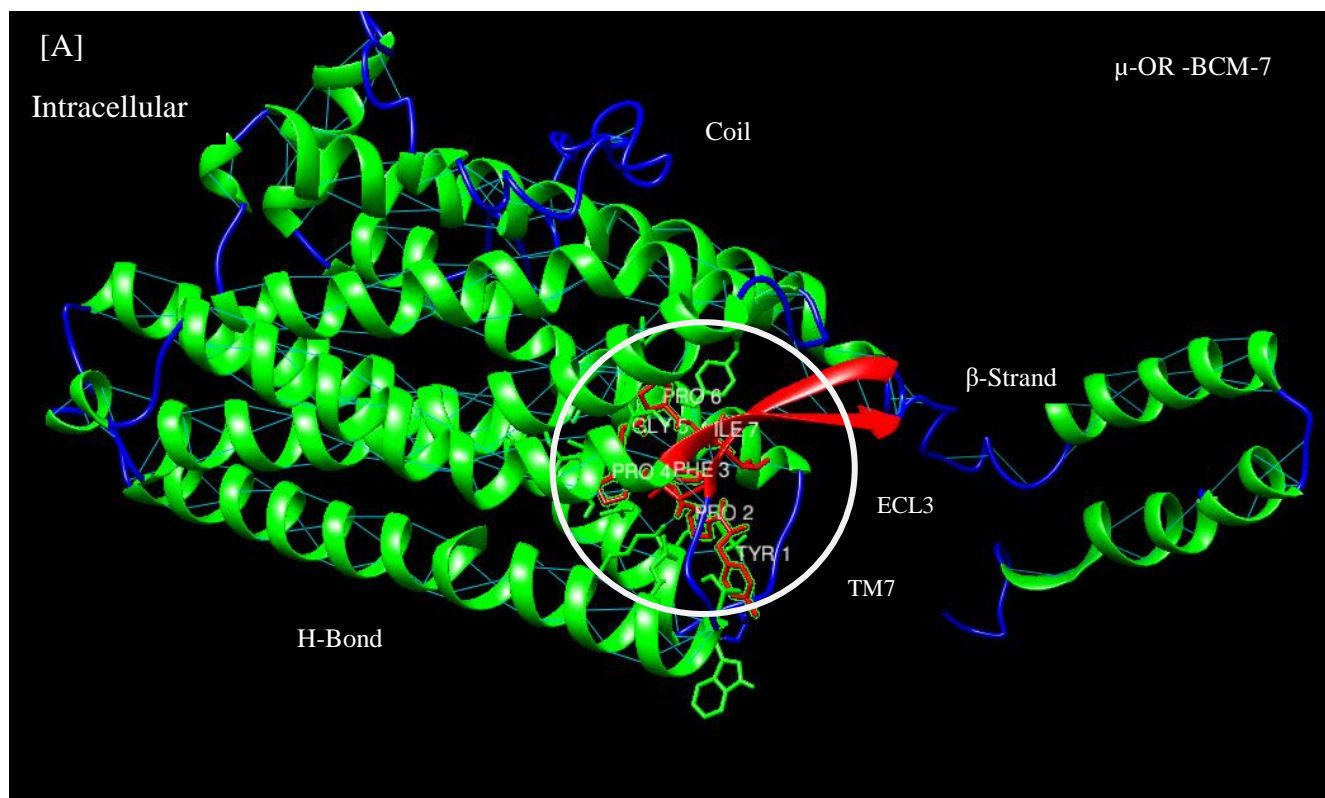


**Fig.4.25 [A & B]** Molecular Docking of MOR with BCMs: [A].Docking with BCM-7 [B].Docking with BCM-9. Where blue colour indicated (coil), red and cyan (β-strand) and red colour BCMs (BCM-7, BCM-9).

MOR-1mRNA, MOR-1U were -58.69,-53.42,-53.39,-60.4,-65.35,-58.69, and -76.01, kcal/mol. This indicates good binding solution for the transcript variants of MOR-B2 with

BCM-7 having the highest binding energy values -53.39 kcal/mol as shown in (Table.4.15).The global energy in which , MOR-1U,MOR-1G and MOR-1D has less binding energy with -76.01, -60.40 and -65.35 kcal/mole; respectively indicating highest binding energy for MOR MOR-1B2 with BCM7. Thus these results strongly supported the FireDocks global energy results confirming that Opioid receptor with a very high binding energy of -53.39 is the most stable. The molecular docking results show the essential role of the relative orientation of the ligand in the  $\mu$ -opioid receptor binding site, inducing the tendency of critical non-covalent interactions that are required to facilitate BCM7/9/MORs interactions and receptor activation. The similar results have been reported by (Stefan M. Noha *et al.*, 2017).

**Table 4.15 Patch Dock and Fire Dock results for each MORs energy for the solution in kcal/mol.**

$\mu$ -Opioid receptor (MOR)	Global energy (KJ/mole)		ACE (KJ/mole)	
	MOR-BCM-7	MOR-BCM-9	MOR-BCM-7	MOR-BCM-9
<b>MOR-1</b>	-58.69	-52.77	-11.31	-4.55
<b>MOR-1A</b>	-53.42	-52.51	-9.94	-8.92
<b>MOR-1-B2</b>	-53.39	-51.14	-10	-9.29
<b>MOR-1D</b>	-60.4	-54.34	-11.65	-4.71
<b>MOR-1G</b>	-65.35	-55.18	-10.39	-4.36
<b>MOR-mRNA</b>	-58.69	-52.77	-11.31	-4.55
<b>MOR-1U</b>	-76.01	-51.55	-18.75	-4.98

The bioactive peptide BCM7/9-MOR complex showed three binding pocket sites such as pocket 1, 2 and 3 which are very close in BCM-7 resulting in strong binding as compared to BCM-9(fig. 4.25). The similar results have been reported by other researchers (Kulp *et al.*, 2012; Blum *et al.*, 2011; Barelier *et al.*, 2015) who also observed multipose binding in many naturally occurring protein-ligand complexes.In the bovine beta-casomorphine-7, presence of tyrosine residue at the N terminal and a phenylalanine residue at the 3<sup>rd</sup> or 4<sup>th</sup> forms the motif, it is bind to the opioid receptor which are pharmecophoric residues. The proline present at the 2<sup>nd</sup> position is crucial for the formation of bioactive conformation of the peptide in order to bind receptor.

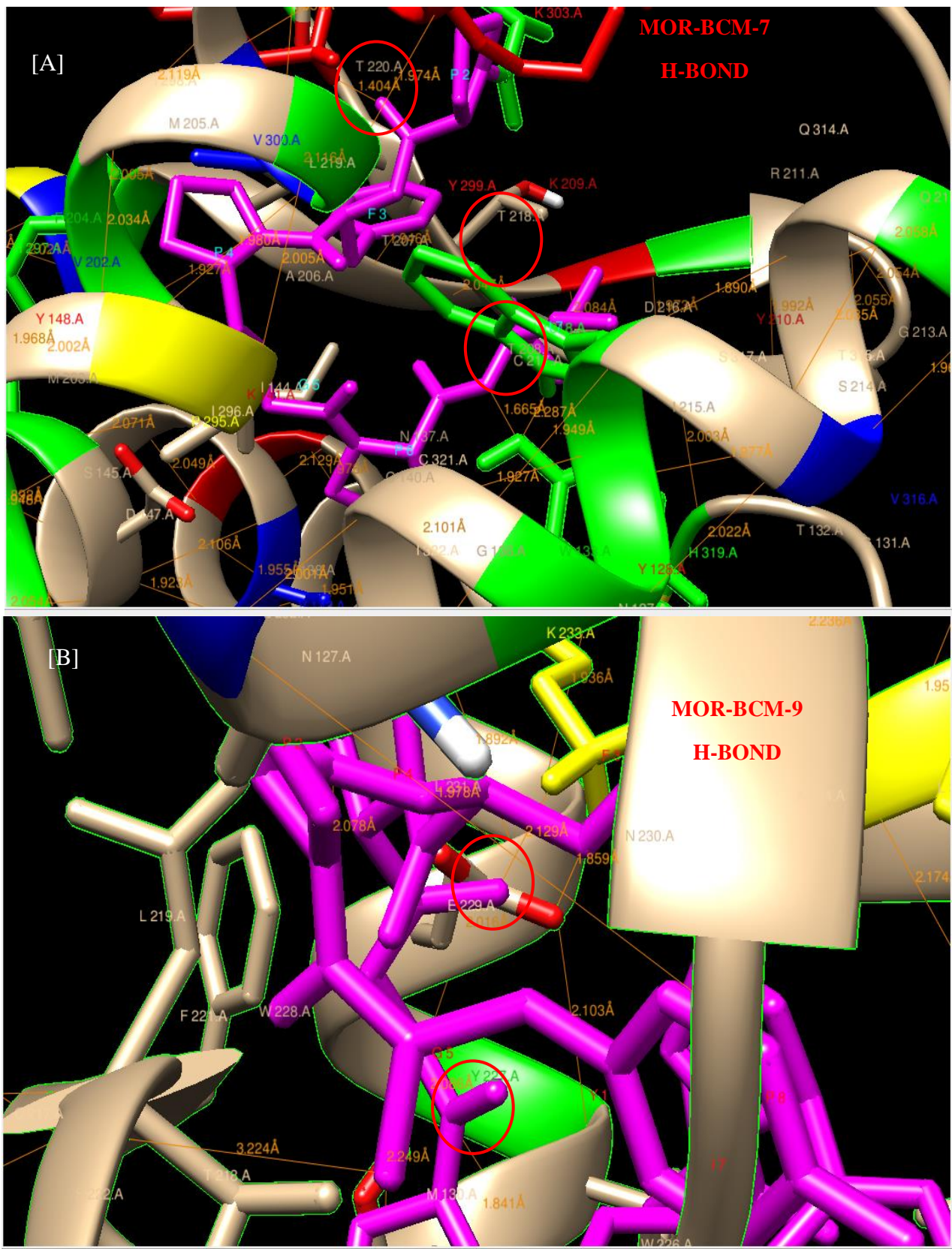


**Fig.4.26 [A&B]:** Representation of H-bonding between MOR and BCM7/9.

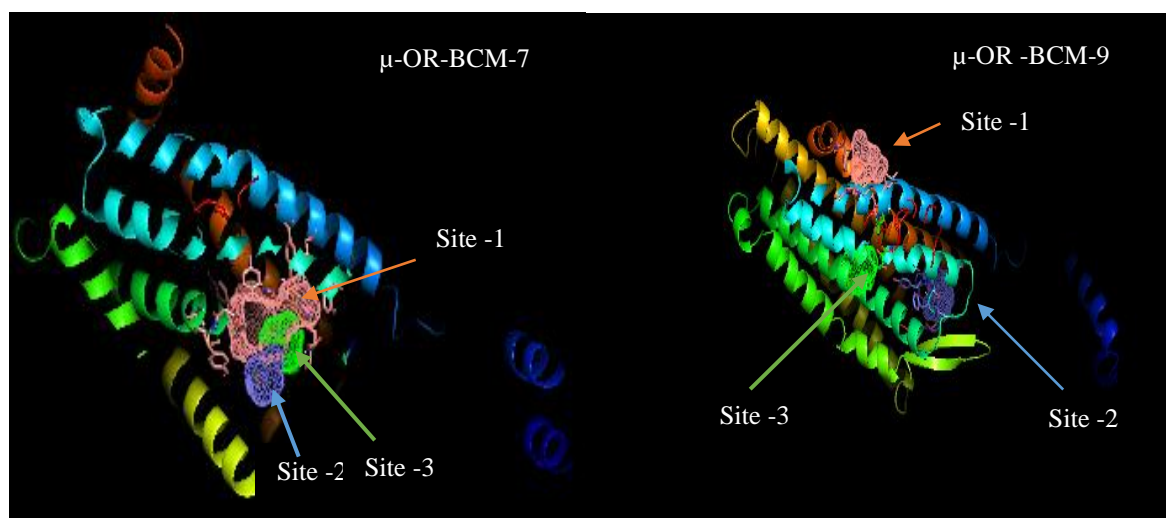


**Fig.4.27** Molecular docking and binding pocket site of  $\mu$ -opioid receptor. All binding pocket (Mesh) of mu-opioid receptor Site-1(Gary), Site-2(Blue), and Site-3(Green)) very close to BCM-7 while In BCM-9 binding pocket site at distinct position.

The proline at 2<sup>nd</sup> position along with the pharmacophoric residues forms the “messenger sequence”. The remaining C terminal sequence forms the “address sequence”. We observed that biologically important residues of Tyr and Phe play a significant role in orienting the conformational change in secondary structure and necessary for opioid activity (Yamazaki *et al.*, 1993, Mierke *et al.*, 1990). In the current study, the binding site was selected based on the amino acid residues, which are involved in binding mu-opioid receptor with beta casomorphins (BCM-7, BCM-9) would be reflected as the best perfect active region (Fig.4.26).

#### 4.3.6 Hydrophobic interactions and functional activity

The average hydrophobically interacting atoms in MORs with BCM7 were 15 (MOR-1B2), 18 (MOR-1M), 17 (MOR-1D) and 14 (MOR-1A) with one or two hydrogen bond. In case of BCM-9, these were 13 (MOR-1B2), 15 (MOR-1M), 16 (MOR-1D) and 13 (MOR-1A) with one or two hydrogen bonds (Fig 4.27). This defines the importance of hydrophobic interactions in ligands proteins and improves the binding affinity of targets. It has been previously described that the binding affinity associated with hydrophobic interactions can be optimized by incorporating them at the site of the hydrogen bonding (Qian *et al.*, 2009). An increase in the number of hydrophobic atoms in the active core of MORs further increases the biological activity.



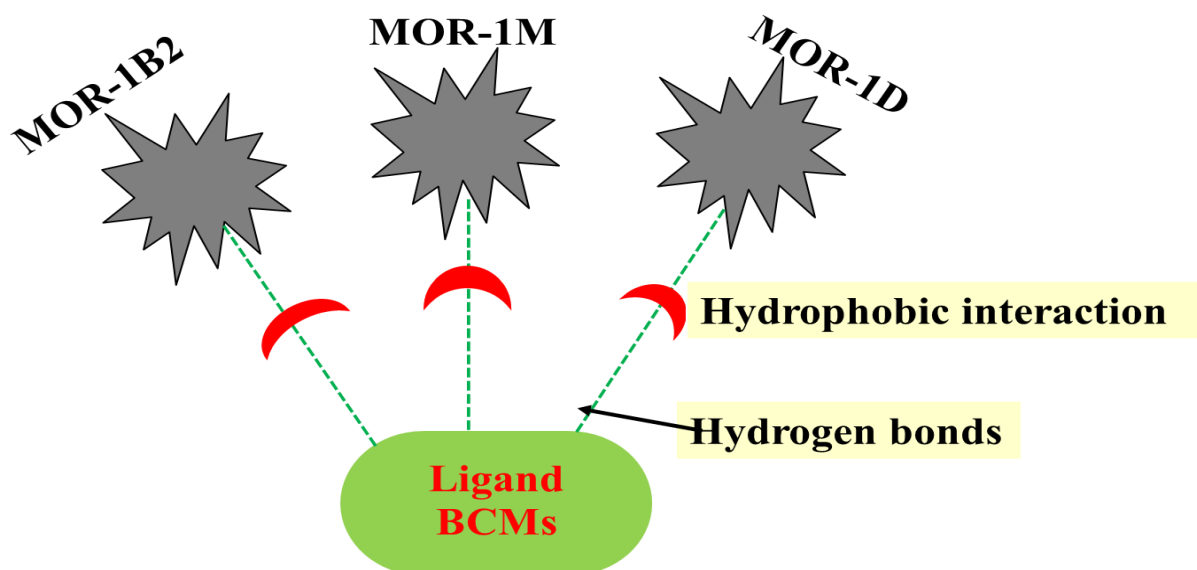


**Fig.4.29** The homology model where the ligand forming hydrogen bonds and hydrophobic interaction.

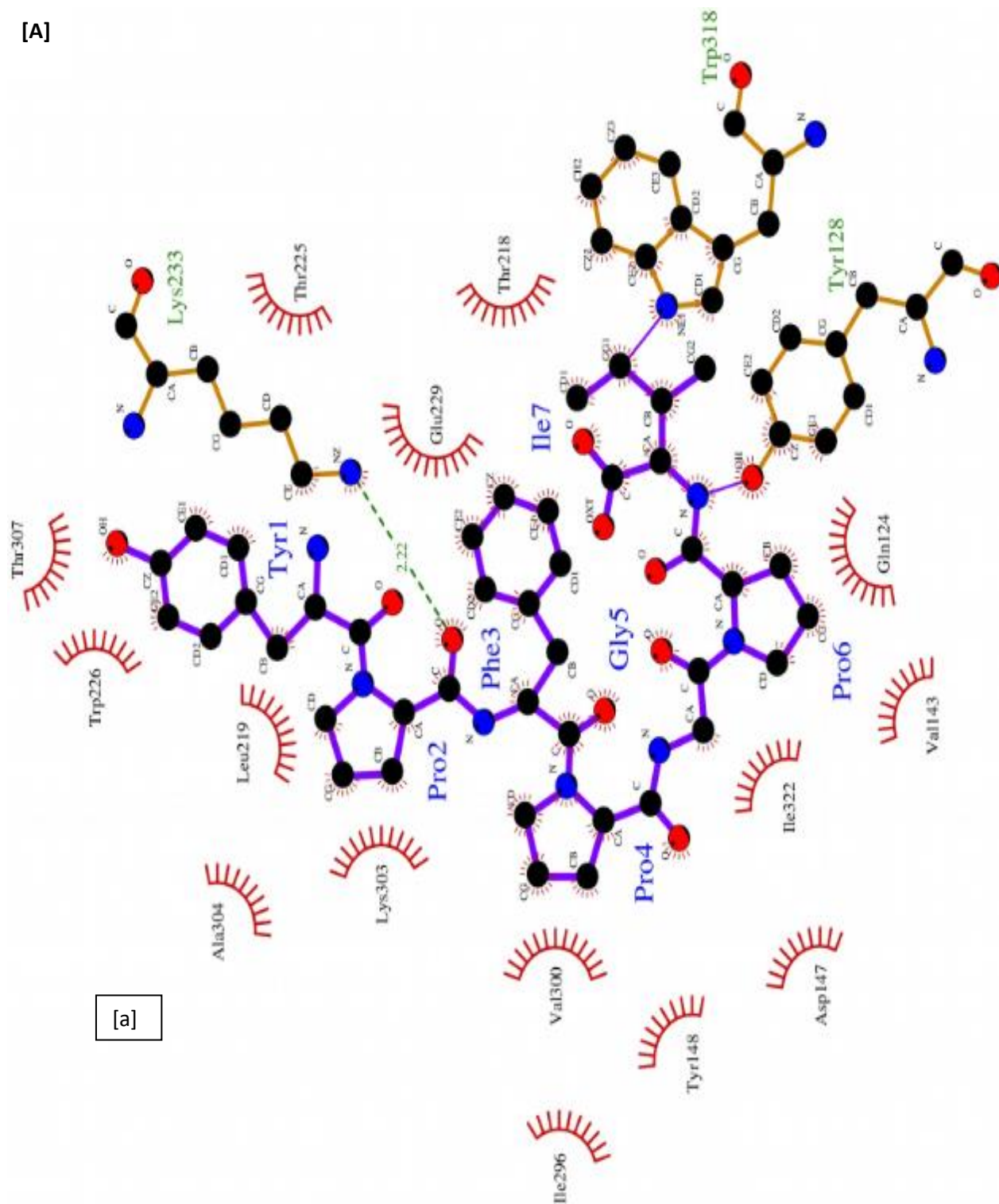
The N-terminal isoleucine at 7<sup>th</sup> position, proline at 2<sup>nd</sup> and 6<sup>th</sup> position interact with the tryptophan residue at Trp<sup>318</sup> (A) position, Lys<sup>223</sup>(A) and Trp<sup>128</sup> (A) residues of mu-opioid receptor respectively. The 16 amino acid residues of mu-opioid receptor showed hydrophobic interaction with BCM-7 including ( Val<sup>300</sup> Gln<sup>124</sup> Ile<sup>322</sup> Ile<sup>296</sup>, 144 Lys303, Lys233 Ala304 Tyr148 Leu219, Tyr326 and Asp147 , Trp226 ,Thr307, Thr225, Glu 229, Thr218 , Trp318 ,Tyr128). It also indicated majority of interactions between BCM-7 and active mu-opioid receptor are hydrophobic or aromatic in nature. In case of BCM-9, bioactive peptide N-terminal proline, asparagine, Phenylalanine at the 4<sup>th</sup>,9<sup>th</sup> and 3<sup>rd</sup> position interact with Lys<sup>233(3.09)</sup>, Glu<sup>310</sup> Aand Leu<sup>219</sup> (A) residues of mu-opioid receptor respectively. The 13 amino acid residues of mu-opioid receptor showed hydrophobic interaction with BCM-7 (Ile<sup>322</sup>, Ile<sup>144</sup>, Lys303, Ala<sup>304</sup> and Asp<sup>216</sup>, Trp<sup>226</sup>, Thr<sup>225</sup>, Glu<sup>229</sup>, Thr<sup>218</sup>, Tyr128, Phe<sup>221</sup>Asn<sup>127</sup>). The most prominent binding site prediction of mu-opioid receptor with BCM7/9 were TYR<sup>128</sup>, TRP<sup>318</sup>, ASN<sup>127</sup>, LYS<sup>233</sup>, GLU<sup>310</sup>LEU<sup>219</sup> (fig 4.28). Thus it can be concluded that these docked atoms help to increase the binding affinity of the target-receptor molecules and optimize the hydrophobic interactions by captivating the hydrogen bonding at the hydrophobic core of the complex.

#### **4.3.7 MOR-BCMs complex energy minimization**

The YASARA (Yet Another Scientific Artificial Reality Application) force field and the homology modelling protocol have been implemented as part of the molecular modelling

program. A web-server can be found at (<http://www.yasara.org/minimizationserver.htm>) which provides access to the YASARA. The YASARA force field defined here addresses these issues by merging the AMBER all-atom force field equation with multi-dimensional knowledge-based torsional potentials and with a consistent set of force field parameters to exploit the accuracy. The energy minimization of docked complex model structure (BCM and BCM-9 with MORs) was done by YASARA server. The full length 7TM transcript variants of BCM-7 showed the greater energy affinity with MOR-1A (-202241.7 kJ/mole), MOR-1 (-184708.6 kJ/mole), MOR-B1 (-178924.8 kJ/mole), MOR-B2 (-191105.7 kJ/mole), MOR-1U (-199434.9 kJ/mole) receptors. Similarly in case of BCM-9, 7 TM transcript variants showed the energy affinity of -184703, -154812.6, -178014.7, -189852.0 and -191018.3 kJ/mole with MOR-1A, MOR-1, MOR-B1, MOR-B2, MOR-1U receptors respectively. The truncated 6TM GPCRs transcript variant in case of BCM-7 showed the energy affinity of -201459.7 and -185062.3 KJ/mole towards MOR-1M and MOR-1N receptors respectively. The truncated 6TM GPCRs transcript variant in case of BCM-7 showed energy affinity of -183604.6 and -154812.6 KJ/mole towards MOR-1M and MOR-1N receptors respectively. Docking of BCM7/9 with mu receptors (MOR) indicated stable binding of BCM7 with mu receptors as compared to BCM9 in terms of interacting amino acids (TYR128, TRP 318, ASN 127, LYS 233, GLU 310 LEU 219), ligand and protein atoms involve in hydrogen bonding (BCM7 = LYS 233(2.22 Å), BCM9 = LYS 233(3.09 Å)), number of hydrophobic interacting amino acid residues (15 in case of BCM7 while 13 in BCM9). Similarly in case of human OPRM-1 receptor the comparative energy minimization for MOR-BCM7 and for MOR-BCM9 showed the energy of -156206.5 and -156113.5 KJ/mole respectively. The comparative energy minimization of docked model for MOR-1A-BCM7- (-202241.7 KJ/mole) and for MOR-1A-BCM9 (-184703.0 KJ/mole) using YASARA server also indicated greater binding affinity of BCM7 towards mu opioid receptor (Table 4.16, Fig. 4.29).

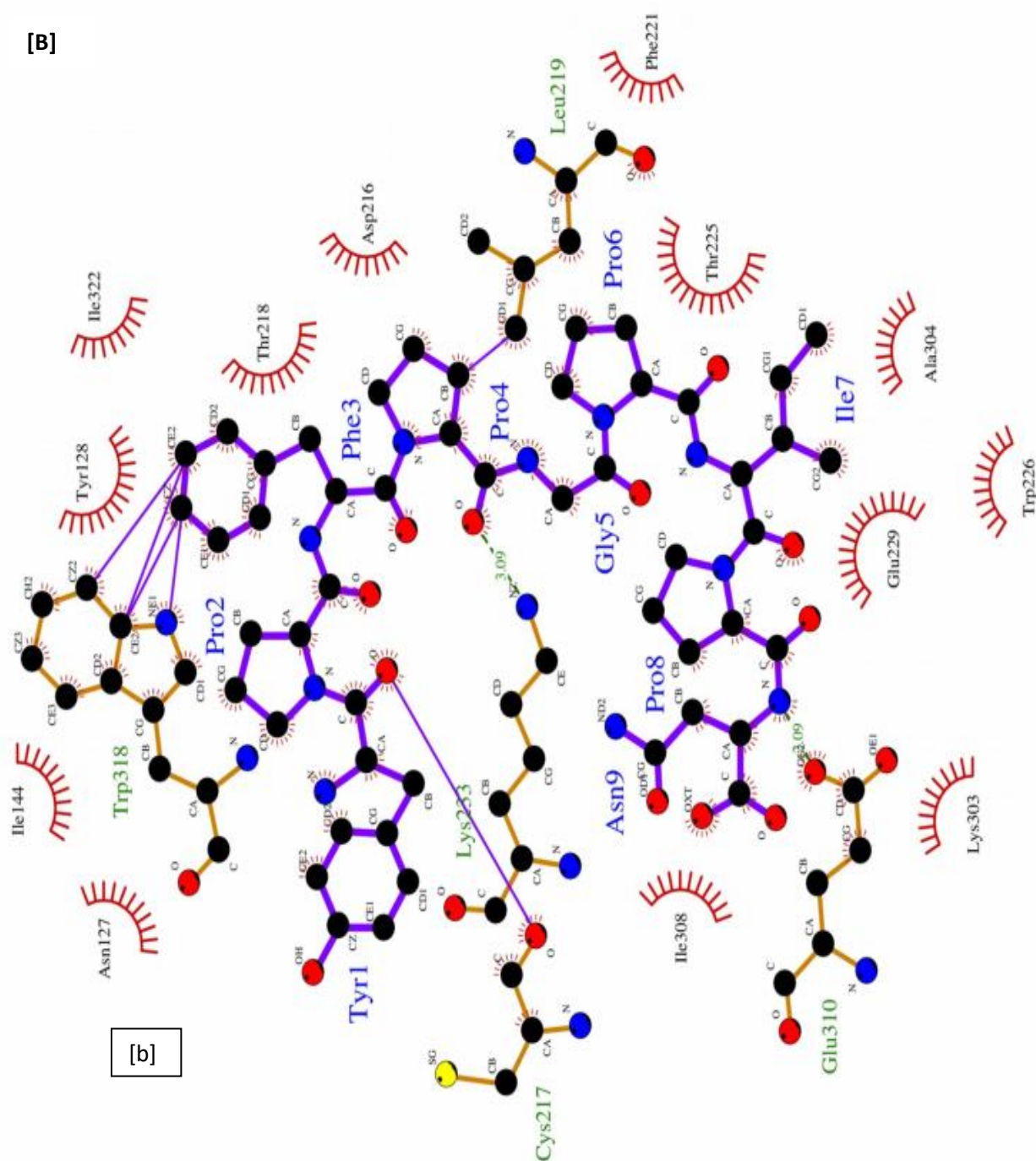
[A]



[a]

**Fig. 4.30 [a]** PDBsum's ligplot results for  $\mu$ -OR-BCM7: The red arc circles indicate hydrophobic interaction; Hydrogen bonds are shown as green dotted lines or green circle while the spoked arcs represent protein residues making non-bonded contacts with the ligand. Amino acid residues involved in polar interactions are illustrated (*i.e.*, Tyr 128, Lys 223 <sup>2.22</sup>, Trp 318, Glu 310 <sup>3.09</sup> Cys127, Leu 219) along with intermolecular hydrogen bonds (green dashed lines).

[B]



[b]

**Fig. 4.30 [b]** PDBsum's ligplot results for  $\mu$ -OR-BCM9: The red arc circles indicate hydrophobic interaction; Hydrogen bonds are shown as green dotted lines or green circle while the spoked arcs represent protein residues making non-bonded contacts with the ligand. Amino acid residues involved in polar interactions are illustrated (*i.e.*, Tyr 128, Lys 223 <sup>2,22</sup>, Trp 318, Glu 310 <sup>3,09</sup> Cys27, Leu 219) along with intermolecular hydrogen bonds (green dashed lines).

**Table 4.16 Energy minimization of complex (MORs-BCMs)**

$\mu$ -Opioid receptor (MOR)	Start Energy (KJ/mole)		END Energy (KJ/mole)	
	MOR-BCM-7	MOR-BCM-9	MOR-BCM-7	MOR-BCM-9
<b>MOR-1</b>	15807339.7	14202835.6	-184708.6	-154812.6
<b>MOR-1A</b>	18443481.1	2647849503.2	-202241.7	-184703.0
<b>MOR-1B2</b>	2194223.4	2689417089.8	-191105.7	-189852.0
<b>MOR-1C</b>	245214.4	133611474137.5	-191105.7	-185062.3
<b>MOR-1D</b>	167778193.5	1284460098.8	-198459.7	-1874389.6
<b>MOR-1M</b>	590839394.1	420659.9	-201459.7	-183604.6
<b>MOR-1mRNA</b>	415488328.8	352375008.2	-199434.9	-171412.2
<b>MOR-1N</b>	245214	14202835.6	-185062.3	-154812.6
<b>MOR-1U</b>	1520130232.5	1689086.8	-199434.9	-191018.3
<b>MOR-1B1</b>	-92222.4	242483887.4	-178924.8	-178014.7

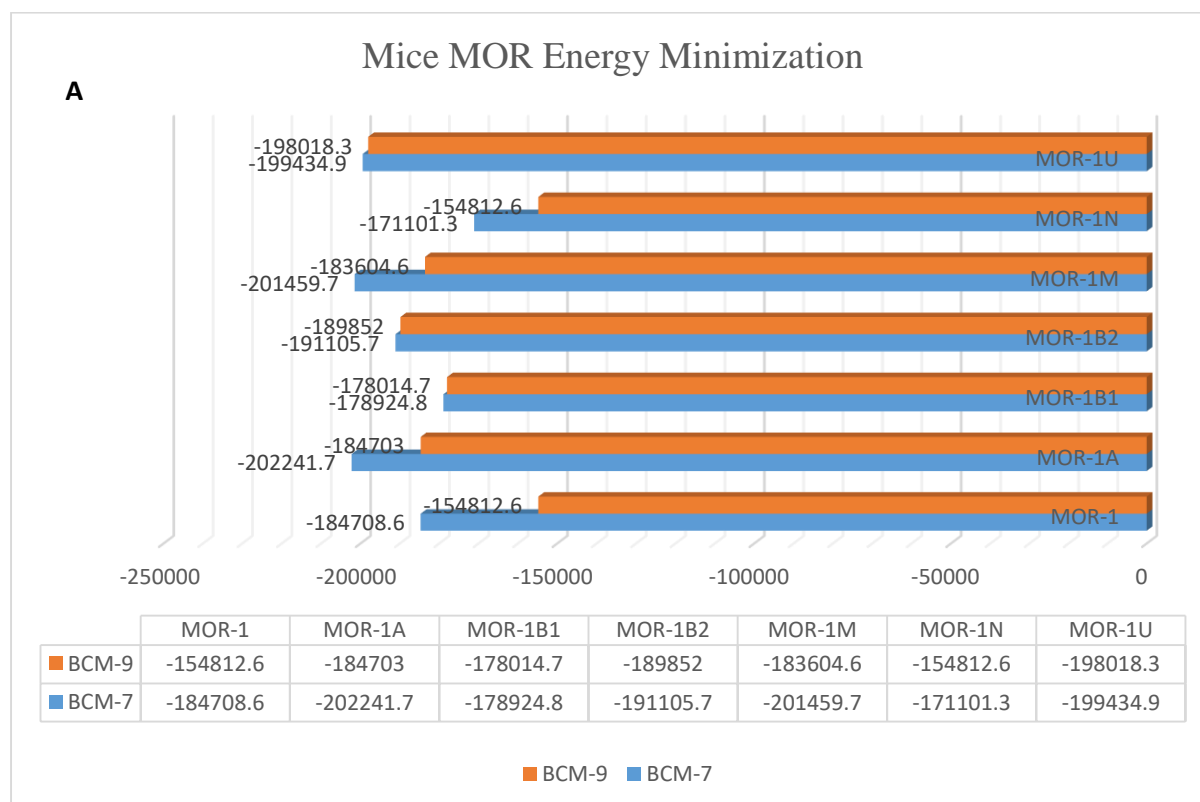


**Fig. 4.31 [A]** Mice MOR Comparative energy analysis of BCMs complex. Blue line energy indicates BCM-7 and orange colour BCM-9 complex.

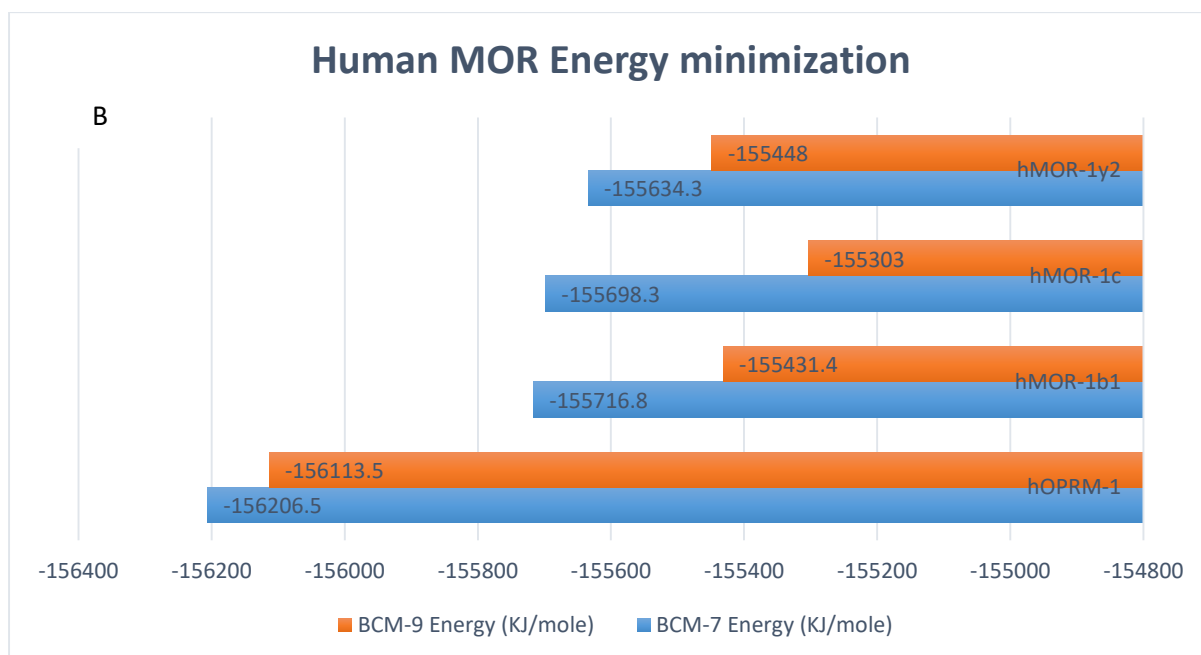


**Fig. 4.31 [B]** Human MOR Comparative energy analysis of BCMs complex. Blue line energy indicates BCM-7 and orange colour BCM-9 complex.

# **CHAPTER -5**

## **Summary and Conclusions**

## SUMMARY AND CONCLUSIONS

---

### **(A) To characterize mu opioid receptor (MOR) and its splice variants in brain and gut tissues of mice**

- Seven splice variants of OPRM-1 gene were identified by amplification of RNA from gut and brain tissue of mice. Sequence characterization of identified splice variants was carried out using ABI 3100 automated DNA Sequencer. Further, to gain insight into all available splice variants, resources like NCBI, UniProt and conserved domain database were also searched. Overall experimentally and from databases a total of 31 MORs transcripts were identified.
- The mice transcript variants were characterized for their location on chromosome, in the cell, exon-intron structure, position of different domains and splicing sites etc. Domain structure of all mice mu receptor genes was conserved and two signature patterns G\_PROTEIN\_RECEP\_F1\_1 and G\_PROTEIN\_RECEP\_F1\_2 were identified. One motif NPxxY was also observed across all the transcript variants. Due to the structural similarity, MORs shared identical binding pockets as well as intra- and extracellular loops.
- The structural organisation of mice transcripts was similar to other mammalian species. At the amino acid level mice MORs showed 93.8 and 92 percent homology to human, rat and cow MORs respectively. Sequence alignments of MOR-1 across species indicated that regions with the highest homology were the transmembrane domains and the three intracellular loops which are important for MORs ligand binding and G protein coupling. The major differences were observed only at the tip of the C –terminus which is the result of splicing.
- The grouping of different MORs on the basis of nucleotide sequences and splicing at different exons resulted in three major groups. Group 1 consisted of 7TM transcript variants resulting from splicing of exon1. All the full length 7TM transcript variants contained exon 1, 2 and 3 which encodes the entire MOR-1 receptor except for the tip of C-terminal 12 amino acid. In addition to these three exons additional exons were also observed in some of the 7 Tm transcript variants including exons 4-5, 7-10, 15, 18 or 19. Group 2 consisted of 6TM transcript variants resulting from splicing of exon 11 and skipping of exon 1. In addition to exon 11 which are observed uniformly, additional exons (4, 7, 8, 9, 11, 13 and 14) in some of the transcript variants of group were also observed. Group 3 consisted of transcript

variants with one trans- membrane domain (1TM) encoded by exon 1. These variants lack exons 2 and 3 but three members (MOR-1H; 1i and -1j) showed additional exons as well.

- The homology search revealed that amongst the 19 splice variants, (MOR-1, MOR-1A, MOR-1B1-1B2, 1B3, 1B4 & 1B5, MOR-1C, MOR-1D, MOR-1F, MOR-1Ei, MOR-1Eii MOR-1Eiii MOR-1Eiv MOR-1Q, MOR-1V, MOR-1W, MOR-1P, MOR-1O,) showed sequence homology from amino acid position 1-360 that is the region including exon 1-3. Variations across these receptors were observed at exon 4. Sequence for Motifs NPXXY (NPVLY) and DRY was conserved in all the 7 transmembrane domains.
- Phylogenetic analysis of MOR gene family distinguished them into three major evolutionary groups wherein members of group III were most divergent and quite dissimilar than from rest of the MOR sequences.

**(B) To clone MOR in Pichia / Bacterial expression system for their over expression and purification**

- The oprm-1M gene was cloned in expression vector pET 28a (+) having T7 promoter and a His-tag sequence that facilitates the purification of recombinant proteins using affinity chromatography. Toxic protein resistance *E.coli* C41 was used as host system. Over-expression of MOR-1M membrane proteins was achieved using 0.4mM IPTG at low temperature (18<sup>0</sup>C).
- The purification of seven Trans membrane protein (7TM) was carried out by using high efficiency membrane protein solubilizing detergents that is 6M urea and 0,8% L-laurylsarcosine.
- The properties of the purified protein were validated. Sufficient quantity of protein was recovered and it can serve as a resource for future studies.

**(C) To undertake interaction studies of MOR with BCM7/9 by in silico approach.**

- Strategy of homology modelling was utilized to generate 3D structure of MORs. For structure prediction, the sequences for major 10 mu receptor isoform were used. Three templates (4n6hA, 5zbh, 4dk1A) satisfying all the criterion for the stable structure were used for homology modeling using I-TASSER. The homology of these templates with mu receptors was 95-98 %.

- Using RAMPAGE Server, 98 % residues of mu receptors were observed to be in the most favored regions indicating energetically and sterically stable conformations of residues.
- The ligand structure prediction (BCM7/9) was carried out by MODELLER server. DOPE score of 0.97 and 0.98 for the structures of BCM7 and 9 respectively, indicated good quality of homology model.
- The PDB files of ligand and target receptor were uploaded to Patch Dock server for docking, using cluster RMSD at default value of 4Å°. Interacting amino acidic residues and prominent binding sites were predicted by PDBsum server and LIGPLOT server respectively. Major forces involved in protein-ligand interactions were Hydrogen bonding in association with other non-covalent interactions such as ionic interactions, hydrophobic interactions, and Van der Waals forces.
- Docking of BCM7/9 with the mu receptors indicated stable binding of BCM7 with mu receptors as compared to BCM9 in terms of interacting amino acids (TYR128, TRP 318, ASN 127, LYS 233, GLU 310LEU 219), ligand and protein atoms involved in hydrogen bonding (BCM7 = LYS233 (2.22 Å°), BCM9 = LYS 233(3.09 Å°)). Further, number of interacting hydrophobic amino acid residues were 15 in case of BCM7 while 13 in BCM9.
- The comparative energy minimization of docked model for  $\mu$ -OR-BCM7 (-191105.7 KJ/mole) and for  $\mu$ -OR-BCM9 (-1898520 KJ/mole) using YASARA server also indicated greater binding affinity of BCM7 towards mu opioid receptor. .

The study helped to characterize the mice mu opioid receptors and its splice variants. Cloning and induced expression mu opioid receptor genes in pET28a (+) vector and E.coli C41 (DE3) host can yield purified protein in large quantities. The 3D structures generated through different software's helped to understand the efficacy of interactions and binding characteristics of MOR with different BCM peptide legends. The interaction of MORs with BCM7 / BCM9 clearly indicated the strong binding of BCM7 with Mu receptors as compared to BCM9. This work form the basis for future studies to understand the impact of different bioactive peptides generated from A1/A2 milk as it is generally believed that binding of MORs with beta-casomorphins (BCMs) might lead to transducing signals and various intracellular pathways that may lead to different health disorders.

---

---

# **Bibliography**

---

---

## BIBLIOGRAPHY

---

- Abbadie., Catherine, Ying-Xian, Pan., and Gavril, W. Pasternak. (2000). Differential distribution in rat brain of mu opioid receptor carboxy terminal splice variants MOR-1C-like and MOR-1-like immunoreactivity: evidence for region-specific processing. *Journal of Comparative Neurology* **419.2**: 244-256.
- Akermoun, M., Koglin, M., Zvalova-Iooss D., Folschweiller, N. and Dowell, SJ. (2005). Characterization of 16 human G protein-coupled receptors expressed in baculovirus-infected insect cells. *Protein Expr Purif* **44**: 65–74.
- Akil, H., Watson, S. J., Young, E., Lewis, M. E., Khachaturian, H., and Walker, J. M. (1984). Endogenous opioids: biology and function. *Annual review of neuroscience*, **7**(1), 223-255.
- Al-Hasani., Ream, and Michael, R. Bruchas. (2011). Molecular mechanisms of opioid receptor-dependent signaling and behavior." *The Journal of the American Society of Anesthesiologists I* **15.6** 20: 1363-1381.
- Alkorta, I., and Loew, G. H. (1996). A 3D model of the  $\delta$  opioid receptor and ligand-receptor complexes. *Protein Engineering, Design and Selection*, **9**(7), 573-583.
- Andoh, T., Yageta, Y., and Konno, M. (2008). Evidence for separate involvement of different mu-opioid receptor subtypes in itch and analgesia induced by supraspinal action of opioids. *J Pharmacol Sci* **106**: 667–70.
- Andre, N., Cherouati, N., Prual, C., Steffan, T., and Zeder-Lutz, G. (2006). Enhancing functional production of G protein-coupled receptors in *Pichia pastoris* to levels required for structural studies via a single expression screen. *Protein Sci* **15**: 1115–1126.
- Anna, Janecka1., Jakub, Fichna1., Marek, Mirowski., and Tomasz, Janecki.(2002).Structure-activity Relationship, Conformation and Pharmacology Studies of Morphiceptin Analogues - Selective  $\mu$ -Opioid Receptor Ligands.**2**: 565-572.
- Arianna, Rath., Mira, Glibowicka., Vincent, G., Nadeau, Gong Chen., and Charles, M. Deber (2009). Detergent binding explains anomalous SDS-PAGE migration of membrane proteins. *Proceedings of the National Academy of Sciences* Feb 2009, 106 (6) 1760-1765; DOI: 10.1073/pnas.0813167106
- Audu, C. O., O’Hara, B., Pellegrini, M., Wang, L., Atwood, W. J., & Mierke, D. F. (2012). Reining in polyoma virus associated nephropathy: Design and characterization of a template mimicking BK viral coat protein cellular binding. *Biochemistry*, **51**(41), 8092-8099.
- Ballesteros, J., and Palczewski, K. (2001). G protein-coupled receptor drug discovery: implications from the crystal structure of rhodopsin. *Current opinion in drug discovery & development*, **4**(5), 561.

- Barak, L. S., Menard, L., Ferguson, S. S., Colapietro, A. M., and Caro, G. (1995). *Biochemistry*. **34**:15407–15414.
- Bare, L. A., Mansson, E., and Yang, D. (1994). Expression of two variants of the human  $\mu$  opioid receptor mRNA in SK-N-SH cells and human brain. *FEBS Lett* **354**:2 13–216.
- Bausch, Suzanne B., Terrell, A., Patterson, Suzanne, M., Appleyard, and Charles, Chavkin. (1995). Immunocytochemical localization of delta opioid receptors in mouse brain. *Journal of chemical neuroanatomy* 8, no. **3**: 175-189.
- Becker, Axel., Gisela, Grecksch., Rudolf, Brödemann., Jürgen, Kraus., Brigitte, Peters., Helmut, Schroeder., Werner, Thiemann., Horace, H., Loh, and Volker Höllt.(2000). Morphine self-administration in  $\mu$ -opioid receptor-deficient mice." *Naunyn-Schmiedeberg's archives of pharmacology* 361, no. **6**: 584-589.
- Berman, HM., Westbrook, J., Feng, Z., Gilliland, G., Bhat, TN., Weissig, H., Shindyalov, IN., and Bourne, PE.(2000). The Protein Data Bank. *Nucleic Acids Res.***28**:235–242.
- Bird, Adrian. (2007). Perceptions of epigenetics. *Nature* **447**.7143: 396.
- Blake, A.D., Bot, G., Li, S., Freeman, J.C. and Reisine, T., (1997). Differential Agonist Regulation of the Human  $\kappa$ -Opioid Receptor. *Journal of neurochemistry*, **68**(5), pp.1846-1852.
- Blumberg, H., and H. B. Dayton. (1973). Naloxone, naltrexone, and related noroxymorphones." *Advances in biochemical psychopharmacology* **8**: 33-43.
- Bockaert, J., Claeysen, S., Bécamel, C., Dumuis, A., and Marin, P. (2006). Neuronal 5-HT metabotropic receptors: fine-tuning of their structure, signaling, and roles in synaptic modulation. *Cell and tissue research*, **326**(2), 553-572.
- Botstein, D., Segev, N., Stearns, T., Hoyt, M. A., Holden, J., and Kahn, R. A. (1988). Diverse biological functions of small GTP-binding proteins in yeast. In Cold Spring Harbor symposia on quantitative biology (Vol. **53**, pp. 629-636). Cold Spring Harbor Laboratory Press.
- Boutrou, R., Gaudichon, C., and Dupont, D. (2013). Sequential release of milk protein-derived bioactive peptides in the jejunum in healthy humans. *American Journal of Clinical Nutrition*. **97**(6):1314–1323. doi:10.3945/ajcn.112.055202.
- Brantl, V., Teschemacher, H., Henschen, A. and Lottspeich, F. (1979) Novel opioid peptides derived from casein (b-casomorphins): I. Isolation from bovine casein peptone. *Hoppe-Seyler's Z PhysiolChem* **360**:1211–1216.
- Bruchas, and Michael, R. (2006). Kappa opioid receptor activation of p38 MAPK is GRK3- and arrestin-dependent in neurons and astrocytes." *Journal of Biological Chemistry* **281**.26: 18081-18089.
- Bruchas, M. R., Macey, T.A., Lowe, J.D. and Chavkin, C. (2006). Kappa opioid receptor activation of p38 MAPK is GRK3- and arrestindependent in neurons and astrocytes. *J BiolChem*; **281**:18081–9.

- Brylinski, M., & Skolnick, J. (2008). A threading-based method (FINDSITE) for ligand-binding site prediction and functional annotation. *Proceedings of the National Academy of sciences*, *105*(1), 129-134.
- Campbell, J. J., Haraldsen, G., Pan, J., Rottman, J., Qin, S., Ponath, P., & Wu, L. (1999). The chemokine receptor CCR4 in vascular recognition by cutaneous but not intestinal memory T cells. *Nature*, **400**(6746), 776.
- Capra, J. A., Laskowski, R. A., Thornton, J. M., Singh, M., & Funkhouser, T. A. (2009). Predicting protein ligand binding sites by combining evolutionary sequence conservation and 3D structure. *PLoS computational biology*, *5*(12), e1000585.
- Chaijale, N.N., Aloyo, V. J., and Simansky, KJ. (2008). A naloxonazine sensitive ( $\mu$ 1 receptor) mechanism in the parabrachial nucleus modulates eating. *Brain Res* **1240**: 111–8.
- Cherny, Nathan., Carla, Ripamonti., Jose, Pereira., Carol, Davis., Marie, Fallon., Henry, McQuay., Sebastiano, Mercadante., Gavril ,Pasternak., Vittorio, Ventafridda., and Expert Working Group of the European Association of Palliative Care Network.(2001). Strategies to manage the adverse effects of oral morphine: an evidence-based report. *Journal of Clinical Oncology* 19, no. **9**: 2542-2554.
- Childers, and Joel, M. (1993). Laparoscopically assisted surgical staging (LASS) of endometrial cancer. *Gynecologic oncology* **51.1**: 33-38.
- Childers, SR., Creese, I., Snowman, A. M, and Synder, SH. (1979). Opiate receptor binding affected differentially by opiates and opioid peptides. *Eur J Pharmacol*; **55**:11–15.
- Christen, and Markus. (2005). The GROMOS software for biomolecular simulation: GROMOS05." *Journal of computational chemistry* **26.16**: 1719-1751.
- Christopoulos, A., and Kenakin, T. (2002).G protein-coupled receptor allostereism and complexing. *Pharmacol Rev.* Jun; **54**(2):323-74.
- Cogoni, Carlo, Nicoletta, Romano, and Giuseppe, Macino. (1994). Suppression of gene expression by homologous transgenes. *Antonie Van Leeuwenhoek* **65.3**: 205-209.
- Contet, C., Kieffer, BL., and Befort, K. (2004). Mu opioid receptor: a gateway to drug addiction. *Curr OpinNeurobiol.* **14**:370–378. [PubMed: 15194118]
- Cregg, James, M., Thomas, S. Vedvick., and William, C. Raschke. (1993). Recent advances in the expression of foreign genes in *Pichia pastoris*. *Nature Biotechnology* **11.8** (1993): 905.
- Dang, V. C., & Christie, M. J. (2012). Mechanisms of rapid opioid receptor desensitization, resensitization and tolerance in brain neurons. *British journal of pharmacology*, **165**(6), 1704-1716.
- Davis, and Ian, W. (2007). MolProbity: all-atom contacts and structure validation for proteins and nucleic acids." *Nucleic acids research* *35.suppl\_2*: W375-W383.

- DeLano, W.L., (2002). The PyMOL Molecular Graphics System. Available online: <http://pymol.Org> (accessed on 25 September 2016).
- Dhawan, BN., Cesselin, F., Raghupir, R., Reisine, T., Bradley, PB. Portoghese, PS., and Hamon, M. (1996). International Union of Pharmacology XII: Classification of opioid receptors. *Pharmacol Rev* **48**:567–92
- Di, Chiara., Gaetano, and R. Alan, North. (1992). Neurobiology of opiate abuse. *Trends in pharmacological sciences* **13**: 185-193.
- Doyle, GA., Rebecca, Sheng, X., Lin, SS., Press, DM., Grice, DE., Buono, RJ., Ferraro, TN., and Berrettini, WH. (2007a). Identification of three mouse mu-opioid receptor (MOR) gene (Oprm1) splice variants containing a newly identified alternatively spliced exon. *Gene* **388**:135–147.
- Du, J., Lei, B., Qin, J., Liu, H., & Yao, X. (2009). Molecular modeling studies of vascular endothelial growth factor receptor tyrosine kinase inhibitors using QSAR and docking. *Journal of Molecular Graphics and Modelling*, *27*(5), 642-654.
- Duhovny, D.; Nussinov, R.; Wolfson, H.J. (2002). Efficient unbound docking of rigid molecules. *Lect. Notes Comput. Sci.* **2452**, **185**–200.
- Elliott, R.B., Harris, D .P. Hill, J.P., Bibby, NJ, and Wasmuth, HE. (1999). Type I (insulin-dependent) diabetes mellitus and cow milk: casein variant consumption. *Diabetologia*, **42**: 292-6.
- Filizola, M., and Weinstein, H. (2002). Structural models for dimerization of G-protein coupled receptors: The opioid receptor homodimers. *Peptide Science: Original Research on Biomolecules*, **66**(5), 317-325.
- Filizola, Marta ., Liisa, Laakkonen., and Gilda, H. Loew. (1999). 3D modeling, ligand binding and activation studies of the cloned mouse  $\delta$ ,  $\mu$  and  $\kappa$  opioid receptors. *Protein engineering* **12.11**: 927-942.
- Flight, Jillian, I., and Adelle, E. Forth. (2007). instrumentally violent youths: The roles of psychopathic traits, empathy, and attachment." *Criminal Justice and Behavior* **34.6**: 739-751.
- Flight, MH. (2007). Epigenetics: methylation and schizophrenia. *Nat Rev Neurosci.*; **8**:**910**–1.
- Flower, DR. (1999). Modelling G-protein-coupled receptors for drug design. *Biochim Biophys Acta* **1422**: 207–234.
- Franklin, TG.and Traynor, JR. (1991). Alkylation with beta-funaltrexamine suggests differences between mu-opioid receptor systems in guinea-pig brain and myenteric-plexus. *Br J Pharmacol* **102**: 718–22
- Fredriksson, R., Lagerstrom, M.C., Lundin, LG., and Schioth, HB. (2003). The G-protein-coupled receptors in the human genome form five main families. Phylogenetic analysis, paralogon groups, and fingerprints. *Mol Pharmacol* **63**: 1256–1272.

- Fritze, O., Filipek, S., Kuksa, V., Palczewski, K., Hofmann, K. P., & Ernst, O. P. (2003). Role of the conserved NPxxY (x) 5, 6F motif in the rhodopsin ground state and during activation. *Proceedings of the National Academy of Sciences*, *100*(5), 2290-2295.
- Gether, U. (2000). Uncovering molecular mechanisms involved in activation of G protein-coupled receptors. *Endocr Rev.* Feb; **21**(1):90-113
- Giuliani, A., Pirri, G., & Nicoletto, S. (2007). Antimicrobial peptides: an overview of a promising class of therapeutics. *Open Life Sciences*, *2*(1), 1-33.
- Grisshammer, R., Tate, CG. (1995). Overexpression of integral membrane proteins for structural studies. *Q Rev Biophys* **28**: 315–422.
- Grunewald, S., Haase, W., Molsberger, E., Michel, H., and Reilander, H. (2004). Production of the human D2S receptor in the methylotrophic yeast *P. pastoris*. *Receptors Channels* **10**: 37–50.
- Gulland, John, Masson, and Robert, Robinson. (1923). CXII.—the morphine group. Part I. A discussion of the constitutional problem. *Journal of the Chemical Society, Transactions* **123**: 980-998.
- Hahn, E. F., Carroll-Buatti, M., Pasternak, GW. (1982). Irreversible opiate agonists and antagonists: the 14-hydroxydihydromorphinone azines. *J Neurosci* **2**: 572–6.
- Hanson, MA, and Stevens, RC. (2009). Discovery of new GPCR biology: one receptor structure at a time. *Structure*. **17**:8–14. [PubMed: 19141277]
- Hassaine, G., Wagner, R., Kempf, J., Cherouati, N, and Hassaine. (2006). Semliki Forest virus vectors for overexpression of 101 G protein-coupled receptors in mammalian host cells. *Protein Expr Purif* **45**: 343–351.
- Hausdorff, W. P., P. T. Campbell., J. Ostrowski., S. S. Yu., M. G. Caron., and R. J. Lefkowitz. (1991). A small region of the  $\beta$ -adrenergic receptor is selectively involved in its rapid regulation. *Proc. Natl. Acad. Sci. USA* **88**: 2979
- Hug, N., Longman, D., and Cáceres, JF. (2016). Mechanism and regulation of the nonsense-mediated decay pathway. *Nucleic Acids Res.*; **44**(4):1483-95.
- Inturrisi, and Charles, E. (2002). Clinical pharmacology of opioids for pain. *The Clinical journal of pain* **18**. S3-S13.
- Janecka, anna, Fichna, J. and Janecki, T. (2004). Opioid Receptors and Their Ligands. *Current Topics in Medicinal Chemistry*. **4**(1):1–17.
- Jinsmaa, Y. and Yoshikawa, M. (1999). Enzymatic release of neocasomorphin and  $\beta$ -casomorphin from bovine  $\beta$ -casein. *Peptides*. **20**(8):957–962. Doi: 10.1016/s0196-9781(99)00088-1.
- Jordan, B. A., and Devi, L. A. (1999). G-protein-coupled receptor heterodimerization modulates receptor function. *Nature*, **399**(6737), 697.
- Kabsch, W. (1976). A solution for the best rotation to relate two sets of vectors. *Acta Cryst.* 1; A **32**:922–923.

- Kenakin, T. (2002). Efficacy at G-protein-coupled receptors. *Nature reviews Drug discovery*, *1*(2), 103.
- Kervestin, S. and Jacobson, A. (2012). NMD: a multifaceted response to premature translational termination. *Nat Rev Mol Cell Biol.* 2012 Nov; **13**(11):700-12.
- Kervestin, S., & Jacobson, A. (2012). NMD: a multifaceted response to premature translational termination. *Nature reviews Molecular cell biology*, *13*(11), 700.
- Kieffer, BL. and Gaveriaux-Ruff, C. (2002). Exploring the opioid system by gene knockout. *Prog Neurobiol* **66**: 285–306.
- Kieffer, BL., and Evans, CJ. (2009). Opioid receptors: From binding sites to visible molecules in vivo. *Neuropharmacology*. **56**:205–212. [PubMed: 18718480]
- Kostyra, E., Sienkiewicz-Szapka, E., Jarmoowska, B., Krawczuk, S. and Kostyra, H. (2004). Opioid peptides derived from milk proteins. *Polish Journal of Nutrition Science* **13**/54: 25–35.
- Kraus, J., Horn, G., Zimprich, A., Simon, T., Mayer, P., and Höllt, V. (1995). Molecular cloning and functional analysis of the rat m opioid receptor gene promoter. *Biochem Biophys Res Commun* **215**:591–597.
- Kulp, J. L., Blumenthal, S. N., Wang, Q., Bryan, R. L., & Guarnieri, F. (2012). A fragment-based approach to the SAMPL3 Challenge. *Journal of computer-aided molecular design*, *26*(5), 583-594.
- Laemmli, U. K. (1970). "Cleavage of Structural Proteins during the Assembly of the Head of Bacteriophage T4". *Nature*. *227* (5259): 680–685.
- Lagerstrom, MC, and Schioth, HB. (2008). Structural diversity of G protein-coupled receptors and significance for drug discovery. *Nat Rev Drug Discov.* **7**:339–357. [PubMed: 18382464]
- LaSalle, JM. (2011). A genomic point-of-view on environmental factors influencing the human brain methylome. *Epigenetics off J DNA Methylation Soc.* **6**:862–9.
- Laskowski, R. A., & Swindells, M. B. (2011). LigPlot+: multiple ligand–protein interaction diagrams for drug discovery.
- Laskowski, RA., MacArthur, MW. Moss D, and Thornton, JM. (1993). PROCHECK: a program to check the stereochemical quality of protein structures. *J Appl Cryst* **26**:283–291. Doi: 10.1107/S0021889892009944.
- Levin, J. M., Robson, B. and Garnier, J. (1986). An algorithm for secondary structure determination in proteins based on sequence similarity. *FEBS Letters*, **205**, 303-308.
- Levitt, M., Gerstein, M. (1998) A unified statistical framework for sequence comparison and structure comparison, *Proc. Natl Acad. Sci. USA*, vol. 95 (pg. 5913-5920)
- Lindahl, Erik, Berk Hess, and David Van Der Spoel. (2001). GROMACS 3.0: a package for molecular simulation and trajectory analysis. *Molecular modeling annual* **7**.8: 306-317.

- Ling, GS, Spiegel, K., Lockhart, SH., and Pasternak, GW. (1985). Separation of opioid analgesia from respiratory depression: evidence for different receptor mechanisms. *J Pharmacol Exp Ther* **232**: 149–55.
- Lykke-Andersen J., Shu M.D., Steitz J.A. (2001). Communication of the position of exon-exon junctions to the mRNA surveillance machinery by the protein RNPS1. *Science*. 293:1836–1839.
- Ma, Y., Kubicek, J, and Labahn, J. (2013). Expression and Purification of Functional Human Mu Opioid Receptor from E.coli. *PLoS ONE* 8(2): e56500. Doi: 10.1371/journal.pone.0056500.
- MacDonald, and Marcy, E. (1993). A novel gene containing a trinucleotide repeat that is expanded and unstable on Huntington's disease chromosomes." *Cell* **72.6**: 971-983.
- Maggio, R., Novi, F., Scarselli, M, and Corsini, GU. (2005).The impact of G-proteincoupled receptor hetero-oligomerization on function and pharmacology. *Febs J*272: 2939–2946.
- Magnan, Jacques, Stewart, J. Paterson, and Hans, W. Kosterlitz. (1992). The interaction of [Met5] enkephalin and [Leu5] enkephalin sequences, extended at the C-terminus, with the  $\mu$ -,  $\delta$ -and  $\kappa$ -binding sites in the guinea-pig brain. *Life sciences***31.12-13**: 1359-1361.
- Mansour, and Alfred. (1988). Anatomy of CNS opioid receptors. *Trends in neurosciences* **11.7**: 308-314.
- Mao, J., Wang, J., Liu, B., Pan, W., Farr III, G.H., Flynn, C., Yuan, H., Takada, S., Kimelman, D., Li, L. and Wu, D.(2001). Low-density lipoprotein receptor-related protein-5 binds to Axin and regulates the canonical Wnt signaling pathway. *Molecular cell*, **7**(4), pp.801-809.
- Matthes, and Hans, WD. (1996).Loss of morphine-induced analgesia, reward effect and withdrawal symptoms in mice lacking the  $\mu$ -opioid-receptor gene. *Nature* **383.6603**: 819.
- Matthes, H. W., Maldonado, R., Simonin, F., Valverde, O., Slowe, S., Kitchen, I., & Tzavara, E. (1996). Loss of morphine-induced analgesia, reward effect and withdrawal symptoms in mice lacking the  $\mu$ -opioid-receptor gene. *Nature*, **383**(6603), 819.
- McLachlan, C.N. (2001). Beta-casein A1, ischaemic heart disease mortality, and other illnesses. *Medical Hypotheses* **56**: 262–72.
- McNicol E, Horowicz-Mehler, N., Fisk, RA., Bennett, K., Gialeli-Goudas, M., Chew, PW, Lau, J., Carr, D. and American Pain Society. (2003). Management of opioid side effects in cancer-related and chronic noncancer pain: A systematic review. *J Pain*; **4**:231–56.
- Melief, and Erica, J. (2010) Ligand-directed c-Jun N-terminal kinase activation disrupts opioid receptor signaling." *Proceedings of the National Academy of Sciences* **107.25**: 11608-11613.

- Melief, EJ, Miyatake, M., Bruchas, MR, and Chavkin, C. (2010). Ligand-directed c-Jun N-terminal kinase activation disrupts opioid receptor signaling. *Proc Natl Acad Sci USA*; **107** 11608–13.
- Michino, M., Abola, E., Dock, G. P. C. R., Brooks III, C. L., Dixon, J. S., Moulton, J., & Stevens, R. C. (2009). Community-wide assessment of GPCR structure modelling and ligand docking: GPCR Dock 2008. *Nature Reviews Drug Discovery*, **8**(6), 455.
- Minami M, and Satoh, M. (1995). Molecular biology of the opioid receptors: structures, functions and distributions. *Neurosci Res. Sep*; **23**(2):121-45.
- Minami M, and Satoh, M. (1995). Molecular biology of the opioid receptors: structures, functions and distributions. *Neurosci Res. Sep*; **23**(2):121-45.
- Mintz, G.S., Popma, J.J., Pichard, A.D., Kent, K.M., Satler, L.F., Chuang, Y.C., Ditrano, C.J. and Leon, M.B., (1995). Patterns of calcification in coronary artery disease: a statistical analysis of intravascular ultrasound and coronary angiography in 1155 lesions. *Circulation*, **91**(7), pp.1959-1965.
- Miroux, B., and Walker, JE. (1996). Over-production of proteins in Escherichia coli: mutant hosts that allow synthesis of some membrane proteins and globular proteins at high levels. *J Mol Biol* **260**: 289–298.
- Mishra, B. P., Mukesh, M., Prakash, B., Sodhi, M., Kapila, R., Kishore, A., Kataria, R. R., Joshi, B. K., Bhasin, V., Rasool, T. J. and Bujarbaruah, K. M. (2009). Status of milk protein, b-casein variants among Indian milch animals. *Indian Journal of Animal Sciences* **79** (7): 722–25.
- Moles, A., Kieffer, BL., and D'Amato, FR. (2004). Deficit in attachment behavior in mice lacking the mu-opioid receptor gene. *Science*. **304**:1983–1986.
- Moles, A., Kieffer, BL., and D'Amato, FR. (2004). Deficit in attachment behavior in mice lacking the mu-opioid receptor gene. *Science*. **304**:1983–1986.
- Moon, R. Y., Horne, R. S., and Hauck, F. R. (2007). Sudden infant death syndrome. *The Lancet*, **370**(9598), 1578-1587.
- Morgan, and Neil, V. (2006). PLA2G6, encoding a phospholipase A 2, is mutated in neurodegenerative disorders with high brain iron." *Nature genetics* **38**.7: 752.
- Murzin, AG, and Bateman, A. (2001). CASP2 knowledge-based approach to distant homology recognition and fold prediction in CASP4. *Proteins. ;Suppl 5*:76–85. doi: 10.1002/prot.10037.
- Nagy, E. and Maquat, L.E. (1998). A rule for termination-codon position within intron-containing genes: when nonsense affects RNA abundance. *Trends Biochem. Sci.* **23**:198–199
- Nestler, and Eric, J. (1993). Regulation of neural gene expression in opiate and cocaine addiction." *NIDA research monograph* **125**: 92-92. *Neuron* **69**:6–8.

- Noha, S. M., Schmidhammer, H., & Spetea, M. (2017). Molecular Docking, Molecular Dynamics, and Structure–Activity Relationship Explorations of 14-Oxygenated N-Methylmorphinan-6-ones as Potent  $\mu$ -Opioid Receptor Agonists. *ACS chemical neuroscience*, *8*(6), 1327-1337.
- Noni, ID. (2008). Release of  $\beta$ -casomorphins 5 and 7 during simulated gastro-intestinal digestion of bovine  $\beta$ -casein variants and milk-based infant formulas. *Food Chemistry*. **110**(4):897–903. doi:10.1016/j.foodchem..02.077.
- Nuyts, S., Van Mellaert, L., Lambin, P., & Anné, J. (2001). Efficient isolation of total RNA from *Clostridium* without DNA contamination. *Journal of microbiological methods*, *44*(3), 235-238.
- Palczewski, K., Kumasaka, T., Hori, T., Behnke, CA. Motoshima, H., Fox, BA., Le, Trong, I. Teller, DC., Okada, T., Stenkamp, RE., Yamamoto, M. and Miyano, M. (2000). Crystal structure of rhodopsin: A G protein-coupled receptor. *Science*. Aug 4; **289**(5480):739-45
- Pan YX, Xu J, Bolan EA, Abbadie C, Chang A, Zuckerman A, Rossi GC, and Pasternak GW (1999). Identification and characterization of three new alternatively spliced mu-opioid receptor isoforms. *Mol Pharmacol* **56**:396–403.
- Pan Y-X, Xu J, Mahurter L, Bolan EA, Xu MM, and Pasternak GW (2001) Generation of the mu opioid receptor (MOR-1) protein by three new splice variants of the Oprm gene. *Proc Natl Acad Sci USA* **98**:14084–14089.
- Pan YX, Xu J, Mahurter, L., Xu M., Gilbert, A. K., Pasternak, GW. (2003). Identification and characterization of two new human mu opioid receptor splice variants, hMOR-10 and hMOR-1X. *Biochem Biophys Res Commun*. Feb 21; **301**(4):1057-61.
- Pan YX, Xu J., Bolan, E., Moskowitz, HS., Xu, M., and Pasternak. GW. (2005b). Identification of four novel exon 5 splice variants of the mouse mu-opioid receptor gene: functional consequences of C-terminal splicing. *Mol Pharmacol* **68**:866–875.
- Pan, L., Xu, J., Yu, R., Xu, M. M., Pan, YX., and Pasternak, GW. (2005a). Identification and characterization of six new alternatively spliced variants of the human mu opioid receptor gene, Oprm. *Neuroscience* **133**:209–220.
- Pan, YX , Xu J, Bolan E, Moskowitz HS, Xu M, Pasternak, GW. (2005). Identification of four novel exon 5 splice variants of the mouse mu-opioid receptor gene: functional consequences of C-terminal splicing. *Mol Pharmacol*. Sep; **68**(3):866-75
- Pan, YX. (2005). Diversity and complexity of the mu opioid receptor gene: alternative pre-mRNA splicing and promoters. *DNA Cell Biol* **24**:736–750.
- Pan, Y-X., Bolan, E., and Pasternak, GW. (2002). Dimerization of morphine and orphanin FQ/nociceptin receptors: generation of a novel opioid receptor subtype. *Biochem Biophys Res Commun* **297**:659–663.

- Pan, Y-X., Cheng, J., Xu, J., and Pasternak. GW. (1994). Cloning, expression and classification of a kappa3-related opioid receptor using antisense oligodeoxynucleotides. *Regul Pept* **54**:217–218.
- Pan, Y-X., Cheng, J., Xu, J., Rossi, GC., Jacobson, E., Ryan-Moro, J., Brooks, AI., Dean, GE., Standifer, KM, and Pasternak, GW .(1995). Cloning and functional characterization through antisense mapping of a kappa 3-related opioid receptor. *Mol Pharmacol* **47**:1180–1188.
- Pasare, Chandrashekhar, and Ruslan, Medzhitov. (2003). Toll pathway-dependent blockade of CD4+ CD25+ T cell-mediated suppression by dendritic cells." *Science* 299.5609: 1033-1036.
- Pasternak GW and Pan YX (2011) Mix and match: heterodimers and opioid tolerance.
- Pasternak, GW, Goodman, R., and Snyder, SH. (1975a).An endogenous morphine-like factor in mammalian brain. *Life Sci* **16**:1765–1769.
- Paul D, and Pasternak GW. (1988). Differential blockade by naloxonazine of two mu opiate actions: analgesia and inhibition of gastrointestinal transit. *Eur J Pharmacol* **149**: 403–4.
- Peysseon, F., & Ricard-Blum, S. (2014). Heparin–protein interactions: from affinity and kinetics to biological roles. Application to an interaction network regulating angiogenesis. *Matrix biology*, 35, 73-81.
- Pierce, KL, Premont, RT., Lefkowitz, and RJ. (2002). Seven-transmembrane receptors. *Nat Rev Mol Cell Biol.* **3**:639–650. [PubMed: 12209124]
- Pierce, KL, Premont, RT., Lefkowitz, and RJ. (2002). Seven-transmembrane receptors. *Nat Rev Mol Cell Biol.* **3**:639–650. [PubMed: 12209124]
- Portoghese, Philip S., A. W. Lipkowski, and A. E. Takemori. (1987). Bimorphinans as highly selective, potent. Kappa. Opioid receptor antagonists." *Journal of medicinal chemistry* **30.2**: 238-239.
- Practical Dietetics, with special reference to diet in disease. (1895). *JAMA: The Journal of the American Medical Association.* **XXV** (13):551. doi:10.1001/jama.1895.02430390037016.
- Pradhan, A.A., Walwyn, W., Nozaki, C., Filliol, D., Erbs, E., Matifas, A., Evans, C. and Kieffer, B.L. (2010). Ligand-directed trafficking of the  $\delta$ -opioid receptor in vivo: two paths toward analgesic tolerance. *Journal of Neuroscience*, **30**(49), pp.16459-16468.
- Premont, R. T., & Gainetdinov, R. R. (2007). Physiological roles of G protein–coupled receptor kinases and arrestins. *Annu. Rev. Physiol.*, **69**, 511-534.
- Probst, W. C., L. A. Snyder, D. I. Schuster, J. Brosius, S. C. Sealfon. (1992). Sequence alignment of the G-protein coupled receptor superfamily. *DNA Cell Biol.* **11**: 1

- Ream Al-Hasani, and Michael R. Bruchas. (2011). Molecular Mechanisms of Opioid Receptor-dependent Signaling and Behavior, *Anesthesiology*, **115**, 6.Regul Pept 54:217–218.
- Robinson, M. S. (1994). The role of clathrin, adaptors and dynamin in endocytosis. *Curr. Opin. Cell. Biol.* 6: 538
- Roche, D., Brackenridge, D., and McGuffin, L. (2015). Proteins and their interacting partners: An introduction to protein–ligand binding site prediction methods. *International journal of molecular sciences*, **16**(12), 29829-29842.
- Roginski, H., Fuquay, J. W., and Fox, P. F. (2003). *Encyclopedia of dairy sciences. Volumes 1-4*. Academic press.
- Rosenbaum, DM, Rasmussen, SG, and Kobilka, BK. (2009). The structure and function of G-protein coupled receptors. *Nature*.**459**:356–363. [PubMed: 19458711]
- Rothman, RB, Jacobson, AE. Rice, KC, Herkenham, M. (1987). Autoradiographic evidence for two classes of mu opioid binding sites in rat brain using [125I] FK33824. *Peptides* **8**: 1015–21.
- Sarramegna, V., Demange, P., Milon, A, and Talmont, F. (2002). Optimizing functional versus total expression of the human mu-opioid receptor in *Pichia pastoris*.*Protein Expr Purif* **24**: 212–220.
- Sarramegna, V., Muller, I., Mousseau, G., Froment, C. and Monsarrat, B. (2005). Solubilization, purification, and mass spectrometry analysis of the human mu opioid receptor expressed in *Pichia pastoris*. *Protein Expr Purif* **43**: 85–93.
- Sarramegna, V., Talmont, F., Demange, P.and Milon, A. (2003). Heterologous expression of G-protein-coupled receptors: comparison of expression systems from the standpoint of large-scale production and purification. *Cell Mol Life Sci* **60**: 1529–1546.
- Sauer, R., Becker, H., Hohenberger, W., Rödel, C., Wittekind, C., Fietkau, R., & Karstens, J. H. (2004). Preoperative versus postoperative chemoradiotherapy for rectal cancer. *New England Journal of Medicine*, **351**(17), 1731-1740.
- Schanen, NC. (2006). Epigenetics of autism spectrum disorders. *Hum Mol Genet.* 15 Spec No 2:R138–50.
- Schlyer S, Horuk R (2006) I want a new drug: G-protein-coupled receptors in drug development. *Drug Discov Today* **11**: 481–493.
- Schneider, Jane C., and Leonard, Guarente. (1991). Regulation of the yeast CYT1 gene encoding cytochrome c1 by HAP1 and HAP2/3/4." *Molecular and Cellular Biology* **11**.10: 4934-4942.
- Schneidman-Duhovny, D.; Inbar, Y.; Nussinov, R.; Wolfson, H.J. (2005). PatchDock and SymmDock: servers for rigidand symmetric docking. *Nucleic Acids Res.* **33**, W363–W367.

- Scholzová, E., Malik, R., Ševčík, J., & Kleibl, Z. (2007). RNA regulation and cancer development. *Cancer letters*, 246(1-2), 12-23.
- Schüttelkopf, Alexander W., and Daan MF Van Aalten. (2004) PRODRG: a tool for high-throughput crystallography of protein–ligand complexes." *Acta Crystallographica Section D: Biological Crystallography* **60.8**: 1355-1363.
- Schweingruber, C., Rufener, SC., Zünd, D., Yamashita, A, and Muehlemann, O. (2013). Nonsense-mediated mRNA decay - mechanisms of substrate mRNA recognition and degradation in mammalian cells. *Biochim Biophys Acta*. Jun-Jul; 1829(6-7):612-23.
- Scorer, and Carol, A. (1994). Rapid selection using G418 of high copy number transformants of *Pichia pastoris* for high–level foreign gene expression." *Nature Biotechnology* **12.2**: 181.
- Singh, M., Rosen, CL., Chang, KJ. and Haddad, GG. (1989). Plasma  $\beta$ -casomorphin-7 Immunoreactive peptide increases after milk intake in newborn but not in adult dogs. *Pediatric Research*. **26**(1):34–38. Doi: 10.1203/00006450-198907000-00011.
- Singh, VK, Bajpai, K., Biswas, S., Haq, W, and Khan, MY. (1997). Molecular biology of opioid receptors: recent advances. *Neuroimmunomodulation* **4**: 285–297.
- Sippl, M. J. (1993). Recognition of errors in three-dimensional structures of proteins. *Proteins: Structure, Function, and Bioinformatics*, **17**(4), 355-362.
- Skolnick, J., Fetrow, J. S., & Kolinski, A. (2000). Structural genomics and its importance for gene function analysis. *Nature biotechnology*, 18(3), 283.
- Sora, Ichiro, Masahiko Funada, and George, R. Uhl. (1997) .The  $\mu$ -opioid receptor is necessary for [D-Pen2, D-Pen5] enkephalin-induced analgesia." *European journal of pharmacology* **324.2-3**: R1-R2.
- Sørensen HP, and Mortensen KK. (2005). Advanced genetic strategies for recombinant protein expression in *Escherichia coli*. *Journal of biotechnology*. **115**(2):113-28.
- Stanasila, L., Massotte, D., Kieffer, BL, and Pattus, F. (1999). Expression of  $\delta$ ,  $\kappa$  and  $\mu$  human opioid receptors in *Escherichia coli* and reconstitution of the high-affinity state for agonist with heterotrimeric G proteins. *European Journal of Biochemistry*.**260** (2):430-8.
- Strahs, Daniel, and Harel, Weinstein. (1997). Comparative modeling and molecular dynamics studies of the delta, kappa and mu opioid receptors.*Protein engineering* 10.9: 1019-1038.
- Sudbery, P.E., Gleeson, M.A., Veale, R.A., Ledebor, A.M. and Zoetmulder, M.C.M. (1988). *Hansenula polymorpha* as a novel yeast system for the expression of heterologous genes.
- Sun H., Gilbert D. J., Copeland N. G., Jenkins N. A. and Nathans J. (1997). Peropsin, a novel visual pigment-like protein located in the apical microvilli of the retinal pigment epithelium. *Proc. Natl Acad. Sci. USA* **94**, 9893–9898.

- Tailford, K. A., Berry, C L., Thomas, A. C. and Campbell, J. H. (2003). A casein variant in cow's milk is atherogenic. *Atherosclerosis* **170**: 13–19.
- Takeda, S., Kadowaki, S., Haga, T., Takaesu, H. and Mitaku, S. (2002). Identification of G protein-coupled receptor genes from the human genome sequence. *FEBS Lett* **520**: 97–101.
- Teschemacher, H. (1993). Atypical opioid peptides. *Opioids*. Springer, Berlin, Heidelberg, 499-528.
- Teschemacher, H. (2003). Opioid receptor ligands derived from food proteins. *Current Pharmaceutical Design* **9**, 1331–1344.
- Thorsdottir, I., Birgisdottir, B. E., Johannsdottir, I. M., Harris, D. P., Hill, J., Steingrimsdottir, L., and Thorsson, A. V. (2000). Different  $\beta$ -casein fractions in Icelandic versus Scandinavian cow's milk may influence diabetogenicity of cow's milk in infancy and explain low incidence of insulin-dependent diabetes mellitus in Iceland. *Pediatrics*, **106**(4), 719-724.
- Tian, Huib., Steven, L., McKnight, and David, W. Russell. (1997). Endothelial PAS domain protein 1 (EPAS1), a transcription factor selectively expressed in endothelial cells." *Genes & development* **11.1**: 72-82.
- Trivedi, MS., Shah, JS, Al-Mughairy, S., Hodgson, NW. Simms, B. and Trooskens, GA. (2014). Food-derived opioid peptides inhibit cysteine uptake with redox and epigenetic consequences. *J Nutr Biochem.*; **25**:1011–8.
- Trompette, A.; Claustre, J.; Caillon, F.; Jourdan, G.; Chayvialle, J.A.; Plaisancie, P. Milk.(2003). bioactive peptides and beta-casomorphins induce mucus release in rat jejunum. *Journal of Nutrition* **133** (11), 3499–3503.
- Tyndall, J .D. Sandilya, R. (2005). GPCR agonists and antagonists in the clinic. *Med Chem* **1**: 405–421.
- Uhl, George R., Ichiro Sora, and Zaijie, Wang. (1999).The  $\mu$  opiate receptor as a candidate gene for pain: polymorphisms, variations in expression, nociception, and opiate responses." *Proceedings of the National Academy of Sciences* **96.14**: 7752-7755.
- UIHaq, M R., Kapila, R., Shandilya, UK, and Kapila, S. (2014). Impact of milk derived  $\beta$ -casomorphins on physiological functions and trends in research: A review. *International Journal of Food Properties*. **17**(8):1726–1741. doi:10.1080/10942912.2012.712077.
- Umbach, M., Teschemacher, H., Praetorius, K., Hirschhäuser, R, and Bostedt, H. (1985). Demonstration of a  $\beta$ -casomorphin immunoreactive material in the plasma of newborn calves after milk intake. *Regulatory Peptides*. **12**(3):223–230. doi:10.1016/0167-0115(85)90063-1.
- Unterholzner, L., 2005. A study of the molecular mechanism of nonsense-mediated mRNA decay in human cells.

- Wagner, S., Baars, L., Ytterberg, AJ. Klussmeier, A, and Wagner CS. (2007). Consequences of membrane protein overexpression in Escherichia coli. *Mol Cell Proteomics* **6**: 1527–1550.
- Walwyn, WM., Miotto, KA, and Evans, CJ. (2010). Opioid pharmaceuticals and addiction: The issues, and research directions seeking solutions. *Drug Alcohol Depend* **108**:156 – 65
- Waly, and Mostafa, I. (2012). Prenatal and postnatal epigenetic programming: implications for GI, immune, and neuronal function in autism. *Autism research and treatment* **2012**.
- Waly, MI., Hornig, M., Trivedi, M., Hodgson, N., Kini R, and Ohta, A. (2012). Prenatal and postnatal epigenetic programming: implications for GI, immune, and neuronal function in autism. *Autism Res Treat*: 19093.
- Wang, HL, Chang, WT., Hsu, CY, Huang, PC. Chow, YW, and Li, AH. (2002). Identification of two C-terminal amino acids, Ser (355) and Thr (357), required for short-term homologous desensitization of mu-opioid receptors. *Biochem Pharmacol*. Jul 15; **64**(2):257-66.
- Waterham, and Hans, R. (1997). Isolation of the Pichia pastoris glyceraldehyde-3-phosphate dehydrogenase gene and regulation and use of its promoter. *Gene* **186.1**: 37-44.
- Weiss HM, and Grisshammer, R. (2002) Purification and characterization of the human adenosine a (2a) receptor functionally expressed in Escherichia coli. *Eur J Biochem* **269**: 82–92.
- Wess J, Nanavati S, Vogel Z, Maggio R. *EMBO J*(1993). 12:331–338. [PMC free article] Probst, W. C., L. A. Snyder, D. I. Schuster, J. Brosius, S. C. Sealfon. 1992. Sequence alignment of the G-protein coupled receptor superfamily. *DNA Cell Biol*. 11: 1.
- Wiederstein, M., and Sippl, MJ. (2007). ProSA-web: interactive webservice for the recognition of errors in three-dimensional structures of proteins. *Nucleic Acids Res* **35**:W407–W410. doi:10.1093/nar/gkm290.
- Wood, Paul L., and Smriti Iyengar. (1988). Central actions of opiates and opioid peptides. The opiate receptors. *Humana Press, Totowa, NJ*, 307-356.
- Woodford, K. B. (2008). A1 beta-casein, type 1 diabetes and links to other modern illnesses.
- Xu J, Xu M, Brown T, Rossi GC, Hurd YL, Inturrisi CE, Pasternak GW, and Pan YX (2013) Stabilization of the m-opioid receptor by truncated single transmembrane splice variants through a chaperone-like action. *J Biol Chem* **288**: 21211–21227.
- Yamazaki, T., Ro S, Goodman, M., Chung, NN, and Schiller, PW. (1993). A topochemical approach to explain morphiceptin bioactivity. *Journal of Medicinal Chemistry*. **36**(6):708–719. doi:10.1021/jm00058a007.
- Yang, J., Roy, A., & Zhang Y. (2013a). BioLiP: A semi-manually curated database for biologically relevant ligand-protein interactions. *Nucleic Acids Res.*; **41**:D1096–1103. doi: 10.1093/nar/gks966.

- Yang, J., Roy, A., & Zhang, Y. (2013). Protein–ligand binding site recognition using complementary binding-specific substructure comparison and sequence profile alignment. *Bioinformatics*, *29*(20), 2588-2595.
- Yang, J., Roy, A., & Zhang, Y. (2013b). Protein-ligand binding site recognition using complementary binding-specific substructure comparison and sequence profile alignment. *Bioinformatics*. ; *29*:2588–2595. doi: 10.1093/bioinformatics/btt447.
- Yang, J., Yan, R., Roy, A., Xu, D., Poisson, J., & Zhang, Y. (2015). The I-TASSER Suite: protein structure and function prediction. *Nature methods*, *12*(1), 7.
- Yasui, D.H., Peddada, S., Bieda, M.C., Vallero, R.O., Hogart, A., Nagarajan, R.P., Thatcher, K.N., Farnham, P.J. and LaSalle, J.M. (2007). Integrated epigenomic analyses of neuronal MeCP2 reveal a role for long-range interaction with active genes. *Proceedings of the National Academy of Sciences*, **104**(49), pp.19416-19421.
- Zhang Y, and Skolnick J. SPICKER. (2004). A clustering approach to identify near-native protein folds. *Journal of computational chemistry*. : **25**:865–871. doi: 10.1002/jcc.20011. [PubMed] [CrossRef]
- Zhang Y. (2009).I-TASSER: fully automated protein structure prediction in CASP8. *Proteins*. *77* Suppl 9(Suppl 9):100-13.
- Zhang Y. (2009).I-TASSER: fully automated protein structure prediction in CASP8. *Proteins*. *77* Suppl 9(Suppl 9):100-13.
- Zhang, Y. (2008). I-TASSER server for protein 3D structure prediction. *BMC bioinformatics*, *9*(1), 40.
- Zhu, Y., King, M. A., Schuller, A. G., Nitsche, J. F., Reidl, M., Elde, R. P., & Pintar, J. E. (1999). Retention of supraspinal delta-like analgesia and loss of morphine tolerance in  $\delta$  opioid receptor knockout mice. *Neuron*, **24**(1), 243-252.
- Zimprich, A., Simon, T. and Höllt, V. (1995). Cloning and expression of an isoform of the rat  $\mu$  opioid receptor (rMOR1B) which differs in agonist induced desensitization from rMOR1. *FEBS Lett* **359**:142–146.

## Appendix I

<b>1. Plastic and Glass wares</b>	<b>Vender</b>
1.1. grade pyrex glass	M/S labco , Ambala, India
1.2. Disposable pasteur pipettes	M/S labco ,Ambala, India
1.3. 15 and 50 ml falcon tubes	Geonaxy
1.4. 0.22 and .45 µm filters	Miliporecorporartion Bedford MA USA
1.5. Disposable tips	M/S Tarsons products Pvt. Ltd, Kolkata India.
<b>2. Chemicals</b>	
2.1. Fluoride	Hi-Media laboratories, Mumbai India
2.2. Yeast Extract	Hi-Media laboratories, Mumbai India
2.3. Tryptone	Hi-Media laboratories, Mumbai India
2.4. NaCl	Hi-Media laboratories, Mumbai India
2.5. Ammonium Acetate	Hi-Media laboratories, Mumbai India
2.6. Phenyl Methyl Sulphonyl	Hi-Media laboratories, Mumbai India
2.7. Agarose powder	Genei
2.8. Sodium Dodecyl Sulphate (SDS)	SRL Mumbai,
2.9. Tris-base	Merck, specialities Pvt. Ltd. Mumbai
2.10. Glycine	Fischer scientific Mumbai
2.11. N-propanol	Fischer scientific Mumbai
2.12. Triton X 114	Sigma Aldrich set Louis, USA
2.13. Acrylamide	Sisco research laboratories Pvt. Ltd. Mumbai
2.14. Tetra-methyl ethylene diamine (TEMED)	stratagene, santa clara, USA
2.15. Ammonium Sulphate	Merck, specialities Pvt. Ltd.
2.16. Beta mercaptoethanol	Merck, specialities Pvt. Ltd.
2.17. Lysozyme	Merck, specialities Pvt. Ltd.
2.18. L lauryl-sorcoc	Merck, specialities Pvt. Ltd.
2.19. Protein molecular weight ladder	Thermo Fischer Scientific
2.20. Gene Ruler (100bp DNA ladder)	Thermo Scientific
2.21. GeneRuler (1kb DNA ladder)	Thermo Scientific
<b>3. Equipment</b>	
Horizontal Agarose gel electrophoresis unit	Bio-Rad laboratories India Pvt.Ltd.
GEL doc	GE Healthcare
Thermal cycler	Bio-Rad laboratories India Pvt.Ltd.
6x histidine	HisTrap
Ni-NTA affinity column	GE Healthcare
Mono Q anion exchange chromatography column	GE Healthcare
HiTrap Heparin affinity column	GE Healthcare